

# **Enzymes and Metabolites in Picric Acid (2,4,6-Trinitrophenol) and 2,4-Dinitrophenol Biodegradation**

Von der Fakultät für Geo- und Biowissenschaften  
der Universität Stuttgart  
zur Erlangung der Würde eines  
Doktors der Naturwissenschaften (Dr. rer. nat.)  
genehmigte Abhandlung

vorgelegt von

**Klaus W. Hofmann**

aus Coburg

Hauptberichter: Prof. Dr. H.-J. Knackmuss  
Mitberichter: PD Dr. Andreas Stolz

Tag der mündlichen Prüfung: 19.12.2003

Institut für Mikrobiologie der Universität Stuttgart  
2003

## Table of Contents

Abbreviations.....	3
Abstract.....	5
Kurzfassung.....	7
1 Introduction.....	9
2 Biodegradation of picric acid and DNP.....	17
2.1 Degrading strains <i>R. (opacus) erythropolis</i> HL PM-1 and <i>N. simplex</i> FJ2-1A.17.....	17
2.2 Initial hydrogenation steps.....	17
2.2.1 Hydrogenation of TNP.....	17
2.2.2 Hydrogenation of H <sup>-</sup> -TNP.....	20
2.3 Tautomerization of 2H <sup>-</sup> -TNP.....	22
2.4 Nitrite elimination from 2H <sup>-</sup> -TNP.....	23
2.5 Hydrogenation of H <sup>-</sup> -DNP.....	26
2.6 Hydrolytic ring fission of 2,4-dinitrocyclohexanone.....	27
2.7 The known pathway and proposed final steps.....	30
3 Literature.....	33
Appendix 1: <i>npd</i> gene functions of <i>Rhodococcus opacus</i> HL PM-1 in the initial steps of 2,4,6-trinitrophenol degradation.....	42
Appendix 2: The role of a tautomerase and a nitrite-eliminating enzyme in 2,4,6-trinitrophenol (picric acid) degradation.....	68
Appendix 3: Hydrolytic ring cleavage in the biodegradation of 2,4,6-trinitrophenol (picric acid) and 2,4-dinitrophenol.....	86
Acknowledgements.....	101
Curriculum Vitae.....	102

## Abbreviations

2,4-DNCH	2,4-Dinitrocyclohexanone
2H <sup>-</sup> -DNP	Dihydride $\sigma$ -complex of DNP
2H <sup>-</sup> -TNP	Dihydride $\sigma$ -complex of TNP
2-NCH	2-Nitrocyclohexanone
4,6-DNH	4,6-Dinitrohexanoate
DNA	Deoxyribonucleic acid
DNP	2,4-Dinitrophenol
F <sub>420</sub> / F <sub>420</sub> H <sub>2</sub>	Oxidized and reduced form of coenzyme F <sub>420</sub>
FPLC	Fast performance liquid chromatography
H <sup>-</sup> -DNP	Hydride $\sigma$ -complex (Meisenheimer complex) of DNP
HTI / II	Hydride transferase I / II
H <sup>-</sup> -TNP	Hydride $\sigma$ -complex (Meisenheimer complex) of TNP
HPLC	High performance liquid chromatography
kDa	Kilodalton
LC-MS	Liquid chromatography, coupled to mass spectroscopy
MALDI-TOF	Matrix-assisted laser desorption time of flight mass spectroscopy
NADPH	Nicotinamide adenine dinucleotide phosphate
NDFR	NADPH-dependent F <sub>420</sub> reductase
NMR	Nuclear magnetic resonance spectroscopy
npd	Nitrophenol degradation
SDS	Sodium dodecylsulphate
TAC	Tricarboxylic-acid cycle
TNP	2,4,6-Trinitrophenol (picric acid)

TNT	2,4,6-Trinitrotoluene
U	Unit [ $\mu\text{mol min}^{-1}$ ]
UV-visible	Ultraviolet and visible spectrum of light

## Abstract

The bacterial strains *Rhodococcus (opacus) erythropolis* HL PM-1 and *Nocardioides simplex* FJ2-1A can use picric acid (TNP) and 2,4-dinitrophenol (DNP) as sole nitrogen source. Enzymes were identified which are isofunctional in both strains, using the same degradation mechanism.

During the initial steps hydride ions were transferred to the aromatic ring of the electron deficient  $\pi$ -system, forming first the hydride  $\sigma$ -complex of TNP,  $H^-$ -TNP, and subsequently the dihydride  $\sigma$ -complex,  $2H^-$ -TNP. The reactions were catalyzed by hydride transferase II (HTII) and hydride transferase I (HTI), respectively, together with the NADPH-dependent  $F_{420}$  reductase (NDFR) and the coenzymes NADPH and  $F_{420}$ . NDFR, HTII, and HTI were cloned and purified as His-tag fusion proteins by Ni-NTA affinity chromatography. Reactions were followed by repeated recording of UV-visible spectra, and intermediates were identified by HPLC, HPLC-MS, and NMR measurements.  $H^-$ -TNP and  $2H^-$ -TNP were chemically synthesized and used as standards and substrates.

In the next step, a nitrite-eliminating enzyme releasing nitrite from  $2H^-$ -TNP and generating the hydride  $\sigma$ -complex of DNP ( $H^-$ -DNP) was identified. A tautomerase was shown to give rise to two tautomeric forms, the *aci*-nitro form and the nitro form of  $2H^-$ -TNP, identified by HPLC and NMR measurements. Since the nitrite-eliminating enzyme used only the *aci*-nitro form as a substrate, it appears that the  $2H^-$ -TNP tautomerase inhibits accumulation of the nitro form. Whereas the  $2H^-$ -TNP tautomerase was cloned and purified as a His-tag fusion protein, the nitrite-eliminating enzyme was isolated by FPLC and the N-terminal sequence was determined. Databank search exhibited no similarities to any known proteins.

HTI and NDFR, together with the coenzymes NADPH and  $F_{420}$ , hydrogenated chemically synthesized  $H^-$ -DNP to  $2H^-$ -DNP. It was shown by HPLC-MS that 2,4-dinitrocyclohexanone (2,4-DNCH) was generated after protonation. A hydrolase was purified by FPLC, catalyzing hydrolytic ring fission of 2,4-DNCH, forming 4,6-dinitrohexanoate (4,6-DNH). 4,6-DNH was identified by HPLC-MS. MALDI-TOF measurements showed that the 2,4-DNCH hydrolase consists of four identical subunits. Since determination of the N-terminal amino acid sequence exhibited that

the corresponding gene was located on the known gene clusters of both strains, the gene function was recognized. Activity for the conversion of 4,6-DNH in crude extracts identified 4,6-DNH as a true intermediate of the degradation pathway of TNP and DNP.

## Kurzfassung

Die Bakterienstämme *Rhodococcus (opacus) erythropolis* HL PM-1 und *Nocardioides simplex* FJ2-1A können Pikrinsäure (TNP) und 2,4-Dinitrophenol (DNP) als alleinige Stickstoffquelle nutzen. Dabei wurden Enzyme eines konvergenten Abbauwegs nachgewiesen, die in beiden Stämmen isofunktionell sind.

Während der Initialschritte wird Hydrid auf den aromatischen Ring des elektronenarmen  $\pi$ -Systems übertragen, wobei sich zeigte, dass zuerst der Hydrid- $\sigma$ -Komplex von TNP,  $H^-$ -TNP, und in einer nachfolgenden Hydridübertragung der Dihydrid- $\sigma$ -Komplex,  $2H^-$ -TNP, entsteht. Die Reaktionen werden von zwei Hydridtransferasen, HTII und HTI, katalysiert, wobei die NADPH-abhängige  $F_{420}$ -Reduktase (NDFR) und die Coenzyme NADPH und  $F_{420}$  für den Umsatz notwendig sind. NDFR, HTII und HTI wurden kloniert und als His-tag-Proteine mittels Ni-NTA-Affinitätschromatographie gereinigt. Die Reaktionen wurden mit Hilfe von UV/Vis-Spektren in zeitlichen Abständen von jeweils einer Minute verfolgt und die Metabolite mit HPLC-MS und NMR-Messungen nachgewiesen.  $H^-$ -TNP und  $2H^-$ -TNP wurden chemisch synthetisiert, um sie sowohl als Standard sowie als Substrat einsetzen zu können.

Im folgenden Abbauschritt wird durch ein Nitrit-eliminierendes Enzym eine Nitro-Gruppe aus  $2H^-$ -TNP in Form von Nitrit abgespalten, wobei der Hydrid- $\sigma$ -Komplex von DNP ( $H^-$ -DNP) entsteht. Eine Tautomerase isomerisiert  $2H^-$ -TNP zu zwei Tautomeren, die *Aci*-nitro- und die Nitro-Form. Dies wurde durch HPLC-MS und NMR-Messungen bestätigt. Da das Nitrit-eliminierende Enzym nur die *Aci*-nitro-Form umsetzen kann, verhindert die  $2H^-$ -TNP-Tautomerase, dass die Nitro-Form als nicht weiter abzubauenendes Produkt akkumuliert. Während die  $2H^-$ -TNP-Tautomerase kloniert und als His-tag-Protein gereinigt wurde, konnte das Nitrit-eliminierende Enzym mittels FPLC isoliert, und die N-terminale Aminosäuresequenz bestimmt werden. Datenbank-Recherchen ergaben keine Ähnlichkeiten zu bekannten Enzymen.

Die HTI und NDFR, zusammen mit den Coenzymen NADPH und  $F_{420}$ , hydrierten chemisch synthetisiertes  $H^-$ -DNP zu  $2H^-$ -DNP. Es zeigte sich, dass anschließend durch Protonierung spontan 2,4-Dinitrocyclohexanon (2,4-DNCH) entstand, was

durch HPLC-MS-Messungen gezeigt wurde. Mittels FPLC wurde eine Hydrolase gereinigt, die eine hydrolytische Ringöffnung von 2,4-DNCH katalysierte, was zu 4,6-Dinitrohexanoat (4,6-DNH) als Produkt führte. 4,6-DNH konnte mit Hilfe von HPLC-MS-Messungen nachgewiesen werden. MALDI-TOF-Messungen ergaben, dass die 2,4-DNCH-Tautomerase wahrscheinlich als Tetramer mit vier identischen Untereinheiten vorliegt. Da die Bestimmung der N-terminalen Aminosäuresequenz der 2,4-DNCH-Hydrolase zeigte, dass das entsprechende Gen auf dem jeweils bekannten Gen-Cluster in beiden Stämmen zu finden war, konnte diesem Gen erstmalig eine Funktion nachgewiesen werden.

Umsatzaktivitäten für 4,6-DNH mit Rohextrakt identifizierten 4,6-DNH als echtes Intermediat im Abbauweg von TNP und DNP.



# 1 Introduction

Picric acid (2,4,6-trinitrophenol, TNP) is industrially produced by treating phenol with concentrated sulfuric acid and subsequently with nitric acid. In the first reaction phenol is sulfonated, in the following step the sulfonic groups are replaced by nitro groups. An alternative way of synthesis is dinitration of chlorobenzene, followed by hydrolysis to 2,4-dinitrophenol (DNP), and further nitration to TNP by nitric acid (13).

TNP was formerly used for dyeing wool, silk, and leather. It is the oldest nitro dye, first obtained by Woulfe in 1771. Nitro dyes have also been used for transfer printing on polyester woven fabrics and in modern reproduction processes, e.g. ink-jet printing, optical data recording, and thermal transfer printing. Further, TNP has been recommended for the colored electrophoretic coating of aluminum as a mixture with alkyd resins (13).

Picric acid was produced as explosive with extensive military use during World War I. Because of its acidity and its ability to form metal picrates, some of which are sensitive and powerful, picric acid is no longer employed as a high explosive. However, ammonium picrate, which is insensitive but not very powerful, is still used (13). Because of its use for many years there are many places heavily contaminated with picric acid, especially the army ammunition plants where explosives were manufactured for much of the 20th century (52).

In analytical chemistry TNP is used as a test reagent, e.g. to identify alkaloids, cardenolids and creatinine. Further, it is used for colorimetric determination of blood sugar and by microanalysis of carbon steel as Igeweskys Reagenz. Fused aromatics are identified with TNP by formation of colored charge-transfer complexes (15).

Dinitrophenols possess a wide range of biocidal activity and were therefore used as insecticides, acaricides, herbicides, and fungicides. The dinitrophenol insecticides uncouple phosphorylation and are highly toxic to plants, insects, higher animals, and humans. Hence, they are not used as insecticides anymore (13).

Nitroaromatics are important synthons in industry due to the versatile chemistry of the nitro group. During the production of nitrobenzene from benzene, TNP and DNP are generated as off-stream chemicals, which accumulate in industrial waste waters. In some factories nitrophenols are removed from the effluents by a thermolytic process under high pressure. Thus, nitrophenols are disintegrated to acetic acid and oxalic acid, which can be biodegraded by microbes in a purification plant. On the other side, sustainable strategies for direct microbial degradation of nitrophenols without thermolytical or chemical treatment is environmentally friendly and might dramatically reduce the costs of removal of nitrophenols not only from waste water but also from contaminated soil and groundwater.

Understanding the pathway by which a compound is degraded is the precondition for the development of an effective bioremediation system. A considerable number of publications described bacterial strains and possible pathways for the biodegradation of nitroaromatic compounds. Fig. 1 summarizes the initial mechanisms of the microbial degradation of nitroaromatics. Initial attack by monooxygenation substitutes the nitro group by a hydroxyl group, accompanied by nitrite elimination. This mechanism was described for 2-nitrophenol (60, 61), 4-nitrophenol (27, 51), 4-chloro-2-nitrophenol (4), and 4-nitroanisole (44). Probably all the monooxygenation reactions involve a quinone intermediate, which was postulated based on the stoichiometry of the cofactor requirements for the reaction (53) or identified and quantitatively analyzed (21, 23). Dioxygenases can hydroxylate the aromatic core yielding a dihydroxy intermediate after nitrite elimination. Several compounds are degraded by this reaction: 2-nitrotoluene (22, 24), 3-nitrobenzoate (36), 1,3-dinitrobenzene (7), and 2,6-dinitrophenol (12). The dihydroxy nitrocyclohexadienes formed by the initial dioxygenase attack undergo spontaneous rearomatization to generate catechols.

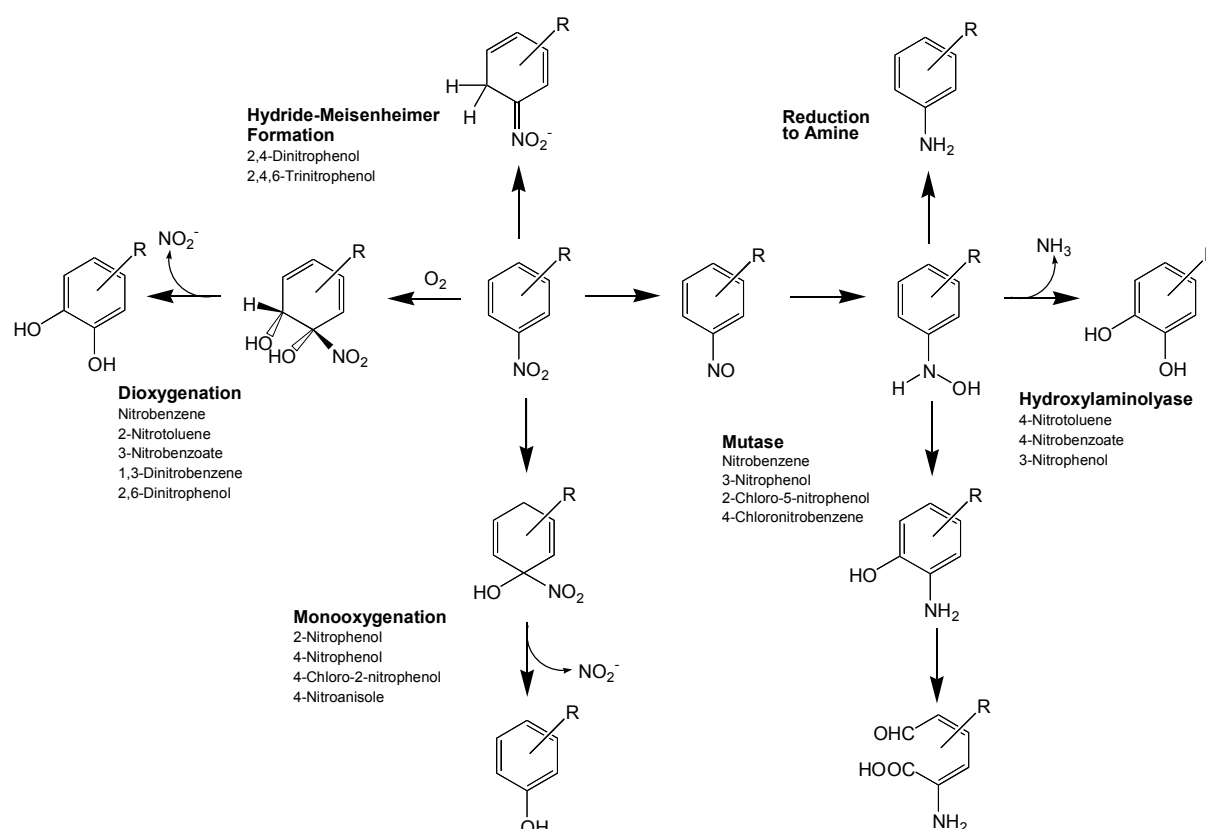


**Fig. 1. Initial mechanisms of the biodegradation of nitroaromatics (37).**

The electrophilic nitro group can be reduced to a nitroso intermediate and further to a hydroxylamino derivative. Mutase-catalyzed intramolecular rearrangement forms an *ortho*-aminophenol. Nitrobenzene (38), 3-nitrophenol 2-chloro-5-nitrophenol (45),(46), and 4-chloronitrobenzene (29) are examples of this mechanism.

The hydroxylamino derivative can also be dihydroxylated by a hydroxylaminolyase accompanied by release of ammonia. Hydroxylamine derivatives of 4-nitrotoluene (22, 40), 4-nitrobenzoate (18, 19), and 3-nitrophenol (35) are further transformed by a hydroxylaminolase to yield pyrocatechol (1,2-dihydroxybenzene) derivatives.

Complete reduction of the nitro group to the amine does not appear to be a mechanism, which is widely used by aerobic bacteria for productive metabolism. This mechanism was observed for anaerobic transformation of 2,4-dinitrophenol (8, 56) and the unproductive metabolism of picric acid forming picramic acid (55).

TNP and DNP were transformed by strains of *Corynebacterium simplex* (20), several *Pseudomonades* (16) (26), *Nocardia alba* (16), and *Arthrobacter* (26) by release of nitrite. However, a pathway or catabolic intermediates were not described.

Whereas in nearly all cases of aerobic breakdown of aromatic compounds the primary attack are oxidative reactions, the negative mesomeric effect of nitro groups at the aromatic carbon ring cause an electron deficiency, which enables hydrogenation at the core rather than oxygenolytic attack. Hence, nitroaromatics with two or more nitro groups are hydrogenated. Picric acid is hydrogenated by this mechanism forming a Meisenheimer complex (hydride  $\sigma$ -complex) (33). Formation of hydride Meisenheimer complexes is a well known chemical reaction, e.g. as intermediates during nucleophilic aromatic substitution of polynitroaromatic compounds by hydrogen (6, 17, 28, 48, 49).

Lenke et al. isolated the strain *Rhodococcus (opacus) erythropolis* HL PM-1 by cultivation on DNP as the sole source of nitrogen, accumulating the orange-red hydride Meisenheimer complex of TNP ( $H^-$ -TNP) (34). Rieger et al. showed that *R. (opacus) erythropolis* HL PM-1 was able to use TNP as a sole source of carbon, nitrogen, and energy (42). The authors characterized the  $H^-$ -TNP by UV-visible and NMR measurements. They proposed that the observed nitrite release occurs from the protonated form of  $H^-$ -TNP, forming DNP (Fig. 2).

Experiments conducted with resting cells showed that prior to denitration  $H^-$ -TNP is further reduced to a dihydride- $\sigma$ -complex,  $2H^-$ -TNP, the dianion of 2,4,6-trinitrocyclohexanone (33). First,  $2H^-$ -TNP was indirectly identified by acidic hydrolysis, forming 1,3,5-trinitropentane after decarboxylation (33, 48). However,  $2H^-$ -TNP was thought to be a dead-end product, because the detection of DNP suggested a gratuitous rearomatization of  $H^-$ -TNP and a concomitant nitrite release (33).

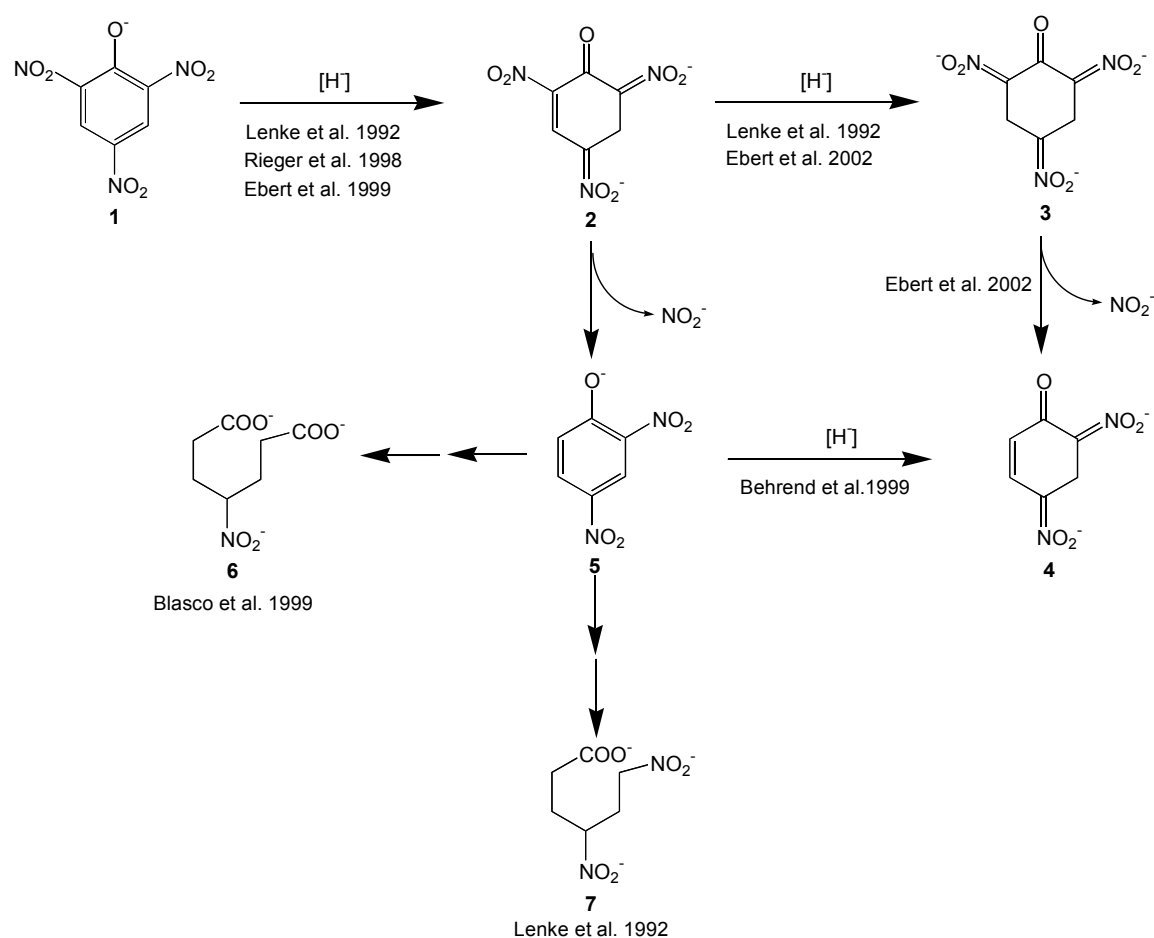


**Fig. 2. Formerly proposed degradation pathway of TNP and DNP. 1: TNP; 2: H<sup>-</sup>-TNP; 3: 2H<sup>-</sup>-TNP; 4: H<sup>-</sup>-DNP; 5: DNP; 6: 3-Nitroadipate; 7: 4,6-DNH.**

Initial hydrogenation of the aromatic ring was also observed during TNT degradation in *R. (opacus) erythropolis* HL PM-1, forming the hydride-Meisenheimer complex of TNT (H<sup>-</sup>-TNT). A subsequent hydrogenation step yields the dihydride-Meisenheimer complex of TNT (2H<sup>-</sup>-TNT) (57, 58). Since no further intermediates or nitrite release were detected, the authors proposed that 2H<sup>-</sup>-TNT formation is due to unproductive misrouting.

The conversion of DNP was also investigated in *Rhodococcus* sp. RB1 (3). In the culture supernatant, with acetate as the carbon source and DNP as the nitrogen source, 3-nitroadipate was isolated and identified by NMR measurements. The authors suggested that hypothetical Meisenheimer intermediates, H<sup>-</sup>-DNP and 2H<sup>-</sup>-

DNP, are generated by two successive hydride transfers. An aerobic *ortho* ring fission of 2H<sup>-</sup>-DNP and a concomitant release of nitrite, catalyzed by an oxygenase, were proposed to form 3-nitroadipate (Fig. 2).

Behrend and Heesche-Wagner gave evidence that H<sup>-</sup>-DNP is formed through hydrogenation of DNP by crude extract of *Nocardioides* sp. CB22-2 (2) and they found that NADPH is required for further degradation. Hence, the authors suggested that a monooxygenolytic hydroxylation at the *para* position might take place, forming 2-nitrohydroquinone after nitrite release.

The first enzymes of the initial TNP degradation were purified and characterized from *Nocardioides simplex* FJ2-1A by Ebert et al. (11). The authors identified a two-enzyme system, which catalyzed hydride transfer to TNP and DNP. One of the protein components functioned as a NADPH-dependent F<sub>420</sub> reductase and the second component was shown to be a hydride transferase, shuttling hydride from reduced coenzyme F<sub>420</sub> to the aromatic ring. TNP was transformed to H<sup>-</sup>-TNP by this mechanism. Ebert et al. showed further that the same enzyme system catalyzes a second hydrogenation, forming 2H<sup>-</sup>-TNP (10). An enzyme activity was enriched, releasing nitrite from 2H<sup>-</sup>-TNP to produce the hydride Meisenheimer complex of DNP (H<sup>-</sup>-DNP). The authors gave evidence that TNP and DNP are degraded via a convergent catabolic pathway with H<sup>-</sup>-DNP as a common metabolite (Fig. 2).

Russ et al. were the first who identified genes of *R. (opacus) erythropolis* HL PM-1 involved in TNP and DNP degradation by mRNA differential display (43, 59). Fig. 3 shows the sequence similarities with protein sequences in the database (1). NpdG exhibited a sequence similarity of 44 % to the F<sub>420</sub>-dependent NADP reductase of *Methanobacterium thermoautotrophicum* (sp | O26350 |). The gene product was shown to reduce F<sub>420</sub> in the presence of NADPH.

Further, a hydride transferring function was found for the gene product of NpdI, which showed a sequence similarity of 46 % to the N<sub>5</sub>,N<sub>10</sub>-Methylene-tetrahydromethanopterin reductase in *Archaeoglobus fulgidus* (gi | 2649522 |) (43). The authors observed that cell extracts of *Escherichia coli* expressing the F<sub>420</sub>-dependent picric acid reductase (NpdI) converted TNP to H<sup>-</sup>-TNP.

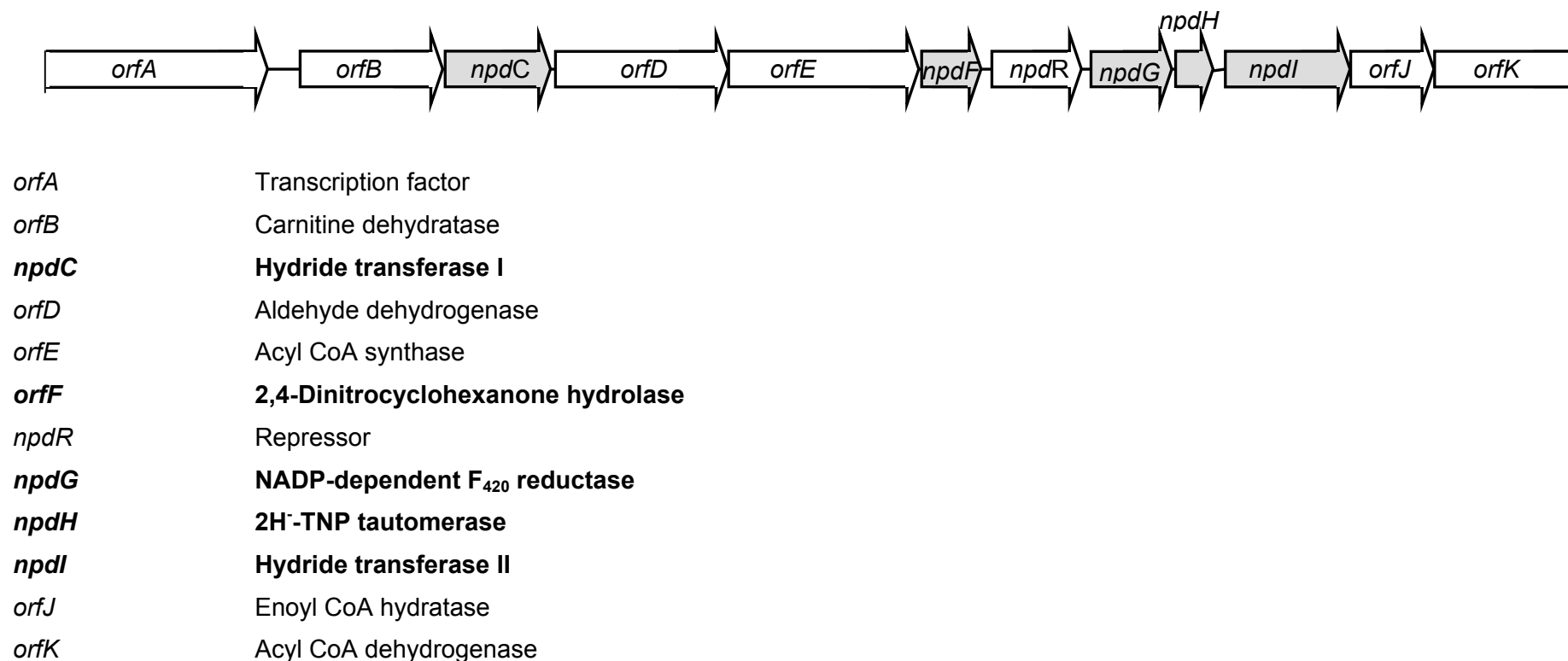


Fig. 3. The picric acid degradation gene cluster of *R. (opacus) erythropolis* HL PM-1 and predicted gene functions, based on sequence similarities with protein sequences in the database. Grey colored genes were biochemically characterized in the present work.

Starting this work, only the two enzymes catalyzing the two initial hydrogenation steps of picric acid degradation had been purified from *N. simplex* FJ2-1A. In contrast, no enzymes of TNP and DNP degradation had been purified from *R. (opacus) erythropolis* HL PM-1 so far. The goal of the present study was to find more catabolic intermediates by instrumental analytics, in order to clarify the complete pathway in both strains. Furthermore, investigation was performed to show if the known gene cluster of *R. (opacus) erythropolis* HL PM-1 harbored additional hitherto unknown degradation enzymes. Another approach to explore the metabolism of polynitrophenols was the purification and characterization of involved enzymes from *R. (opacus) erythropolis* HL PM-1 and *N. simplex* FJ2-1A. Comparison of enzyme functions and metabolites were supposed to show common or different bacterial strategies of polynitroaromatic degradation.



## 2 Biodegradation of Picric Acid and DNP

### 2.1 Degrading strains *R. (opacus) erythropolis* HL PM-1 and *N. simplex* FJ2-1A

In the present study, two TNP degrading strains were investigated to identify metabolites and enzymes involved in TNP and DNP degradation. The strain *R. erythropolis* HL PM-1 was originally isolated by the ability to grow with DNP as a nitrogen source by Lenke et al. (33). Heiss et al. proposed a reclassification as *R. (opacus) erythropolis*, confirmed by 16S rDNA analysis (25).

*N. simplex* FJ2-1A was isolated from TNP containing wastewater and identified by 16S rDNA analysis by Rajan et al. (39).

Both strains were grown with TNP, DNP, or 2-nitrocyclohexanone (2-NCH) as a sole nitrogen source in mineral medium. Since cell lysis of these Gram-positive strains was very difficult to perform, especially for *R. (opacus) erythropolis* HL PM-1 (41), new growth conditions were introduced to improve disruption of the cells. 3-liter unbaffled shaking flasks were filled with 1 liter of medium. Possibly, limited oxygen supply in the culture promoted growth of the cells and the expression of the enzymes of the non-oxygenolytic pathway. In addition, the unbaffled shaking flasks reduced mechanical stress in comparison to cultivation in a fermenter or in baffled flasks. Growing under these conditions, cells of both strains could be lysed by French Press.

### 2.2 Initial hydrogenation steps

#### 2.2.1 Hydrogenation of TNP

Aerobic degradation of aromatic compounds is usually initiated by the attack of mono- or dioxygenases. In contrast, the initial step of TNP biodegradation is a hydrogenation reaction, yielding the hydride Meisenheimer complex of TNP (H<sup>-</sup>-TNP).

TNP possesses an electrophilic aromatic nucleus, due to the negative mesomeric effects of the nitro groups. In addition, the nitrogen and the oxygen atoms are electronegative and therefore attract the  $\pi$ -electrons of the ring (negative inductive

effect). The electron density at the nitro groups makes them easily reducible, which is observed in most cases during 2,4,6-trinitrotoluene (TNT) decomposition: by one-electron transfer or two-electron transfer a nitroso derivative is formed, followed by two consecutive electron transfers, producing a hydroxylamine and an aromatic amine (14).

The electron withdrawing effects of the nitro groups also facilitate a nucleophilic attack at the aromatic ring. A hydride ion, e.g. provided by  $\text{NaBH}_4$ , reduces the aromatic nucleus to form a Hydride-Meisenheimer  $\sigma$ -complex. This reaction is observed for TNT and TNP. The TNP degrading strains, investigated in this work, both use the hydrogenation mechanism of the aromatic nucleus.

Enzymes were found to be encoded by the gene cluster in *R. (opacus) erythropolis* HL PM-1, which are responsible for providing hydride ions and the concomitant hydrogenation of the aromatic ring (43). The authors cloned *npdG* ( $F_{420}$  / NADPH oxidoreductase) and *npdI* (Acyl-CoA dehydrogenase) and expressed both genes in *E. coli*. A mixture of the cell-free extracts with overexpressed NpdG and NpdI, respectively, was shown to transform TNP to H-TNP. No enzyme assays were conducted with purified enzymes.

The aim of the present work was to unequivocally show the function of *npdG* and *npdI*. Hence, both genes were cloned and the gene products were expressed as His-Tag fusion proteins and purified by Ni-NTA affinity chromatography for further enzyme characterization. All genes of the *R. (opacus) erythropolis* HL PM-1 gene cluster, involved in TNP degradation, were named *npd* for nitrophenol degradation (25). NpdG (NADPH-dependent  $F_{420}$  reductase, NDFR) showed a 44 % sequence similarity to a  $F_{420}$ -dependent NADP reductase of *Methanobacterium thermoautotrophicum* in the database (43, 50, 59). Furthermore, the first 27 amino acids of the translation product exhibited a 66 % sequence identity to the N-terminal region of the NADPH-dependent  $F_{420}$  reductase of *N. simplex* FJ2-1A (11).

Recently, a gene cluster from *N. simplex* FJ2-1A was sequenced (9), exhibiting similar genes to *npdG*, *npdH*, and *npdI* in the *R. (opacus) erythropolis* HL PM-1

cluster. Therefore, *npdG* was cloned also from *N. simplex* FJ2-1A, to compare both NDFRs biochemically. The gene product was expressed as a His-tag fusion protein, and purified by Ni-NTA affinity chromatography. To confirm NDFR functions in both strains, assays were performed at 400 nm (pH = 5.5) together with the coenzymes  $F_{420}$  and NADPH. Decrease in absorbance indicated the reduction of  $F_{420}$  and the formation of  $F_{420}H_2$  by a concomitant oxidation of NADPH. The NDFR of *R. (opacus) erythropolis* HL PM-1 exhibited a  $V_{max}$  of  $17.27 \pm 2.46$  U  $mg^{-1}$  and a  $K_m$  value of  $9.86 \pm 2.89$   $\mu M$ , whereas a specific activity of  $31.7$  U  $mg^{-1}$  and a  $K_m$  value of  $15.64 \pm 3.93$   $\mu M$  was calculated for the NDFR of *N. simplex* FJ2-1A. NDFRs of both strains reduced only  $F_{420}$  and had no reducing activity with flavins, like FAD (flavin adenine dinucleotide) or FMN (flavin mononucleotide).  $F_{420}H_2$ , formed in the described reaction, serves as a hydride donor for the hydrogenation of TNP.

The gene product of *npdI* in the *R. (opacus) erythropolis* gene cluster was named hydride transferase II (HTII). HTII exhibited a sequence similarity of 46 % to an  $F_{420}$ -dependent *N5,N10*-methylene-tetrahydromethanopterin reductase from *Archaeoglobus fulgidus* (30, 43). In addition, the first 27 amino acids showed a 77 % sequence identity to the N-terminal region of the hydride transferase of *N. simplex* FJ2-1A, which converts TNP to  $H^-$ -TNP, as described by Ebert et al. (11).

Together with the NDFR, the purified HTII hydrogenated TNP at the *meta* position of the carbon ring, forming the hydride complex,  $H^-$ -TNP (Fig. 4).

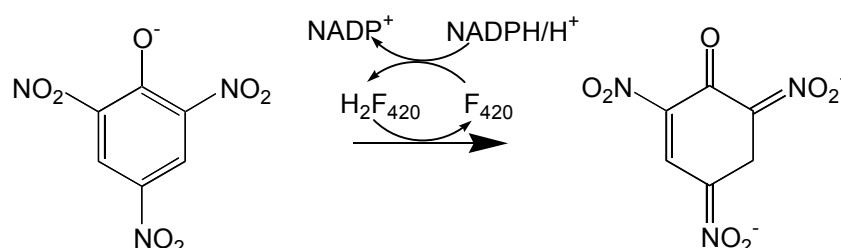


**Fig. 4: Hydrogenation of TNP by NDFR and HTII, generating  $H^-$ -TNP.**

Conversion of TNP was followed by repeated recording of UV-visible spectra, displaying the disappearance of TNP and the concomitant formation of  $H^-$ -TNP. Transformation was also followed by HPLC measurements. Therefore, authentic  $H^-$ -

TNP was used as an analytical standard, synthesized by hydrogenation of TNP with  $(\text{H}_3\text{C})_4\text{NB}_3\text{H}_8$  (42). Chemical identification of  $\text{H}^-$ -TNP was carried out by UV-visible, HPLC, and LC-MS analysis.

Further experiments showed, that HTII had no activity with 2-nitrophenol or 4-nitrophenol as substrates. Obviously the enzyme requires at least two nitro groups, one in *ortho* and another in *para* position to the hydroxyl group.

For investigation of the hydride transferase II from *N. simplex* FJ2-1A, *npdI* of the gene cluster was cloned and the gene product purified as a His-tag fusion protein. The HTIIs of *R. (opacus) erythropolis* HL PM-1 and *N. simplex* FJ2-1A exhibited the same enzyme function, hydrogenation of TNP and DNP. Whereas the HTII of *R. (opacus) erythropolis* HL PM-1 revealed a  $K_m$  value of 0.2  $\mu\text{M}$  using TNP as substrate, the HTII of *N. simplex* FJ2-1A exhibited a  $K_m$  value of 1.7  $\mu\text{M}$ . Both HTIIs showed inhibition of the hydride transfer at higher substrate concentrations.

### 2.2.2 Hydrogenation of $\text{H}^-$ -TNP

Previously, it was hypothesized that rearomatization occurs to the protonated form of  $\text{H}^-$ -TNP, generating DNP (34, 42). Recent investigations have shown that  $\text{H}^-$ -TNP is further hydrogenated to produce  $2\text{H}^-$ -TNP as an intermediate of the pathway (10, 25, 34).

The hydride transferring enzyme system (NDFR and HTII), isolated from *N. simplex* FJ2-1A, was shown to hydrogenate  $\text{H}^-$ -TNP in a subsequent step, generating the dihydride  $\sigma$ -complex,  $2\text{H}^-$ -TNP (10). In contrast, HTII from HL PM-1 showed only a minimal activity for  $\text{H}^-$ -TNP. Though the HTIIs of both strains, FJ2-1A and HL PM-1, seem to be functionally alike, they obviously possess a different substrate spectrum.

As a consequence, HL PM-1 was expected to harbor a gene encoding for another hydride transferase. Indeed, database comparison revealed a hydride transferase gene in the gene cluster, *npdC*, which showed a sequence similarity of 42 % to an N5,N10-methylene-tetrahydromethanopterin reductase of *Methanococcus jannaschii*

(5, 43). *npdC* was cloned and the gene product, named hydride transferase I (HTI), was expressed and purified as a His-tag fusion protein.

Chemically synthesized  $\text{H}^-$ -TNP was used as a substrate for turnover with purified HTI. Enzyme assays gave evidence, that HTI converts  $\text{H}^-$ -TNP to the dihydride complex of TNP ( $2\text{H}^-$ -TNP) by a hydride transfer to the carbon ring at the C5 position. Like HTII, it requires the NDFR and the coenzymes NADPH and  $\text{F}_{420}$  to provide hydride, which is transferred to  $\text{H}^-$ -TNP. Repeated recording of UV-visible spectra displayed the disappearance of  $\text{H}^-$ -TNP and the concomitant formation of  $2\text{H}^-$ -TNP. In addition, the reaction was followed by HPLC and LC-MS measurements, to identify  $2\text{H}^-$ -TNP as the product.

$2\text{H}^-$ -TNP was synthesized as an analytical standard by reduction of  $\text{H}^-$ -TNP with  $\text{NaBH}_4$  (48, 49). Chemical confirmation of the structure  $2\text{H}^-$ -TNP was obtained by UV-visible spectrum, HPLC analysis, NMR, and LC-MS measurements.

Using the DNA sequence of *npdC* encoding for HTI of *R. (opacus) erythropolis* HL PM-1, a gene was found in *N. simplex* FJ2-1A, which exhibited a 78 % similarity to *npdC* (54). The gene was cloned and overexpressed in *E. coli* BL21 (DE3), and enzyme assays were performed with crude extract and  $\text{H}^-$ -TNP as substrate. It was shown, that the HTIs of both strains, HL PM-1 and FJ2-1A, possess the same enzyme function:  $\text{H}^-$ -TNP was converted to  $2\text{H}^-$ -TNP, whereas TNP was not transformed (Fig. 5).

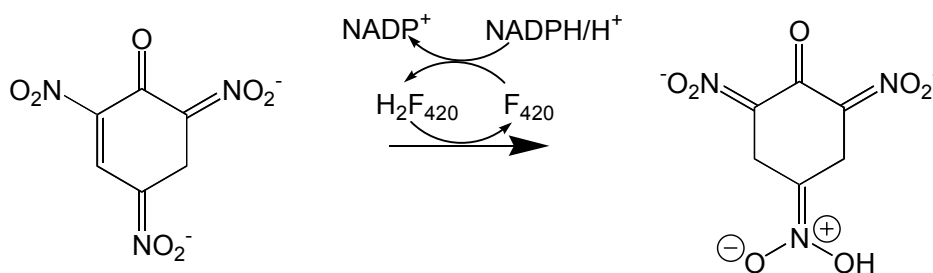


**Fig. 5. Hydrogenation of  $\text{H}^-$ -TNP by NDFR and HTII, forming  $2\text{H}^-$ -TNP.**

An explanation for this mechanism, preferring hydrogenation instead of DNP formation by rearomatization, derives from the energy profile during degradation:  $\text{H}^-$ -TNP possesses a higher potential energy in comparison to TNP, because the aromatic system is abolished. A consecutive hydrogenation step leads to  $2\text{H}^-$ -TNP as an intermediate, which is less stable than DNP because of its higher potential energy. Thus, it seems more efficient to keep the energy profile at a high level, before the next low energy intermediate is generated. Following this mechanism saves energy in the course of the pathway.

Obviously, both hydride transferases (HTI and HTII) in FJ2-1A can hydrogenate  $\text{H}^-$ -TNP. Furthermore, HTI was also shown to play a decisive role in further degradation by hydrogenation of the Hydride-Meisenheimer complex of 2,4-DNP as described in 2.5.

### 2.3 Tautomerization of $2\text{H}^-$ -TNP

Under alkaline conditions (pH 12), chemically synthesized  $2\text{H}^-$ -TNP showed only one peak in the HPLC spectrum, whereas at pH < 8 slowly another peak of a new product X occurred. This reaction was dramatically accelerated by a small enzyme (NpdH) of *R. (opacus) erythropolis* HL PM-1. LC-MS measurements showed that  $2\text{H}^-$ -TNP and product X had the same molecular mass, which suggested that two tautomeric structures of  $2\text{H}^-$ -TNP are present in the reaction mixture. This assumption was proven by  $^1\text{H}$ -NMR measurements, which showed that protonated  $2\text{H}^-$ -TNP exists in two tautomeric forms, the *aci*-nitro and the nitro form, whereas the enamine form was not detected (Fig. 6). The observed product X appeared to be the nitro form. In equilibrium, the estimated concentration ratio of the tautomers was 20:80 (*aci*-nitro:nitro form), determined by HPLC (peak areas at a wavelength of 390 nm). Since the nitro form could not be chemically purified, it was impossible to determine its extinction coefficient. Therefore absolute concentrations could not be calculated and the enzyme activity could not be quantified. As the equilibration rate was shown to be pH-dependent, the time taken to reach the final concentration ratio was measured by following the reaction course by HPLC. The result confirmed that the equilibration



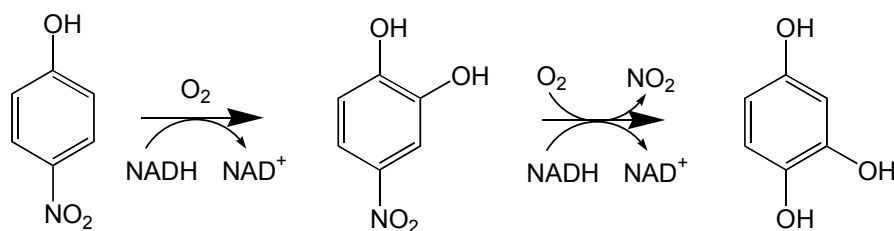


**Fig. 7: Transformation of *p*-nitrophenol to 4-nitrocatechol (27)**

A similar mechanism of nitrite elimination follows an initial vicinal dioxygenation producing a dihydroxy intermediate, observed for 2-nitrotoluene (24) or 2,6-dinitrophenol (12, 37). All described mechanisms have the use of oxygen for nitrite elimination in common. In contrast, TNP because of its high electron deficiency is not attacked by oxygenases, but hydrogenated to 2H<sup>-</sup>-TNP which is the catabolite for nitrite release.

Recently, Ebert et al. described nitrite release from 2H<sup>-</sup>-TNP by an enriched enzyme from *N. simplex* FJ2-1A, which was not fully identified nor characterized (10). In the present work, the described enzyme was purified and evidence was given for the enzyme function.

Turnover of 2H<sup>-</sup>-TNP by crude extracts of *R. (opacus) erythropolis* HL PM-1 or *N. simplex* FJ2-1A yielded H<sup>-</sup>-DNP with a concomitant release of nitrite in stoichiometric amounts, measured photometrically. Behrend and Heesche-Wagner had detected H<sup>-</sup>-DNP formerly with resting cell experiments by *Nocardioides* sp. CB 22-2 during the conversion of TNP (2). In the present studies the nitrite-eliminating activity was isolated by FPLC from cell extracts of *N. simplex* FJ2-1A. Initial purification procedures contained a further step: after native PAGE the gel was stained in a solution containing 1 mM 2H<sup>-</sup>-TNP. The dark yellow band with the nitrite-eliminating enzyme was cut and further separated by SDS-PAGE and blotted on a PDF-membrane. Although pure, the enzyme could not be sequenced, because the N-terminus was chemically blocked in the course of the electrophoresis or blotting procedure, which hindered the attack of phenyl isothiocyanate during the Edman degradation.



Improved growth conditions (2.2.1) promoted protein expression and after anion exchange, ammonium sulfate precipitation, hydrophobic interaction, gel filtration, and centrifugal concentration the enzyme was purified 45-fold to a specific activity of 57 U mg<sup>-1</sup> of protein. SDS-PAGE indicated a purity of >95 % and a molecular weight of 35.3 kDa, which was in agreement with m/z 30.50 kDa, determined by MALDI-TOF measurements. The N-terminus of the nitrite-eliminating enzyme was sequenced and database search showed no similarity to any known protein sequences. Hence, the nitrite-eliminating enzyme is not encoded by any gene of the known gene clusters of *R. (opacus) erythropolis* HL PM-1 or *N. simplex* FJ2-1A.

Authentic 2H<sup>-</sup>-TNP was used as a substrate for the purified nitrite-eliminating enzyme, which was shown to remove a nitro group at the *ortho* position (Fig. 8). Stoichiometric amounts of nitrite were released, quantified by colorimetric tests. Repeated recording of UV-visible spectra showed the conversion of 2H<sup>-</sup>-TNP to the hydride Meisenheimer complex of DNP (H<sup>-</sup>-DNP), which was identified by UV-visible, HPLC, and LC-MS measurements.

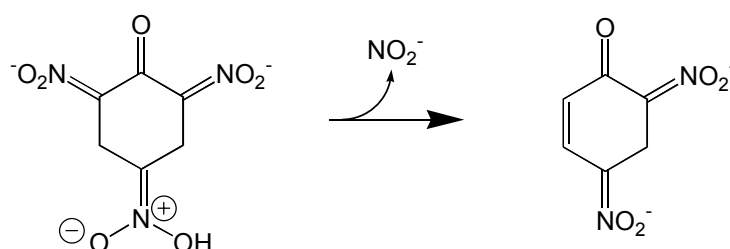


**Fig. 8: Release of nitrite from 2H<sup>-</sup>-TNP by the nitrite-eliminating enzyme.**

The nitrite-eliminating enzyme was specific for 2H<sup>-</sup>-TNP and showed no activity with other hydride complexes of TNP degradation, such as H<sup>-</sup>-TNP or H<sup>-</sup>-DNP. In addition to analyses made by Behrend & Heesche-Wagner (2), H<sup>-</sup>-DNP was synthesized as an authentic standard by reduction of DNP with NaBH<sub>4</sub> at 4 °C. It was generated a stable sodium salt, which was stored at -20°C to avoid disproportionation. The structure of H<sup>-</sup>-DNP was confirmed by LC-MS and NMR spectra.

Since 2H<sup>-</sup>-TNP was shown to be the substrate for the nitrite-eliminating enzyme, it was interesting to know which tautomer, the *aci*-nitro or the nitro form, was catabolized. HPLC measurements revealed, that only the *aci*-nitro form was

converted to H<sup>-</sup>-DNP by the nitrite-eliminating enzyme (Fig. 8). This observation explains the role of the 2H<sup>-</sup>-TNP tautomerase, which is necessary to tautomerize the inert nitro form to the *aci*-nitro form that is further metabolized. This mechanism avoids accumulation of the nitro form as a dead-end product.

## 2.5 Hydrogenation of H<sup>-</sup>-DNP

In the previous chapter H<sup>-</sup>-DNP was shown to be the product of denitration of 2H<sup>-</sup>-TNP. H<sup>-</sup>-DNP is also produced by hydrogenation of 2,4-dinitrophenol (DNP). The HTII is not only specific for TNP, but also possesses activity for DNP. Whereas the HTI did not convert DNP, the HTII hydrogenated DNP, though the carbon ring is less electron deficient than that of TNP. H<sup>-</sup>-DNP was shown to be the common metabolite of the converging pathways of TNP and DNP. However, its fate in further degradation appeared to be unclear.

When Behrend & Heesche-Wagner investigated degradation of picric acid in *Nocardioides* sp. strain CB 22-2, they showed that H<sup>-</sup>-DNP is further transformed at the expense of NADPH (2). Therefore, the authors suggested that *para*-hydroxylation of H<sup>-</sup>-DNP could result in 2-nitrohydroquinone, which means that a Meisenheimer complex is the substrate for a monooxygenase (Fig. 9).

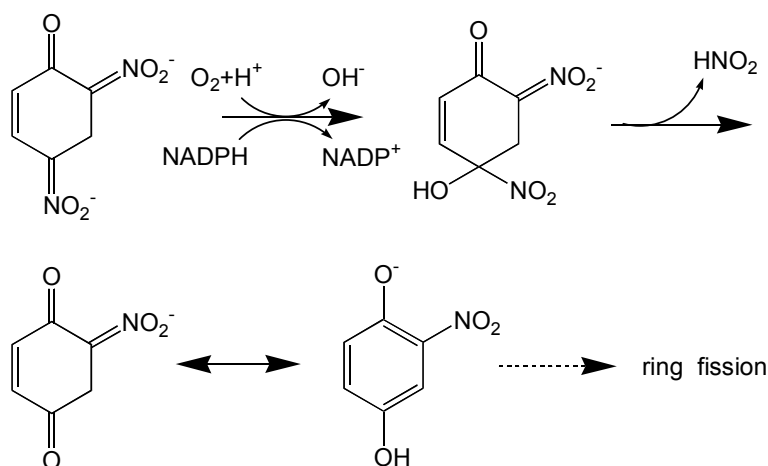
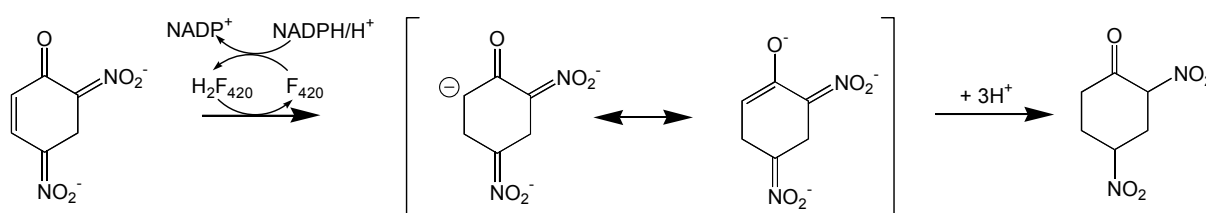


Fig. 9. Hypothetical mechanism for NADPH-dependent conversion of H<sup>-</sup>-DNP (2).

This hypothetical pathway was refuted in the present work. Evidence was given by LC-MS, that the HTI transfers hydride to H<sup>-</sup>-DNP, forming the dihydride  $\sigma$ -complex of DNP (2H<sup>-</sup>-DNP) (Fig. 10). The reaction was also followed by repeated recording of UV-visible spectra, showing the disappearance of H<sup>-</sup>-DNP and a concomitant increase in absorbance at 340 nm. Under physiological conditions 2H<sup>-</sup>-DNP is protonated, yielding 2,4-dinitrocyclohexanone (2,4-DNCH) with a characteristic maximum of absorbance at 340 nm.



**Fig. 10. Hydrogenation of H<sup>-</sup>-DNP by NDFR and HTI, yielding 2,4-DNCH.**

In contrast to the HTIs of *R. (opacus) erythropolis* HL PM-1 and *N. simplex* FJ2-1A, the HTIIs showed no activity with H<sup>-</sup>-DNP.

## 2.6 Hydrolytic ring fission of 2,4-dinitrocyclohexanone

Crude extracts of *R. (opacus) erythropolis* HL PM-1 or *N. simplex* FJ2-1A degraded both, commercially available 2-nitrocyclohexanone (2-NCH) and biologically generated 2,4-DNCH. Both strains were able to grow with 2-NCH as the sole nitrogen source in the medium. Since it was supposed that the carbon ring of the cyclohexanone is cleaved during the reaction, the interesting question was, if ring fission occurred by an oxygenolytic or a hydrolytic mechanism.

Blasco et al. investigated the degradation of DNP in *Rhodococcus* sp. strain RB1 (3). When the authors identified 3-nitroadipate in culture supernatants, they proposed formation of hypothetical Meisenheimer intermediates followed by aerobic *ortho* ring fission, producing 3-nitroadipate (Fig. 11).

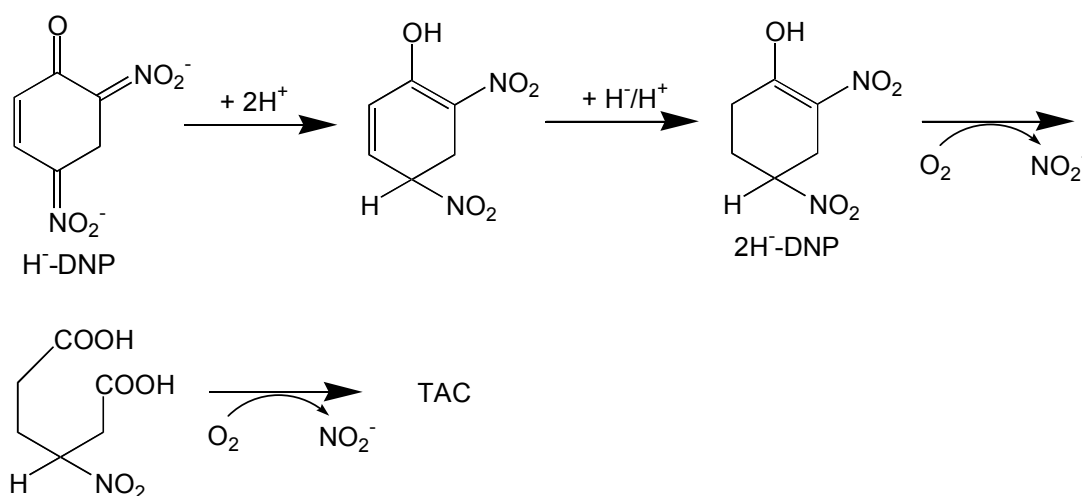


**Fig. 11. Proposed degradation of H-DNP by formation of 3-nitroadipate (3)**

In contrast to this mechanism, Lenke et al. suggested two possible pathways (32): the unproductive conversion of 2H-TNP to 2,4,6-trinitrocyclohexanone, which was chemically hydrolyzed to 1,3,5-trinitropentane after decarboxylation at pH 2. Further, they hypothesized the formation of 2,4-DNCH, followed by hydrolysis yielding 4,6-DNH.

None of these pathways have been confirmed. The only way to find out the real mechanism was the identification of enzymes and metabolites involved in the step of C-C-cleavage. Therefore, cell extracts of *N. simplex* FJ2-1A were subjected to FPLC purification, using 2-NCH as a test substrate. After anion exchange, ammonium sulfate precipitation, hydrophobic interaction, gel filtration, and centrifugal concentration, an enzyme with a purity of >98 % was isolated. MALDI-TOF measurements revealed a molecular mass of 16.989 kDa. Since the molecular weight of the purified enzyme estimated from gel filtration was 63 kDa, it can be assumed that the enzyme consists of four identical subunits. Results of N-terminal amino acid sequencing proved that the gene is located on the known DNA sequence (*orf3*) of *N. simplex* FJ2-1A (9), because the gene product showed 100 % sequence identity. Furthermore, a sequence similarity of 78 % to the N-terminal end of the gene product of *orfF*, which encodes a putative lyase in *R. (opacus) erythropolis* HL PM-1, was found. As the gene product of *orfF* is an enzyme of TNP degradation, the gene was named *npdF*.

Since chemical synthesis of 2,4-DNCH has not been successful, the extinction coefficient could not be calculated. Therefore it was impossible to quantify the enzyme activity. The enzyme function was proven by periodically scanned UV-visible spectra, which showed the disappearance of 2,4-DNCH. Furthermore, HPLC and LC-MS measurements gave evidence that 4,6-dinitrohexanoate (4,6-DNH) is the product of ring fission. The purified enzyme was shown to catalyze hydrolytic ring opening of 2,4-DNCH at the  $\alpha$ -nitro keto grouping and was consequently named 2,4-DNCH hydrolase (Fig. 12). Since 2-NCH was also converted by the 2,4-DNCH hydrolase, it can be assumed that the nitro group in *para* position has no influence on the enzyme substrate interaction.

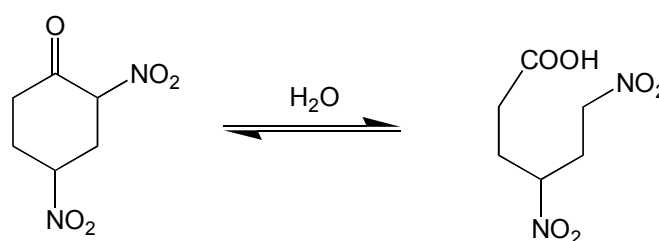


**Fig. 12. Hydrolytic ring fission of 2,4-DNCH by the 2,4-DNCH hydrolase and generation of 4,6-DNH.**

The spontaneous reaction is slow at physiological conditions, but it is accelerated under acidic conditions. Indeed, the ring of 2-NCH was cleaved at pH < 6, whereas the reverse reaction (condensation) was observed at pH > 8. Hydrolysis of 2,4-DNCH was also observed, forming 4,6-DNH spontaneously at low pH values, a reversible reaction which was turned the other way by addition of sodium hydroxide. Therefore, the 2,4-DNCH hydrolase is obviously necessary to ensure effective ring fission for further degradation under physiological conditions.

In all known mechanisms of aerobic breakdown of aromatic compounds, the ring-cleaving step is an oxidative reaction by mono- or dioxygenases. Hydrolytic ring fission was observed so far only in anaerobic bacteria. For instance, cell-free extracts of a fermenting *Clostridium* strain converted resorcinol (1,3-benzenediol) to cyclohexanedione. This is subject to hydrolytic C-C-cleavage, probably by a

nucleophilic attack on one of the carbonyl carbon atoms as shown in Fig. 13 (31), (47).

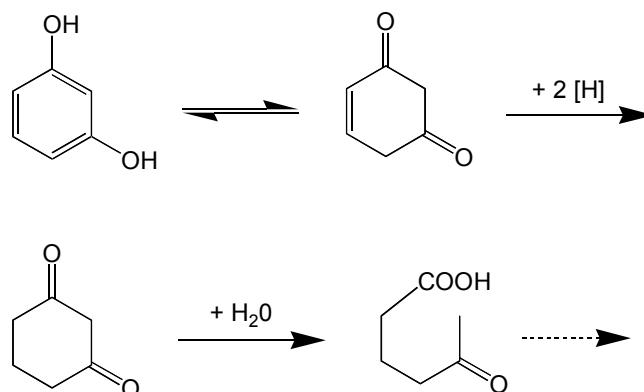


**Fig. 13. Anaerobic degradation of resorcinol by a fermenting *Clostridium* strain (47).**

The present investigation gives evidence, that TNP or DNP utilizing bacteria can degrade 2,4-DNCH by a ring-cleavage mechanism which is typical for anaerobic strains.

HPLC measurements showed that 4,6-DNH was further degraded by crude extract of *R. (opacus) erythropolis* HL PM-1 and *N. simplex* FJ2-1A, which proved that 4,6-DNH is a real metabolite. However, a new product could not be identified by HPLC.

## 2.7 The known pathway and proposed final steps

Fig. 14 summarizes the pathway known so far and shows all enzyme functions characterized in the present work. The enzymes biochemically investigated in the present work are shown in Table 1.

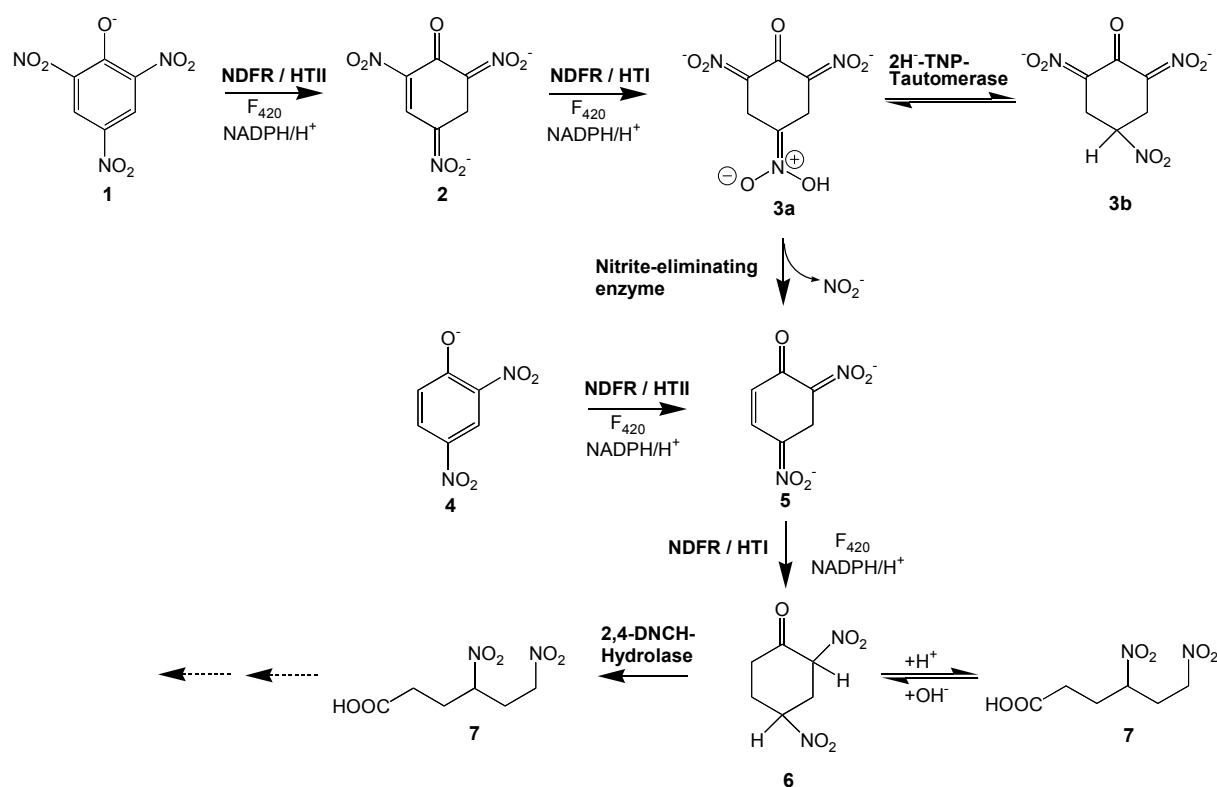


**Fig. 14. Metabolites and enzymes of TNP and DNP degradation by *R. (opacus) erythropolis* HL PM-1 and *N. simplex* FJ2-1A. (1) TNP, (2) H-TNP, (3a) aci-nitro form of 2H-TNP, (3b) nitro form of 2H-TNP, (4) DNP, (5) H-DNP, (6) 2,4-DNCH, (7) 4,6-DNH.**

Though deep insights in the biodegradation of TNP and DNP derived from this work, questions still remain how 4,6-DNH is assimilated. Probably 4,6-DNH is further degraded yielding an acetic acid derivative which can be channeled into the tricarboxylic acid cycle. Therefore, it can be expected that the remaining two nitro groups are cleaved first. There are two possible mechanisms for nitrite elimination. A nitrite-eliminating enzyme as described in section 2.4 can displace nitrite from 4,6-DNH, though no activity was found for this reaction. However, a similar enzyme could use the same mechanism to remove nitrite, implying that no oxygen is needed for degradation. An alternative route can be imagined by oxygenases catalyzing nitrite elimination as shown in Fig. 7. Further experiments conducted under aerobic and anaerobic conditions should elucidate which mechanism is really used.

**Table 1. Enzymes involved in TNP and DNP degradation.**

<b>Enzyme</b>	<b><i>R. (opacus) erythropolis</i> HL PM-1</b>	<b><i>N. simplex</i> FJ2-1A</b>
NDFR (NpdG)	His-tag fusion protein	His-tag fusion protein
HTII (NpdI)	His-tag fusion protein	His-tag fusion protein
HTI (NpdC)	His-tag fusion protein	Overexpressed in <i>E. coli</i> BL21
2H-TNP-Tautomerase (NpdH)	His-tag fusion protein	His-tag fusion protein
Nitrite-eliminating enzyme	Activity in crude extract	Purified by FPLC
2,4-DNCH-Hydrolase (NpdF)	Activity in crude extract	Purified by FPLC

The degradation genes and enzymes of *R. (opacus) erythropolis* HL PM-1 and *N. simplex* FJ2-1A identified here can be useful tools for future research efforts. The unusual catabolic mechanism that distinguishes itself by including initial hydrogenations and a pathway that at least up to the level of ring cleavage does not require oxygen, may open new possibilities for nitroaromatic biodegradation under reduced oxygen supply. It has to be examined whether other polynitroaromatics like TNT are degraded by similar enzymes and mechanisms to make progress in environmental remediation.



### 3 Literature

1. **Altschul, S. F., T. L. Madden, A. A. Schaffer, J. Zhang, Z. Zhang, W. Miller, and D. J. Lipman.** 1997. Gapped BLAST and PSI-BLAST: a new generation of protein database search programs. *Nucleic Acids Res.* **25**:3389-3402.
2. **Behrend, C. and K. Heesche-Wagner.** 1999. Formation of hydride-Meisenheimer complexes of picric acid (2,4,6-trinitrophenol) and 2,4-dinitrophenol during mineralization of picric acid by *Nocardioides* sp. strain CB 22-2. *Appl. Environ. Microbiol.* **65**:1372-1377.
3. **Blasco, R., E. Moore, V. Wray, D. Pieper, K. Timmis, and F. Castillo.** 1999. 3-nitroadipate, a metabolic intermediate for mineralization of 2,4-dinitrophenol by a new strain of a *Rhodococcus* species. *J. Bacteriol.* **181**:149-152.
4. **Bruhn, C., R. C. Bayly, and H. J. Knackmuss.** 1988. The in vivo construction of 4-chloro-2-nitrophenol assimilatory bacteria. *Arch. Microbiol.* **150**:171-177.
5. **Bult, C. J., O. White, G. J. Olsen, and 37 other authors.** 1996. Complete genome sequence of the methanogenic archaeon, *Methanococcus jannaschii*. *Science* **273**:1058-1073.
6. **Buncel, E.** 1982. The chemistry of amino, nitroso, and nitro compounds and their derivatives, p. 1225-1260. John Wiley & Sons, New York.
7. **Dickel, O. and H. J. Knackmuss.** 1991. Catabolism of 1,3-dinitrobenzene by *Rhodococcus* sp. QT-1. *Arch. Microbiol.* **157**:76-79.

8. **Dolon, B. A., E. Razo-Flores, G. Lettinga, and J. A. Field.** 1996. Continuous detoxification, transformation, and degradation of nitrophenols in upflow anaerobic sludge blanket (USAB) reactors. *Biotechnol. Bioeng.* **51**:439-449.
9. **Ebert, S.** 2001. Enzyme, Gene und Mechanismen des oberen Abbauweges von Pikrinsäure und 2,4-Dinitrophenol durch *Nocardioides simplex* FJ2-1A. Ph.D. thesis. University of Stuttgart, Stuttgart, Germany.
10. **Ebert, S., Fischer P., and H. J. Knackmuss.** 2002. Converging catabolism of 2,4,6-trinitrophenol (picric acid) and 2,4-dinitrophenol by *Nocardioides simplex* FJ2-1A. *Biodegradation* **12**:367-376.
11. **Ebert, S., P. G. Rieger, and H. J. Knackmuss.** 1999. Function of coenzyme F<sub>420</sub> in aerobic catabolism of 2,4,6-trinitrophenol and 2,4-dinitrophenol by *Nocardioides simplex* FJ2-1A. *J. Bacteriol.* **181**:2669-2674.
12. **Ecker, S., T. Widmann, H. Lenke, Dickel O., Fischer P., C. Bruhn, and H. J. Knackmuss.** 1992. Catabolism of 2,6-dinitrophenol by *Alcaligenes eutrophus* JMP 134 and JMP 222. *Arch. Microbiol.* **158**:149-154.
13. **Elvers, B., S. Hawkins, and G. Schulz.** 1991. Ullmann's Encyclopedia of Industrial Chemistry. Verlag Chemie, Weinheim.
14. **Esteve-Nunez, A., A. Caballero, and J. L. Ramos.** 2001. Biological degradation of 2,4,6-trinitrotoluene. *Microbiol. Mol. Biol. Rev.* **65**:335-52.
15. **Falbe, J. and M. Regitz.** 1999. Römpp Lexikon Chemie. Georg Thieme Verlag, Stuttgart, New York.

16. **Germanier, R. and K. Wuhrmann.** 1963. Über den aeroben mikrobiellen Abbau aromatischer Nitroverbindungen. *Path. Microbiol.* **26**:569-578.
17. **Gold, V., A. Y. Miri, and S. R. Robinson.** 1980. Sodium borohydride as a reagent for nucleophilic aromatic substitution by hydrogen: the role of hydride Meisenheimer adducts as reaction intermediates. *J. Chem. Soc. Perkin Trans. II* 243-249.
18. **Groenewegen, P. E., P. Breeuwer, J. M. van Helvoort, A. A. Langenhoff, F. P. de Vries, and J. A. de Bont.** 1992. Novel degradative pathway of 4-nitrobenzoate in *Comamonas acidovorans* NBA-10. *J. Gen. Microbiol.* **138**:1599-1605.
19. **Groenewegen, P. E., J. A. M. de Bont, and P. E. J. de Bont.** 1992. Degradation of 4-nitrobenzoate via 4-hydroxylaminobenzoate and 3,4-dihydroxybenzoate in *Comamonas acidovorans* NBA-10. *Arch. Microbiol.* **158**:381-386.
20. **Gundersen, K. and H. L. Jensen .** 1956. A soil bacterium decomposing organic nitrocompounds. *Acta Agric. Scand.* **6**:100-114.
21. **Haigler, B. E., S. F. Nishino, and J. C. Spain.** 1994. Biodegradation of 4-methyl-5-nitrocatechol by *Pseudomonas* sp. strain DNT. *J. Bacteriol.* **176**:3433-3437.
22. **Haigler, B. E. and J. C. Spain .** 1993. Biodegradation of 4-nitrotoluene by *Pseudomonas* sp. strain 4NT. *Appl. Environ. Microbiol.* **59**:2239-2243.

23. **Haigler, B. E., W. C. Suen, and J. C. Spain.** 1996. Purification and sequence analysis of 4-methyl-5-nitrocatechol oxygenase from *Burkholderia* sp. strain DNT. *J. Bacteriol.* **178**:6019-6024.
24. **Haigler, B. E., W. H. Wallace, and J. C. Spain.** 1994. Biodegradation of 2-nitrotoluene by *Pseudomonas* sp. strain JS42. *Appl. Environ. Microbiol.* **60**:3466-3469.
25. **Heiss, G., K. W. Hofmann, N. Trachtmann, D. M. Walters, P. Rouviere, and H. J. Knackmuss.** 2002. *npd* gene functions of *Rhodococcus (opacus) erythropolis* HL PM-1 in the initial steps of 2,4,6-trinitrophenol degradation. *Microbiology* **148**:799-806.
26. **Jensen, H. L. and G. Lautrup-Larsen.** 1967. Microorganisms that decompose nitroaromatic compounds, with special reference to dinitro-*ortho*-cresol. *Acta Agric. Scand.* **17**:115-126.
27. **Kadiyala, V. and J. C. Spain.** 1998. A two-component monooxygenase catalyzes both the hydroxylation of p-nitrophenol and the oxidative release of nitrite from 4-nitrocatechol in *Bacillus sphaericus* JS905. *Appl. Environ. Microbiol.* **64**:2479-2484.
28. **Kaplan, L. A. and A. R. Siedle .** 1971. Studies in boron hydrides. IV. Stable hydride Meisenheimer adducts. *J. Org. Chem.* **36**:937-939.
29. **Katsivela, E., V. Wray, D. H. Pieper, and R. M. Wittich.** 1999. Initial reactions in the biodegradation of 1-chloro-4-nitrobenzene by a newly isolated bacterium, strain LW1. *Appl. Environ. Microbiol.* **65**:1405-1412.

30. **Klenk, H. P., R. A. Clayton, J. F. Tomb & 22 other authors.** 1997. The complete genome sequence of the hyperthermophilic, sulphate-reducing archaeon *Archaeoglobus fulgidus*. *Nature* **390**:364-370.
31. **Kluge, C., A. Tschech, and G. Fuchs.** 1990. Anaerobic metabolism of resorcylic acids (*m*-dihydroxybenzoic acids) and resorcinol (1,3-benzenediol) in a fermenting and in a denitrifying bacterium. *Arch. Microbiol.* **155**:68-74.
32. **Lenke, H., C. Achtnich, and H. J. Knackmuss.** 2000. Perspectives of bioelimination of polynitroaromatic compounds, p. 91-126. *In* J. C. Spain, J. B. Hughes, and H. J. Knackmuss (eds.), *Biodegradation of nitroaromatic compounds and explosives*. Lewis Publishers, Boca Raton.
33. **Lenke, H. and H. J. Knackmuss.** 1992. Initial hydrogenation during catabolism of picric acid by *Rhodococcus erythropolis* HL 24-2. *Appl. Environ. Microbiol.* **58**:2933-2937.
34. **Lenke, H. and H. J. Knackmuss.** 1996. Initial hydrogenation and extensive reduction of substituted 2,4-dinitrophenols. *Appl. Environ. Microbiol.* **62**:784-790.
35. **Meulenberg, R., M. Pepi, and J. A. de Bont.** 1996. Degradation of 3-nitrophenol by *Pseudomonas putida* B2 occurs via 1,2,4-benzenetriol. *Biodegradation* **7**:303-311.
36. **Nadeau, L. J. and J. C. Spain.** 1995. Bacterial degradation of *m*-nitrobenzoic acid. *Appl. Environ. Microbiol.* **61**:840-843.

37. **Nishino, S. F., G. C. Paoli, and J. C. Spain.** 2000. Aerobic degradation of dinitrotoluenes and pathway for bacterial degradation of 2,6-dinitrotoluene. *Appl. Environ. Microbiol.* **66**:2139-2147.
38. **Nishino, S. F. and J. C. Spain.** 1995. Oxidative pathway for the biodegradation of nitrobenzene by *Comamonas* sp. strain JS765. *Appl. Environ. Microbiol.* **61**:2308-2313.
39. **Rajan, J., K. Valli, R. E. Perkins, F. S. Sariaslani, S. M. Barns, A. L. Reysenbach, S. Rehm, M. Ehringer, and N. R. Pace.** 1996. Mineralization of 2,4,6-trinitrophenol (picric acid): characterization and phylogenetic identification of microbial strains. *J. Ind. Microbiol.* **16**:319-324.
40. **Rhys-Williams, W., S. C. Taylor, and P. A. Williams.** 1993. A novel pathway for the catabolism of 4-nitrotoluene by *Pseudomonas*. *J. Gen. Microbiol.* **139**:1967-1972.
41. **Rieger, P. G.** 1996. University of Stuttgart. Aerober Abbau von 2,4,6-Trinitrophenol und Strukturanaloga durch *Rhodococcus erythropolis*: Die Rolle der H<sup>-</sup>- $\sigma$ -Komplexbildung. Ph.D. thesis. University of Stuttgart, Stuttgart, Germany.
42. **Rieger, P. G., V. Sinnwell, A. Preuss, W. Francke, and H. J. Knackmuss.** 1999. Hydride-Meisenheimer complex formation and protonation as key reactions of 2,4,6-trinitrophenol biodegradation by *Rhodococcus erythropolis*. *J. Bacteriol.* **181**:1189-1195.

43. **Russ, R., D. M. Walters, H. J. Knackmuss, and P. E. Rouviere.** 2000. Identification of genes involved in picric acid and 2,4-dinitrophenol degradation by mRNA differential display, p. 127-143. *In* J. C. Spain, J. B. Hughes, and H. J. Knackmuss (eds.), Biodegradation of nitroaromatic compounds and explosives. Boca Raton, Fla.
44. **Schäfer, A., H. Harms, and A. J. B. Zehnder.** 1996. Biodegradation of 4-nitroanisole by two *Rhodococcus* spp. *Biodegradation* **7**:249-255.
45. **Schenzle, A., H. Lenke, Fischer P., P. A. Williams, and H. J. Knackmuss.** 1997. Catabolism of 3-nitrophenol by *Ralstonia eutropha* JMP134. *Appl. Environ. Microbiol.* **63**:1421-1427.
46. **Schenzle, A., H. Lenke, J. C. Spain, and H. J. Knackmuss.** 1999. Chemoselective nitro group reduction and reductive dechlorination initiate degradation of 2-chloro-5-nitrophenol by *Ralstonia eutropha* JMP134. *Appl. Environ. Microbiol.* **65**:2317-2323.
47. **Schink, B., B. Philipp, and J. Muller.** 2000. Anaerobic degradation of phenolic compounds. *Naturwissenschaften* **87**:12-23.
48. **Severin, T. and M. Adam.** 1963. Umsetzung von Nitroaromaten mit Borhydrid II. *Chem. Ber.* **96**:448-452.
49. **Severin, T. and R. Schmitz.** 1962. Umsetzung von Nitroaromaten mit Natriumborhydrid. *Chem. Ber.* **95**:1417-1419.

50. **Smith, D. R., L.A. Doucette-Stamm, C. Deloughery & 22 other authors.** 1997. Complete genome sequence of *Methanobacterium thermoautotrophicum* deltaH: functional analysis and comparative genomics. *J. Bacteriol.* **179**:7135-7155.
51. **Spain, J. C. and D. T. Gibson.** 1991. Pathway of biodegradation of *p*-nitrophenol in *Moraxella* sp. *Appl. Environ. Microbiol.* **57**:812-819.
52. **Spain, J. C., J. B. Hughes, and H. J. Knackmuss.** 2000. Biodegradation of nitroaromatic compounds and explosives. Lewis Publishers, Boca Raton, Fla.
53. **Spain, J. C., O. Wyss, and D. T. Gibson.** 1979. Enzymatic oxidation of *p*-nitrophenol. *Biochem. Biophys. Res. Comm.* **88**:634-641.
54. **Trachtmann, N.** 2003. Personal Communication.
55. **Tsukamura, M.** 1960. Enzymatic reduction of picric acid. *J. Biochem.* **48**:662-671.
56. **Uberoi, V. and S. K. Bhattacharya.** 1997. Toxicity and degradeability of nitrophenols in anaerobic systems. *Water Environmental Research* **69**:146-156.
57. **Vorbeck, C., H. Lenke, P. Fischer, and H. J. Knackmuss.** 1994. Identification of a hydride-Meisenheimer complex as a metabolite of 2,4,6-trinitrotoluene by a *Mycobacterium* strain. *J. Bacteriol.* **176**:932-934.



- 
58. **Vorbeck, C., H. Lenke, P. Fischer, J. C. Spain, and H. J. Knackmuss.** 1998. Initial reductive reactions in aerobic microbial metabolism of 2,4,6-trinitrotoluene. *Appl. Environ. Microbiol.* **64**:246-252.
  59. **Walters, D. M., R. Russ, H. J. Knackmuss, and P. E. Rouviere.** 2001. High-density sampling of a bacterial operon using mRNA differential display. *Gene* **273**:305-315.
  60. **Zeyer, J. and P. C. Kearney.** 1984. Degradation of *o*-nitrophenol and *m*-nitrophenol by *Pseudomonas putida*. *J. Agric. Food Chem.* **32**:238-242.
  61. **Zeyer, J. and H. P. Kocher.** 1988. Purification and characterization of a bacterial nitrophenol oxygenase which converts ortho-nitrophenol to catechol and nitrite. *J. Bacteriol.* **170**:1789-1794.

## Appendix 1

# ***npd* Gene Functions of *Rhodococcus opacus* HL PM-1 in the Initial Steps of 2,4,6-Trinitrophenol Degradation**

Published in Microbiology, 2002, 148, p. 799-806

**Gesche Heiss<sup>1</sup>, Klaus W. Hofmann<sup>1</sup>, Natalie Trachtmann<sup>1</sup>,  
Dana M. Walters<sup>2</sup>, Pierre Rouvière<sup>2</sup> and Hans-Joachim, Knackmuss<sup>1</sup>**

<sup>1</sup> Institute of Microbiology, University of Stuttgart, Allmandring 31, 70550 Stuttgart, Germany

<sup>2</sup> DuPont de Nemours Company, Wilmington, Delaware, USA

Author for correspondence: Gesche Heiss. Tel: +49 711 685 5489. Fax: +49 711 685 5725. e-mail: [gesche.heiss@po.uni-stuttgart.de](mailto:gesche.heiss@po.uni-stuttgart.de)

## Summary

*Rhodococcus (opacus) erythropolis* HL PM-1 grows on 2,4,6-trinitrophenol (picric acid) or 2,4-dinitrophenol (2,4-DNP) as sole nitrogen source. A gene cluster involved in picric acid degradation was recently identified. The functional assignment of three of its genes, *npdC*, *npdG*, and *npdI*, and the tentative functional assignment of a fourth one, *npdH*, is reported. The genes were expressed in *Escherichia coli* as His-tag fusion proteins that were purified by Ni-affinity chromatography. The enzyme activity of each protein was determined by spectrophotometry and HPLC analyses. NpdI, a hydride transferase, catalyses a hydride transfer from reduced  $F_{420}$  to the aromatic ring of picric acid, generating the hydride  $\sigma$ -complex (hydride Meisenheimer complex) of picric acid ( $H^-$ -PA). Similarly, NpdI also transformed 2,4-DNP to the hydride  $\sigma$ -complex of 2,4-DNP. A second hydride transferase, NpdC catalysed a subsequent hydride transfer to  $H^-$ -PA, to produce a dihydride  $\sigma$ -complex of picric acid ( $2H^-$ -PA). All three reactions required the activity of NpdG, an NADPH-dependent  $F_{420}$  reductase, for shuttling the hydride ions from NADPH to  $F_{420}$ . NpdH converted  $2H^-$ -PA to a hitherto unknown product, X. The results show that *npdC*, *npdG* and *npdI* play a key role in the initial steps of picric acid degradation, and that *npdH* may prove to be important in the later stages.

### Abbreviations:

$H^-$ -PA, hydride  $\sigma$ -complex of picric acid; 2,4-DNP, 2,4-dinitrophenol;  $H^-$ -2,4-DNP, hydride  $\sigma$ -complex of 2,4-dinitrophenol;  $2H^-$ -PA, dihydride  $\sigma$ -complex of picric acid

## Introduction

Nitrophenols such as 2,4-dinitrophenol (2,4-DNP) and 2,4,6-trinitrophenol (picric acid) have been introduced into the environment through their use as explosives, synthetic intermediates, dyes and pesticides (Nishino *et al.*, 2000; Spain, 2000). Although several bacteria exist which mineralize these compounds (Behrend & Heesche-Wagner, 1999; Blasco *et al.*, 1999; Ebert *et al.*, 1999; Hess *et al.*, 1990; Lenke *et al.*, 1992; Rajan *et al.*, 1996), their general recalcitrance (Lenke *et al.*, 2000) and toxic properties pose a threat to the environment (Aguirre *et al.*, 1993; Andres *et al.*, 1996; Linsinger *et al.*, 1999). Hence, although the bacterial biodegradation of nitrophenols has been studied for a long time, we need to deepen our understanding of the enzymes involved, particularly in the catabolism of polynitrophenols. This will increase the possibilities of finding simple biotechnological measures to remove nitrophenols from industrial waste streams or contaminated soil.

Picric acid and 2,4-DNP are degraded by an initial reductive attack on the aromatic ring (Lenke *et al.*, 1992; Lenke & Knackmuss, 1992). The orange-red hydride  $\sigma$ -complex of picric acid ( $H^-$ -PA, or hydride Meisenheimer complex of picric acid) is the first metabolite produced during mineralization of picric acid by *Rhodococcus (opacus) erythropolis* HL PM-1 (Lenke *et al.*, 1992; Lenke & Knackmuss, 1992; Lenke & Knackmuss, 1996; Rieger *et al.*, 1999). However, because of the difficulty in lysing the cells, the enzymes involved have, until now, remained unknown.

*Nocardioides simplex* FJ2-1A was shown to contain a hydride transferase (HTES, or hydride transferring enzyme system) involved in the hydride transfer to the aromatic ring of picric acid, giving rise to  $H^-$ -PA (Ebert *et al.*, 1999). The HTES also catalyses a second hydride transfer, converting  $H^-$ -PA to the dihydride  $\sigma$ -complex of picric acid ( $2H^-$ -PA; Ebert *et al.*, 2002). Both hydride transfer reactions require the NADPH-dependent  $F_{420}$  reductase (previously referred to as component A) as an electron shuttle from NADPH to  $F_{420}$ .

Recently, a gene cluster of about 12.5 kb, involved in picric acid degradation, was identified in *R. (opacus) erythropolis* HL PM-1 using differential display and sequenced (Russ *et al.*, 2000; Walters *et al.*, 2001). We have named these genes *npd* for nitrophenol degradation. Our goal was to determine the function of *npdC* (previously ORF3), *npdG* (previously ORF7), *npdH* (previously undetected) and *npdI* (previously ORF8) by overexpressing the genes in *Escherichia coli*. Herewith, we have proven that the genes encode enzymes involved in picric acid catabolism.

## Methods

### Bacterial strains, plasmids and bacterial culture.

Strains and plasmids used are listed in Table 1. Recombinant *E. coli* strains were grown at 37°C in Luria-Bertani (LB) medium supplemented with ampicillin (100 µg/ml). For gene expression, overnight cultures of *E. coli* JM109 (pNTG3), *E. coli* JM109 (pNTG6), *E. coli* BL21 (DE3)(pNTG11) or *E. coli* TOP10 (pDMW10) were inoculated into LB and incubated for 1.5-3 h at 37°C. The cultures were induced for 4-5 h at 30°C with IPTG (1 mM) for *E. coli* TOP10 (pDMW10) or *E. coli* BL21 (pNTG11), and with L-rhamnose (0.2% w/v) for *E. coli* JM109 (pNTG6) and *E. coli* JM109 (pNTG3). *R. (opacus) erythropolis* HL PM-1 was grown at 30°C in 50 mM KH<sub>2</sub>PO<sub>4</sub>/Na<sub>2</sub>HPO<sub>4</sub> buffer (pH 7.4) containing 45 mM CaCl<sub>2</sub>, 50 mM acetate and mineral salts solution (Dorn *et al.*, 1974), modified by adding 0.5 mM 2,4-DNP or 0.7 mM picric acid instead of (NH<sub>4</sub>)<sub>2</sub>SO<sub>4</sub>.

### Molecular techniques.

Standard protocols were used for manipulation of DNA (Ausubel *et al.*, 2001; Sambrook *et al.*, 1989). Plasmid DNA was isolated using the FlexiPrep Kit (Amersham Pharmacia Biotech). *E. coli* was transformed according to Inoue *et al.* (1990). Sequencing was performed by MWG Biotech AG (Ebersberg).

### Fatty acid and mycolic acid analyses.

Fatty acid analysis and analysis of mycolic acids were performed by the DSMZ GmbH (Braunschweig, Germany).

### Sequence comparisons and database searches.

Pairwise sequence comparisons and database searches were carried out using Blastn, Blastp, Blastx and NCBI ORFfinder software (Altschul *et al.*, 1990; Tatusova & Madden, 1999). Translations were achieved using the Translation Machine from the EMBL Outstation European Bioinformatics Institute. Conserved motif searches were performed using the programs CD-search, Pfam, Proscan and Block

(<http://www.ncbi.nlm.nih.gov/Structure/cdd/wrpsb.cgi>; <http://www.sanger.ac.uk>;  
[http://npsa-pbil.ibcp.fr/cgi-bin/pattern\\_prosite.pl](http://npsa-pbil.ibcp.fr/cgi-bin/pattern_prosite.pl); [http://blocks.fhcrc.org/blocks-bin/blocks\\_search](http://blocks.fhcrc.org/blocks-bin/blocks_search)).

**Table 1. *Escherichia coli* strains and plasmids used**

Bacterial strain/plasmid	Genotype/phenotype	Reference/source
<b><i>E. coli</i> strain</b>		
JM109	<i>endA1 recA1 gyrA96 thi hsdR17</i> ( $r_K, m_K^+$ ) <i>relA1 supE44</i> $\lambda^- \Delta(lac-proAB)(F' traD36$ <i>proAB lac^Z \Delta M15) \lambda^-</i>	Yanisch-Perron <i>et al.</i> (1985)
TOP10	$F^- mcrA \Delta(mrr-hsdRMS-mcrBC)$ 80 <i>dlac \Delta M15 \Delta lacX74 deoR recA1 araD139</i> $\Delta(ara-leu)7697 galU galK rpsL (strR) endA1$ <i>nupG</i>	Invitrogen
BL21 (DE3)	$F^- ompT hsdS$ ( $r_B, m_B^-$ ) <i>gal</i> ( $\lambda clts857 ind1$ <i>sam7 nin5 lacUV5-T7 gene 1</i> )	Calbiochem-Novabiochem
<b>Plasmid</b>		
pTrcHis2-TOPO	$Ap^r$ ; $P_{tre}$ ; ColE1 origin; C-terminal tag containing six polyhistidine residues and <i>myc</i> epitope	Invitrogen
pBAD/Thio-TOPO	$Ap^r$ ; $P_{araBAD}$ ; ColE1 origin; C-terminal tag containing six polyhistidine residues and V5 epitope; His-Patch thioredoxin as an N- terminal fusion partner	Invitrogen
pJoe2702	$Ap^r$ ; $P_{rhaBAD}$ ; ColE1 origin	Stump <i>et al.</i> (2000)
pBW22	$Ap^r$ ; $P_{rhaBAD}$ ; ColE1 origin; C-terminal tag containing six polyhistidine residues	Wilms <i>et al.</i> (2001)
pQE-30	$Ap^r$ ; phage T5 promoter; ColE1 origin; N- terminal tag containing six polyhistidine residues	Qiagen
pET11a*	$Ap^r$ ; phage T7 promoter; ColE1 origin; contains a polylinker with additional restriction sites: <i>SmaI</i> , <i>KpnI</i> , <i>XhoI</i> , <i>Sall</i> .	Calbiochem-Novabiochem
pDMW10	PCR fragment containing <i>npdG</i> in pTrcHis2- TOPO	This work
pNTG3	<i>NdeI/HindIII</i> fragment containing <i>npdI</i> and His-tag from pQE-30 in pJoe2702	This work
pNTG6	<i>NdeI/HindIII</i> fragment containing <i>npdC</i> and His-tag from pBAD/Thio-TOPO in pJoe2702	This work
pNTG11	<i>NdeI/HindIII</i> fragment containing <i>npdH</i> and His-tag from pBW22 in pET11a	This work

### Cloning and expression of *npdC*, *npdG*, *npdH* and *npdI*.

*npdI* was amplified from *R. (opacus) erythropolis* HL PM-1 chromosomal DNA with specific primers. Primer P63 was designed with a *Bam*H1 site (underlined) 5'-GGATCCATGATCAAAGGCAT 3' and primer P68 was designed with a *Hind*III site (underlined) 5'-GCCTGCGTGCAAAGCTTTCATGCG 3'. Following digestion with *Bam*H and *Hind*III, the resulting PCR product was ligated into the expression vector pQE-30 to yield plasmid pDMW4. *npdC* was amplified with primers P33 (5'-ATGAAGGTCGGAATCAGGAT-3') and P34 (5'-GGGCAGGTTGTGTGCGGTGG-3'). The resulting PCR product was cloned into the pBAD/topo thio fusion expression system (Invitrogen) to yield pDMW7. *npdG* was amplified with primers P56 (5'-ATGAAGAGCAGCAAGATCGC-3') and P57 (5'-CGCAGCTCGTGGATCATGAA-3'). The resulting PCR product was cloned into pTrcHis2-topo (Invitrogen) to yield pDMW10.

For expression, the *npdC* and *npdI* genes were amplified from pDMW7 and pDMW4, respectively. Primers were designed to incorporate *Nde*I and *Hind*III (underlined), and the His-tag sequence at the 3' end of *npdC* (5'-TTT TCA TAT GAA GGT CGG AAT CAG GAT CC-3' and 5'-TTT AAG CTT TCA ATG GTG ATG GTG ATG ATG-3') and the 5' end of *npdI* (5'-CGT CAT ATG AGA GGA TCG CAT CAC CAT CAC-3' and 5'-CCC AAG CTT GGG TCA TGC GAG CTC CGG CAG GAC-3').

*npdH* was cloned into pBW22 by amplification, the primers being designed to contain *Nde*I and *Bam*HI sites (underlined) (5'-TTT TCA TAT GAT CCA CGA GCT GCG-3' and 5'-TTT TGG ATC CGG AGC GGG CGT ATG AC-3'). Subsequently, *npdH* was subcloned from pBW22 (including the His-tag) into pET11a\*: pBW22 containing *npdH* was cut with *Nde*I and *Hind*III. The *Hind*III site was filled in with DNA polymerase I (large Klenow fragment; NEB) to create a blunt end and ligated into pEt11a\* (*Nde*I/*Sma*I).

The PCR reaction mixtures contained 1 ng template DNA, 0.5 U Vent polymerase (New England Biolabs), 2 mM MgSO<sub>4</sub>, 4% DMSO, 0.2 mM of each dNTP and 50 pmol of each primer. Twenty-five amplification cycles were performed as follows:



95°C 30 s, 55°C 40 s, 72°C 1 min 40s. Primers were purchased from MWG Biotech. PCR fragments were eluted from agarose using an Easypure DNA purification kit (Biozym Diagnostics), restricted with the appropriate restriction enzymes and ligated into the vector (Table 1).

### **Preparation of cell extracts and SDS-PAGE.**

Cells suspended in 50 mM  $\text{KH}_2\text{PO}_4/\text{K}_2\text{HPO}_4$  (pH 7.8) plus imidazole (5mM) were lysed with a French press (Aminco) at 80 MPa. Cell debris was removed by centrifugation at 100.000 g for 45 min at 4°C. The protein concentration was determined by the method of Bradford (1976) using a dye reagent concentrate (Bio-Rad protein assay). Bovine serum albumin served as the standard. SDS-PAGE was performed by the method of Laemmli (1970) on a Mini-PROTEAN II electrophoresis cell (Bio-Rad).

### **Purification of His-tag fusion proteins.**

His-tag fusion proteins were purified by Ni-NTA metal affinity chromatography (Qiagen), as described by the manufacturer. Fractions were tested for enzyme activity. Purified fractions were desalted by utilizing pD10 Desalting Columns (Amersham Pharmacia Biotech) and subsequently concentrated with a Vivaspin 2 ml concentrator (Sartorius).

### **Determination of the Concentration of $F_{420}$ .**

$F_{420-2}$ , purified from *Methanobacterium thermoautotrophicum* using a QAE column, was obtained from Lacy Daniels (Peck, 1989). The lyophilized powder was dissolved in 50 mM Tris, pH 7.5 and the absorbance determined at 420 nm. The concentration was calculated using an extinction coefficient of  $41400 \text{ M}^{-1} \text{ cm}^{-1}$  (Purwantini & Daniels, 1996).

### **Enzyme assays and kinetic measurements.**

Enzyme assays and kinetic assays were performed with a Varian Cary 50 Biospectrophotometer controlled by Cary WinUV Biopackage software. All enzyme

reactions were done in a total volume of 1 ml. The enzyme activity of NpdG in standard tests was measured in citrate-phosphate buffer (50 mM, pH 5.5) containing 10-100  $\mu\text{M}$  NADPH, 10  $\mu\text{M}$   $F_{420}$  and 0.25  $\mu\text{g}$  enzyme. The decrease in absorbance was monitored at 400 nm. The  $K_m$  constant and  $V_{\text{max}}$  were determined for NpdG only. Reaction rates were calculated by taking an extinction coefficient of  $25700 \text{ M}^{-1} \text{ cm}^{-1}$  (Eirich *et al.*, 1978). One unit of enzyme activity was taken as the amount of enzyme which converts 1  $\mu\text{mol}$  of  $F_{420} \text{ min}^{-1}$ . For determination of the  $K_m$  constant, the concentration of  $F_{420}$  was varied from 2 to 35  $\mu\text{M}$ . The  $K_m$  and  $V_{\text{max}}$  values for  $F_{420}$  were calculated by using Sigma Plot for Windows, version 5.00 (SPSS).

Enzyme activities of NpdC, NpdH and NpdI were detected by repeated recording of UV-visible spectra (280 – 600 nm). Spectra were recorded every minute. Reactions with NpdC and NpdI were performed in 50 mM  $\text{KH}_2\text{PO}_4/\text{K}_2\text{HPO}_4$ , pH 7.8, containing 125  $\mu\text{M}$  NADPH, 11  $\mu\text{M}$   $F_{420}$ , 100  $\mu\text{M}$  substrate (picric acid, H<sup>-</sup>-PA or 2,4-DNP), 5  $\mu\text{g}$  NpdG, and 30  $\mu\text{g}$  NpdI or NpdC. The first recording was performed in buffer containing  $F_{420}$  and NADPH only. After addition of NpdG, the second spectrum was recorded. The reaction was then commenced by the addition of NpdI or NpdC. Testing for enzyme activities in the absence of  $F_{420}$  or NADPH served as negative controls. Reactions with NpdH were performed in 50 mM  $\text{KH}_2\text{PO}_4/\text{K}_2\text{HPO}_4$ , pH 7.8, containing 100  $\mu\text{M}$  2H<sup>-</sup>-PA and 30  $\mu\text{g}$  NpdH.

### HPLC analyses.

Metabolites were detected by means of HPLC (Chromeleon Chromatography Data Systems 4.30, equipped with a Dionex UV/Vis detector UVD 170S/340S, a Dionex pump, P 580, and a Dionex autosampler, Gina50). Samples were resolved on Gromsil 100 Octyl-4 columns (125 x 4 mm or 250 x 4 mm, particle size 5  $\mu\text{m}$ ; Grom) using 30 or 40% (v/v) methanol, respectively, plus 5 mM PicA (tetrabutylammonium hydrogensulfate), pH 7.8, as the mobile phase. The precolumn was a Gromsil 100 Octyl-4 column (20 x 4 mm particle size 5  $\mu\text{m}$ ; Grom). Enzyme reactions were terminated by freezing samples in liquid nitrogen prior to HPLC analysis.

### Mass spectra.

Liquid chromatography (LC) mass spectra were obtained by negative-mode electrospray ionization (ESI) on a high performance liquid chromatograph (Dionex P580A HPG) with a Dionex diode array detector, DAD 340, coupled to a TSQ 7000 mass spectrometer. Metabolites were resolved on an LC column [Luna RP18(2); Phenomenex; 3 $\mu$ , 150mm x 2.1mm] cooled to 15°C by a Dionex column oven, STH 585. The initial mobile phase comprised 4% (v/v) acetonitrile / 0.0005% (v/v) ammonia which was maintained at a flow rate of 250  $\mu$ l min<sup>-1</sup> for 3 min. The percentage of acetonitrile was then linearly increased to 50% (v/v) over a time period of 8 min and sustained for 1 min. Finally, the gradient was linearly decreased to 4% (v/v) within 1 min and maintained for 6 min.

### Chemicals.

H<sup>-</sup>PA was synthesized as described previously with modifications (Rieger *et al.*, 1999). Picric acid (650 mg; lyophilized) was dissolved in 7 ml absolute acetonitrile. Subsequently, tetramethylammonium octahydridotriborate (345 mg, dissolved in 7 ml absolute acetonitrile) was added to the picric acid/acetonitrile solution under argon as a protective atmosphere at -20°C. The precipitating dark powdery crystals were filtered through a sintered glass filter, followed by washing with ice cold, absolute acetonitrile and finally dried in a vacuum (Christ Alpha I-5). 2H<sup>-</sup>PA was prepared according to Severin & Schmitz (1962).

## Results

### Reclassification of strain HL PM-1

Fatty acid and mycolic acid analyses (chain length of 48-54 carbon atoms) of *R. erythropolis* HL PM-1 suggest that it should be reclassified as *Rhodococcus opacus*. The almost complete 16S rDNA sequence of strain HL PM-1 (accession no. AF435009) was obtained and showed 99% sequence identity to the 16S rRNA gene of *R. opacus* strain 1CP and *R. opacus* strain GM-29. The first 500 bp revealed 99% sequence identity to *R. opacus* RB1 (Blasco *et al.*, 1999) and the type strain *R. opacus* DSM 43205 (Klatte *et al.*, 1994). Hence, we propose that *R. erythropolis* HL PM-1 should be reclassified as *R. opacus* HL PM-1.

### Expression of *npdC*, *npdG*, *npdH* and *npdI*

All genes were expressed as His-tag fusion proteins (Table 1). *npdG* was cloned into pTrcHis2-TOPO and the resulting recombinant plasmid was designated pDMW10. In induced cultures of *E. coli* TOP10 (pDMW10), the enzyme constituted approximately 20% of the total cellular protein as estimated by SDS-PAGE. In non-induced cultures, no protein band of the expected size was detectable. Hence, NpdG was purified from *E. coli* TOP10 (pDMW10).

*npdC* and *npdI* were originally cloned into pBAD/Thio-TOPO and pQE-30, respectively. Recombinant cells carrying *npdC* or *npdI* in pBAD/Thio-TOPO or pQE-30 contained a substantial amount of inclusion bodies. Hence, *npdC* and *npdI* were amplified from the respective vectors and ligated with pJoe2702 to create pNTG6 and pNTG3, respectively. SDS-PAGE showed no enhanced protein bands of the expected sizes in cell extracts prepared from JM109 (pNTG3) or JM109 (pNTG6), although the respective enzyme activities could be measured. Hence, the strains were used for subsequent protein production and purification.

*npdH* was first cloned into pBW22. The resulting recombinant cells showed very low levels of activity. *npdH* was then subcloned into pET11a\* to form pNTG11. Cell

extracts of BL21(DE3)(pNTG11) indicated that NpdH comprised 30% of the total cellular protein. Consequently, BL21(DE3)(pNTG11) was used for protein purification.

### **Characterization of NpdC, NpdG, NpdH and NpdI**

NpdG showed a 44% sequence similarity to an F<sub>420</sub>-dependent NADP reductase of *Methanobacterium thermoautotrophicum* in the database (Russ *et al.*, 2000; Smith *et al.*, 1997; Walters *et al.*, 2001). Further, the first 27 aa of the translation product, NpdG, exhibited a 66% sequence identity to the amino-terminal region of the NADPH-dependent F<sub>420</sub> reductase of *N. simplex* FJ2-1A (Ebert *et al.*, 1999). NpdC exhibited a sequence similarity of 42% to an N5,N10-methylene-tetrahydromethanopterin reductase of *Methanococcus jannaschii* (Bult *et al.*, 1996; Russ *et al.*, 2000) and NpdI possessed a sequence similarity of 46% to a F<sub>420</sub>-dependent N5,N10-methylene-tetrahydromethanopterin reductase from *Archaeoglobus fulgidus* (Klenk *et al.*, 1997; Russ *et al.*, 2000). In addition, the first 27 aa of NpdI exhibited a 77% sequence identity to the amino-terminal region of the hydride transferase of *N. simplex* FJ2-1A (Ebert *et al.*, 1999).

Detailed sequence analyses of the picric acid degradation gene cluster revealed a short ORF (*npdH*) of 318 bp between *npdG* and *npdI* (Fig. 1). Database searches with NpdH showed no significant similarity to any known sequence.

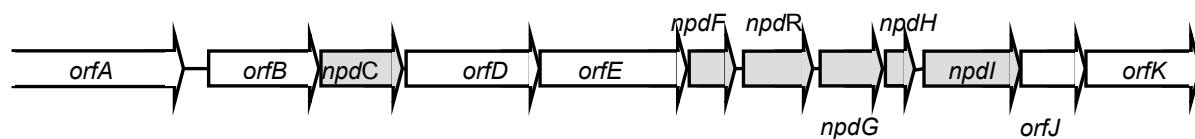


**Fig. 1.** The picric acid degradation gene cluster of *R. (opacus) erythropolis* HL PM-1 (accession no. AF323606; see also Russ *et al.*, 2000). The ORFs and direction of transcription are indicated by the operon arrows. *npdC* encodes hydride transferase I; *npdG* encodes NADPH-dependent F<sub>420</sub> reductase; *npdH* encodes the protein converting 2H<sup>-</sup>PA to product X; *npdI* encodes hydride transferase II.

No conserved motifs were detected using the programs CD-search, Pfam, Proscan or Block.

From SDS polyacrylamide gels, the molecular weight of NpdG, NpdC, NpdI and NpdH were calculated to be 28.8, 43.4, 41.7 and 13.8 kDa, respectively. The sizes of NpdG and NpdH were consistent with the predicted molecular weight of 27 and 12.9 kDa, respectively (taking fusion of the vector-encoded His-tag, *myc* and V5 epitopes into account). The predicted molecular weights for NpdC and NpdI were considerably smaller (35.9 and 32.9 kDa, respectively) than those calculated from SDS-PAGE. We have no explanation for this presently, except that the conditions used for SDS-PAGE (salts and SDS) may cause abnormal migration of the proteins.

NpdC, NpdG and NpdH were largely purified to complete homogeneity. NpdI could only be purified to 90%. NpdC, NpdG and NpdI were unstable in the presence of imidazole, a constituent of the elution buffer used for purification. Hence, imidazole was removed from purified protein solutions by pD10 Desalting Columns. All four enzymes were stable at -20°C for several weeks in 50 mM KH<sub>2</sub>PO<sub>4</sub>/K<sub>2</sub>HPO<sub>4</sub> buffer (pH 7.8) plus 20% glycerol.

### Reduction of F<sub>420</sub> by NpdG

Purified enzyme was incubated with NADPH and F<sub>420</sub> in citrate-phosphate buffer (50 mM pH 5.5). A reduction in absorbance was observed at 400 nm, indicating the reduction of F<sub>420</sub> and the formation of F<sub>420</sub>H<sub>2</sub> (Purwantini *et al.*, 1992). The  $K_m$  value was determined to be  $9.68 \pm 2.89$   $\mu$ M. The enzyme possessed a  $V_{max}$  of  $17.27 \pm 2.46$  U  $mg^{-1}$ . The standard deviations were calculated from at least three repetitions. No activity was observed when F<sub>420</sub> was replaced by FAD (flavin adenine dinucleotide) or FMN (flavin mononucleotide).

### NpdI catalyses a hydride transfer to picric acid or 2,4-DNP

To demonstrate that NpdI catalyses the conversion of picric acid to H<sup>-</sup>-PA, NpdI was incubated with picric acid, NADPH, F<sub>420</sub> and NpdG. No enzyme activity was detected in the absence of F<sub>420</sub>. Enzyme activities were detected by repeated spectral scans. An increase in absorbance at 420 and 490 nm ( $\lambda_{max}$  of H<sup>-</sup>-PA at pH 7.8) was the same as described before for H<sup>-</sup>-PA formation (Behrend & Heesche-Wagner 1999; Lenke *et al.*, 1992). Further, the spectral changes corresponded to a colour change from yellow to orange. The spectrum measured during HPLC analysis ( $\lambda_{max}$  422, 490 nm) was indistinguishable from the chemically synthesized H<sup>-</sup>-PA and from that described previously. The retention volumes were 4.0 ml [40% (v/v) methanol plus 5 mM PicA, pH 7.8; 250 mm column] or 4.9 ml [30% (v/v) methanol plus 5 mM PicA; 125 mm column]. Coupled HPLC-ESI-MS proved the identity of the chemically synthesized H<sup>-</sup>-PA. At a retention volume of 4.3 ml, the mass spectrum of the H<sup>-</sup>-PA revealed a single peak at an ion mass of  $m/z$  230, which corresponded to the molecular ion [M]<sup>-</sup>. A decrease in the concentration of picric acid coincided with a stoichiometric increase in concentration of H<sup>-</sup>-PA, indicating that picric acid was completely converted to H<sup>-</sup>-PA.

Incubation of NpdI with 2,4-DNP, NADPH, F<sub>420</sub> and NpdG showed that NpdI converted 2,4-DNP to the hydride  $\sigma$ -complex of 2,4-DNP (H<sup>-</sup>-2,4-DNP). Spectrophotometrically, an increase in absorbance was detected at 420 nm, which was typical for H<sup>-</sup>-2,4-DNP (Behrend & Heesche-Wagner, 1999). Further, the spectrum measured during HPLC analysis ( $\lambda_{max}$  258, 306 and 440 nm) corresponded

to the UV/Vis spectrum of the  $\text{H}^-$ -2,4-DNP described by Behrend & Heesche-Wagner (1999). The retention volume of the  $\text{H}^-$ -2,4-DNP was 1.3 ml [40% (v/v) methanol plus 5 mM PicA, pH 7.8; 250 mm column] or 1.7 ml [30 (v/v) methanol plus 5 mM PicA; 125 mm column].

### **NpdC catalyses a hydride transfer to $\text{H}^-$ -PA**

Spectroscopic scans were performed with NpdC plus  $\text{H}^-$ -PA, NADPH,  $\text{F}_{420}$  and NpdG. As for NpdI, no enzyme activity of NpdC was detected when omitting  $\text{F}_{420}$  from the enzyme assay. Enzyme activity was detected as spectral changes exhibiting a decrease in absorbance at 420 and at 490 nm (Fig. 2). This coincided with a colour change from orange to yellow. HPLC analysis showed that the new product possessed a retention volume of 2.6 ml [40% (v/v) methanol plus 5 mM PicA, pH 7.8; 250 mm column] or 2.4 ml [30 (v/v) methanol plus 5 mM PicA; 125 mm column]. The spectrum derived from HPLC analysis showed absorbance maxima at  $\lambda_{\text{max}}$  of 229 and 383 nm. These corresponded to  $2\text{H}^-$ -PA as described previously (Ebert *et al.*, 2002) and to the chemically synthesized  $2\text{H}^-$ -PA. Coupled HPLC-ESI-MS of the latter confirmed the structure:  $2\text{H}^-$ -PA was detected at a retention volume of 0.9 ml. Two signals at  $m/z$  232 and 185 were due to the molecular ion  $[\text{M}]^-$  and the molecular ion after elimination of  $\text{HNO}_2$ ,  $[\text{M}-\text{HNO}_2]^-$ .



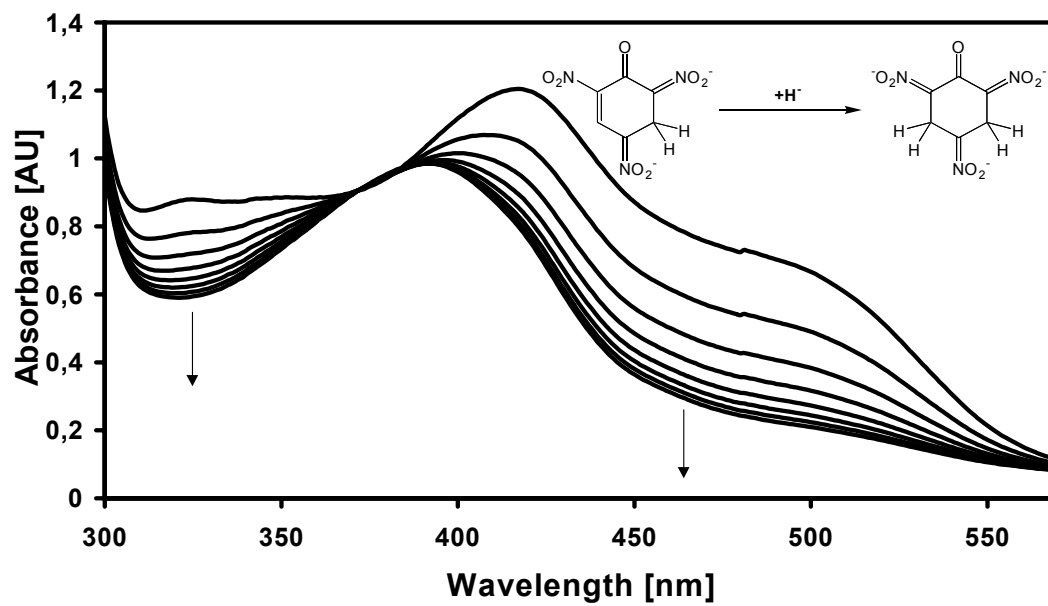


**Fig. 2:** Absorption spectrum showing the conversion of H<sup>-</sup>-PA to 2H<sup>-</sup>-PA by NpdG plus NpdC. The NpdG/NpdC assay contained F<sub>420</sub>, NADPH and H<sup>-</sup>-PA in 50 mM KH<sub>2</sub>PO<sub>4</sub>/K<sub>2</sub>HPO<sub>4</sub>, pH 7.8. Scans were recorded every 60 s over a period of 10 min.

### NpdH converts 2H<sup>-</sup>-PA to product X

NpdH converted 2H<sup>-</sup>-PA to a new product, X. This was shown by repeated recording of spectroscopic scans; an increase in absorbance occurred at 389 nm (Fig. 3).

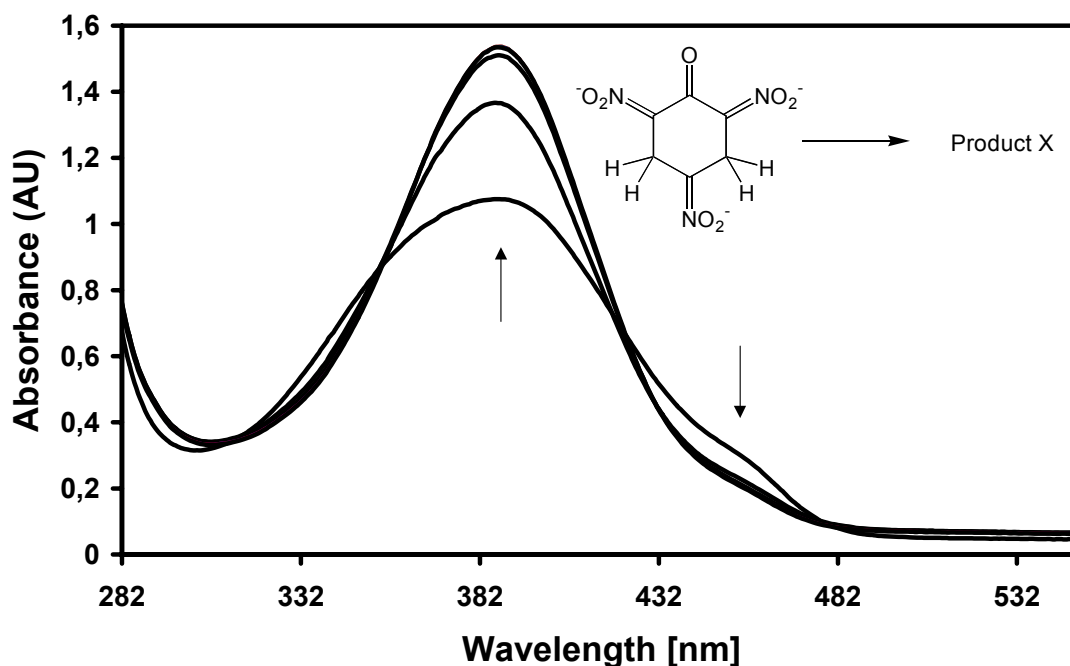


**Fig. 3.** Absorption spectrum showing the conversion of 2H<sup>-</sup>-PA to product X by NpdH. The NADPH assay contained 2H<sup>-</sup>-PA in 50 mM KH<sub>2</sub>PO<sub>4</sub>/K<sub>2</sub>HPO<sub>4</sub>, pH 7.8. Scans were recorded every 60 s over a period of 10 min.

HPLC analysis of product X showed a retention volume of 3.4 ml [40% (v/v) methanol plus 5 mM PicA, pH 7.8; 250 mm column] or 3.0 ml [30 (v/v) methanol plus 5 mM PicA; 125 mm column]. The spectrum obtained from HPLC analysis had absorbance maxima of 203, 236 and 390 nm. Coupled HPLC-ESI-MS showed a retention volume of 1.2 ml. The signal at  $m/z$  232 corresponded to the molecular anion of the protonated 2H<sup>-</sup>-PA. From this ion, nitrite was eliminated, giving rise to the negative fragment ions at  $m/z$  46 [NO<sub>2</sub>]<sup>-</sup> and  $m/z$  185 [M-HNO<sub>2</sub>]<sup>-</sup>, respectively. Since 2H<sup>-</sup>-PA was in equilibrium with product X, it was not completely converted to product X.

## Discussion

In the present study, NpdI, or hydride transferase II (plus NpdG, the NADPH-dependent  $F_{420}$  reductase), was shown to catalyse a hydride transfer to picric acid, forming  $H^-$ -PA. NpdC, the hydride transferase I (plus NpdG), was shown to catalyse the hydride transfer to  $H^-$ -PA, giving rise to  $2H^-$ -PA (Fig. 4). Based on *in vivo* transformations,  $2H^-$ -PA has, until recently, been believed to be a dead-end metabolite as part of a non-productive route of picric acid degradation (Lenke *et al.*, 1992; Lenke & Knackmuss, 1992). Only recently was it shown that  $2H^-$ -PA is an intermediate of the productive route (Ebert *et al.*, 2002). The authors showed that the purified HTES of *N. simplex* FJ2-1A (comprising a hydride transferase and an NADPH-dependent  $F_{420}$  reductase) not only converts picric acid to  $H^-$ -PA, but also performs a second hydrogenation from  $H^-$ -PA to  $2H^-$ -PA.

Since NpdC, NpdI and the hydride transferase of *N. simplex* FJ2-1A all catalyse hydride transfers, they are functionally alike. At the sequence level, no sequence similarity was detected between NpdC and the amino-terminal region of the hydride transferase of strain FJ2-1A. On the other hand, NpdI exhibited a sequence identity of 77% to the latter. Hence, we regarded NpdI as the immediate counterpart of the hydride transferase of strain FJ2-1A, not NpdC. Functionally, both the hydride transferase of strain FJ2-1A and NpdI convert picric acid to  $H^-$ -PA, requiring  $F_{420}H_2$  as the electron donor. Yet, the hydride transferase of strain FJ2-1A appears to possess a broader substrate specificity than NpdI: while the former has the ability to transfer a hydride ion to both picric acid and to  $H^-$ -PA, NpdI exhibited only minimal activity for  $H^-$ -PA. Instead, NpdC transferred hydride ions to  $H^-$ -PA, giving rise to  $2H^-$ -PA (Fig. 4). This suggests that *R. (opacus) erythropolis* HL PM-1 has evolved an additional enzyme for this step. However, this does not exclude the possibility that *N. simplex* FJ2-1A may also harbour another hydride transferase.

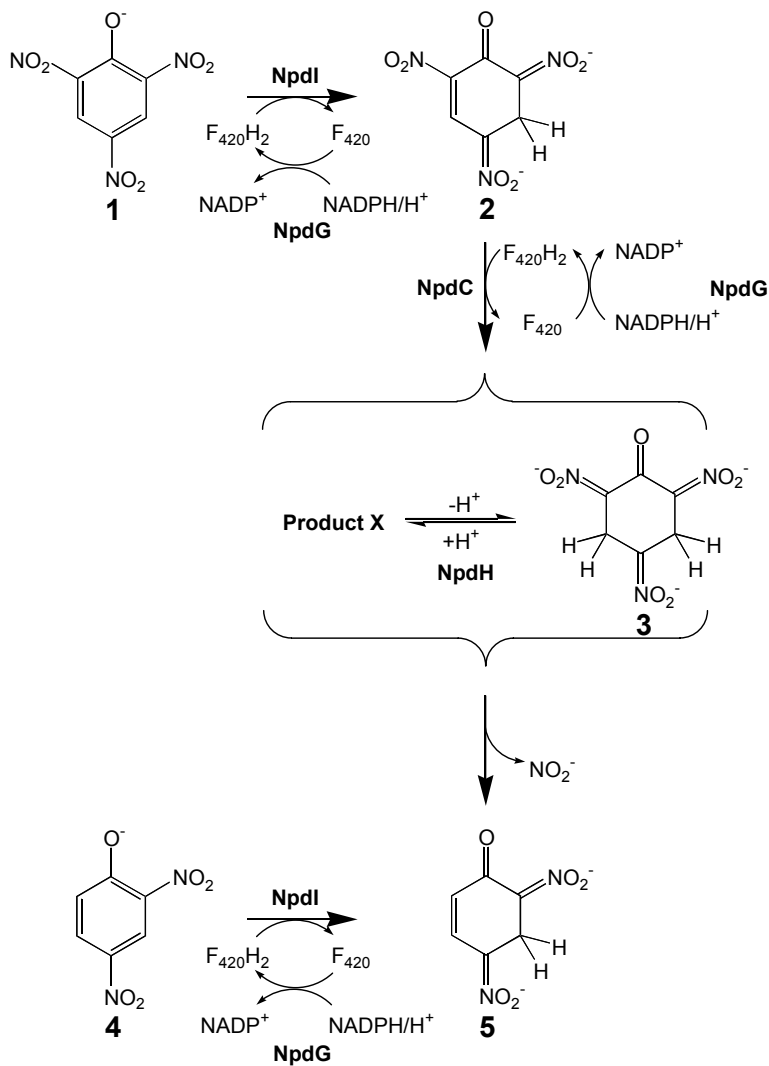


**Fig. 4.** Proposed upper picric acid degradation pathway showing the enzymes involved in *R. (opacus) erythropolis* HL PM-1. 1, Picrate; 2, H<sup>-</sup>-PA; 3, 2H<sup>-</sup>-PA; 4, 2,4-dinitrophenolate; 5, H<sup>-</sup>-2,4-DNP.

Comparable to the hydride transferase of strain FJ2-1A, NpdI converted 2,4-DNP to H<sup>-</sup>-2,4-DNP. Behrend & Heesche-Wagner (1999) initially described the H<sup>-</sup>-2,4-DNP as a metabolite of picric acid degradation by *Nocardioides* sp. CB 22-2. Furthermore, H<sup>-</sup>-2,4-DNP would be expected to be the product of nitrite release from 2H<sup>-</sup>-PA, as proposed for *N. simplex* FJ2-1A (Ebert *et al.*, 2002). Indeed, cell-free extracts of *R. (opacus) erythropolis* HL PM-1 convert 2H<sup>-</sup>-PA to H<sup>-</sup>-2,4-DNP, suggesting it to be a true metabolite of picric acid degradation in the strain.

NpdG was shown to be essential for the hydride transfer reactions to take place by regenerating  $F_{420}H_2$ . An interesting aspect is that NpdG appears to only use  $F_{420}$  as a substrate. It cannot reduce flavins such as FAD or FMN. Enzymes playing a role in general metabolism, with  $F_{420}$  being involved, are known in mycobacteria, streptomycetes and *Archaea* (Berk & Thauer, 1997; Eker *et al.*, 1989; Purwantini & Daniels, 1996). For this reason, even though specific for  $F_{420}$ , NpdG may not necessarily be restricted to picric acid or 2,4-DNP degradation strains. Research is under way to test this hypothesis.

Although we cannot assign an explicit function to *npdH*, the gene product may well play an essential role in preparing  $2H^-PA$  for nitrite release. Since the molecular masses of the  $2H^-PA$  and product X were indistinguishable, while the retention volumes and the absorbance spectra differed, this suggests that product X may be a tautomeric form of protonated  $2H^-PA$ . This might be required to facilitate subsequent nitrite release. Vorbeck *et al.* (1998) made a similar observation in the course of TNT degradation, where the hydride complex of TNT ( $H^-TNT$ ) undergoes a second hydride attack, followed by protonation and subsequent tautomerization of the resulting dihydride complex of TNT ( $2H^-TNT$ ). Various other groups studying bacterial TNT degradation have detected several protonated forms of  $2H^-TNT$  (French *et al.*, 1998; Pak *et al.*, 2000). That the UV/Vis spectrum of product X (pH 7.8) was indistinguishable from that of  $2H^-PA$  (pH 12; at  $\geq 280$  nm) could be due to the same longer wavelength chromophore in both structures. Work is in progress to characterize product X, to show it to be part of a productive catabolic route of picric acid degradation and to assign an explicit function to NpdH.

## **Acknowledgements**

Many sincere thanks to Lacy Daniels for the generous supply of coenzyme F<sub>420</sub> (Department of Microbiology, University of Iowa, Iowa City, USA), Josef Altenbuchner for the vectors pJoe2702 and pBW22 (Department of Industrial Genetics, University of Stuttgart, Germany), and Ed Hendrickson and Roz Young for the 16S rDNA sequence (Dupont, Wilmington, DE, USA). We acknowledge Michael Spiteller and Thomas Pfeifer (Institute of Environmental Research, University of Dortmund, Germany) for enabling us to determine the mass spectra. The work was supported by the German Research Foundation (DFG).

## References

**Aguirre, A., Sanz de Galdeano, C., Oleaga, J. M., Eizaguirre X. & Diaz Perez J. L. (1993).** Allergic contact dermatitis from picric acid. *Contact Dermatitis* 28, 291.

**Andres, M. I., Repetto, G., Sanz, P. & Repetto, M. (1996).** Comparative effects of the metabolic inhibitors 2,4-dinitrophenol and iodoacetate on mouse neuroblastoma cells *in vitro*. *Toxicology* 110,123-32.

**Altschul, S. F., Gish, W., Miller, W., Myers, E. W. & Lipman, D. J. (1990).** Basic local alignment search tool. *J Mol Biol* 215, 403-410.

**Ausubel, F. M., Brent R., Kingston R. E., Moore D. D., Seidman J.G., Smith J. A. & Struhl, K. (2001).** *Current Protocols in Molecular Biology*. John Wiley & Sons, Inc.

**Berk, H. & Thauer R. K. (1997).** Function of coenzyme F<sub>420</sub>-dependent NADP reductase in methanogenic Archaea containing an NADP-dependent alcohol dehydrogenase. *Arch Microbiol* 168, 396-402.

**Behrend, C. & Heesche-Wagner, K. (1999).** Formation of hydride-Meisenheimer complexes of picric acid (2,4,6-trinitrophenol) and 2,4-dinitrophenol during mineralization of picric acid by *Nocardioides* sp. strain CB 22-2. *Appl Environ Microbiol* 65, 1372-1377.

**Blasco, R., Moore, E., Wray, V., Pieper, D., Timmis, K. & Castillo, F. (1999).** 3-nitroadipate, a metabolic intermediate for mineralization of 2,4-dinitrophenol by a new strain of a *Rhodococcus* species. *J Bacteriol* 181, 149-152.

**Bult C. J., White, O., Olsen, G.J. & 20 other authors (1996).** Complete genome sequence of the methanogenic archaeon, *Methanococcus jannaschii*. *Science* **273**, 1058-1073.

**Dorn, E., Hellwig, M., Reineke, W. & Knackmuss, H.-J. (1974).** Isolation and characterization of a 3-chlorobenzoate degrading pseudomonad. *Arch Microbiol* **99**, 61-70.

**Ebert, S., Rieger, P. G. & Knackmuss, H.-J. (1999).** Function of coenzyme F<sub>420</sub> in aerobic catabolism of 2,4,6-trinitrophenol and 2,4-dinitrophenol by *Nocardioides simplex* FJ2-1A. *J Bacteriol* **181**, 2669-2674.

**Ebert, S., Fischer, P. & Knackmuss, H.-J. (2001).** Converging catabolism of 2,4,6-trinitrophenol (picric acid) and 2,4-dinitrophenol by *Nocardioides simplex* FJ2-1A. *Biodegradation* (in press).

**Eker, A. P., Hessels, J. K. & Meerwaldt, R. (1989).** Characterization of an 8-hydroxy-5-deazaflavin:NADPH oxidoreductase from *Streptomyces griseus*. *Biochim Biophys Acta* **990**, 80-86.

**Inoue, H., Nojima, H. & Okayama, H. (1990).** High efficiency transformation of *Escherichia coli* with plasmids. *Gene* **96**, 23-28.

**Klatte, S., Kroppenstedt, R. M. & Rainey, F. A.. (1994).** *Rhodococcus opacus* sp. nov., an unusual nutritionally versatile *Rhodococcus* species. *System Appl Microbiol* **17**, 355-360.

**Klenk, H. P., Clayton, R. A., Tomb, J. F. & 22 other authors (1997).** The complete genome sequence of the hyperthermophilic, sulphate-reducing archaeon *Archaeoglobus fulgidus*. *Nature* **390**, 364-370.



**Laemmli, U. K. (1970).** Cleavage of structural proteins during the assembly of the head of bacteriophage T4. *Nature* **227**, 680-685.

**Lenke, H. & Knackmuss, H.-J. (1992).** Initial hydrogenation during catabolism of picric acid by *Rhodococcus erythropolis* HL 24-2. *Appl Environ Microbiol* **58**, 2933-2937.

**Lenke, H., Pieper, D. H., Bruhn, C., & Knackmuss, H.-J. (1992).** Degradation of 2,4-dinitrophenol by two *Rhodococcus erythropolis* strains, HL 24-1 and HL 24-2. *Appl Environ Microbiol* **58**, 2928-2932.

**Lenke, H., Achtnich, C. & Knackmuss, H.-J. (2000).** Perspectives of bioelimination of polynitroaromatic compounds. In *Biodegradation of Nitroaromatic Compounds and Explosives*, pp. 91-126. Edited by J. C. Spain, J. B. Hughes & H. J. Knackmuss. Lewis Publishers, Boca Raton: CRC Press.

**Linsinger, G., Wilhelm, S., Wagner, H. & Hacker, G. (1999).** Uncouplers of oxidative phosphorylation can enhance a *Fas* death signal. *Mol Cell Biol* **19**, 3299-3311.

**Peck, M. W. (1989).** Changes in concentrations of coenzyme F<sub>420</sub> analogs during batch growth of *Methanosarcina barkeri* and *Methanosarcina mazei*. *Appl Environ Microbiol* **55**, 940-945.

**Purwantini, E., Mukhopadhyay, B., Spencer, R. W. & Daniels, L. (1992).** Effect of temperature on the spectral properties of coenzyme F<sub>420</sub> and related compounds. *Anal Biochem* **205**, 342-350.

**Purwantini, E., & Daniels, L. (1996).** Purification of a novel coenzyme F<sub>420</sub>-dependent glucose-6-phosphate dehydrogenase from *Mycobacterium smegmatis*. *J Bacteriol* **178**, 2861-2866.

**Rajan, J., Valli, K., Perkins, R. E., Sariaslani, F. S., Barns, S. M., Reysenbach, A. L., Rehm, S., Ehringer, M. & Pace, N. R. (1996).** Mineralization of 2,4,6-trinitrophenol (picric acid): characterization and phylogenetic identification of microbial strains. *J Ind Microbiol* **16**, 319-324.

**Rieger, P.G., Sinnwell, V., Preuss, A., Francke, W. & Knackmuss H.-J. (1999).** Hydride-Meisenheimer complex formation and protonation as key reactions of 2,4,6-trinitrophenol biodegradation by *Rhodococcus erythropolis*. *J Bacteriol* **181**, 1189-1195.

**Russ, R., Walters, D. M., Knackmuss, H.-J. & Rouviere, P. E. (2000).** Identification of genes involved in picric acid and 2,4-DNP degradation by mRNA differential display. In *Biodegradation of Nitroaromatic Compounds and Explosives*, pp. 127-143. Edited by J. C. Spain, J. B. Hughes & H. J. Knackmuss. Lewis Publishers, Boca Raton: CRC Press.

**Severin, T., & Schmitz, R. (1962).** Umsetzung von Nitroaromaten mit Natriumborhydrid. *Chemische Berichte* **95**, 1417-1419.

**Smith, D. R., Doucette-Stamm, L. A., Deloughery, C. & 22 other authors (1997).** Complete genome sequence of *Methanobacterium thermoautotrophicum* deltaH: functional analysis and comparative genomics. *J Bacteriol* **179**, 7135-7155.

**Tatusova, T. A. & Madden, T. L. (1999).** BLAST 2 Sequences, a new tool for comparing protein and nucleotide sequences. *FEMS Microbiol Lett* **174**, 247-250.

**Walters, D.M., Russ, R., Knackmuss, H.-J. & Pouviere, P.E. (2001).** High-density sampling of a bacterial operon using mRNA differential display. *Gene* **273**, 305-315.

**Wilms, B., Hauck, A., Reuss, M., Sylatk, C., Mattes, R., Siemann, M. & Altenbuchner, J. (2001).** High-cell-density fermentation for production of  $\text{L-N}$ -carbamoylase using an expression system based on the *Escherichia coli rhaBAD* promoter. *Biotechnol Bioeng* **73**, 95-103.

**Yanisch-Perron, C., Vieira, J. & Messing, J. (1985).** Improved M13 phage cloning vectors and host strains: nucleotide sequences of the M13mp18 and pUC19 vectors. *Gene* **33**, 103-119.

## **Appendix 2**

# **The Role of a Tautomerase and a Nitrite-Eliminating Enzyme in 2,4,6-Trinitrophenol (Picric Acid) Degradation**

(Submitted at Appl. Environ. Microbiology)

**Klaus W. Hofmann, Hans-Joachim Knackmuss\*, and Gesche Heiss**

Institute of Microbiology, University of Stuttgart, Allmandring 31, 70569 Stuttgart,  
Germany

\*Corresponding author: Phone: +49-(0)7152-52930. e-mail: [imbhjk@po.uni-stuttgart.de](mailto:imbhjk@po.uni-stuttgart.de)

## Abstract

A 2H<sup>-</sup>-TNP tautomerase from the 2,4,6-trinitrophenol degrading strains *Rhodococcus (opacus) erythropolis* HL PM-1 and *Nocardioides simplex* FJ2-1A was each purified as a His-tag fusion protein. Both 2H<sup>-</sup>-TNP tautomerases were shown to catalyze a proton-shift isomerization of the dihydride complex of 2,4,6-trinitrophenol (2H<sup>-</sup>-TNP). The protonated 2H<sup>-</sup>-TNP existed in two tautomeric forms, the *aci*-nitro and the nitro form. From the crude extract of *N. simplex* FJ2-1A a nitrite-eliminating enzyme was purified and characterized. The same activity was found in crude extracts of *R. (opacus) erythropolis* HL PM-1. Nitrite elimination occurred only from the *aci*-nitro form of 2H<sup>-</sup>-TNP, not from the nitro form. This suggests that the 2H<sup>-</sup>-TNP tautomerase is necessary to avoid accumulation of the nitro form as an inert metabolite. The product of nitrite release was identified as the hydride complex of 2,4-dinitrophenol (H<sup>-</sup>-DNP) by <sup>1</sup>H-NMR and LC-MS.

## Abbreviations:

DNP, 2,4-dinitrophenol; H<sup>-</sup>-DNP, hydride  $\sigma$ -complex of 2,4-dinitrophenol; H<sup>-</sup>-TNP, hydride  $\sigma$ -complex of 2,4,6-trinitrophenol; 2H<sup>-</sup>-TNP, dihydride  $\sigma$ -complex of 2,4,6-trinitrophenol; HTI, hydride transferase I; HTII, hydride transferase II; TNP, 2,4,6-trinitrophenol; NDFR, NADPH-dependent F<sub>420</sub> reductase.

## Introduction

2,4,6-Trinitrophenol (TNP) and 2,4-dinitrophenol (DNP) are nitroaromatic compounds of versatile use in chemical synthesis. They occur as off-stream chemicals during the production of aniline as a starting material for synthesis of pesticides and azo dyes. Furthermore, TNP and its salts have been used as explosives. Large quantities of TNP in waste streams of aniline production necessitate bioremediation strategies. Several bacteria with the ability to use TNP as a growth substrate have been identified (3, 4, 11, 21). This opens up possibilities for biological bioremediation approaches once the mechanisms of degradation are understood.

It was established that two initial hydrogenation reactions take place (7, 10, 15, 22). First, TNP is hydrogenated at the aromatic nucleus by the hydride transferase II (HTII, encoded by *npdI*) and the NADPH-dependent  $F_{420}$  reductase (NDFR, encoded by *npdG*). The hydride Meisenheimer complex of TNP ( $H^-$ -TNP) thereby formed is further hydrogenated by the hydride transferase I (HTI, encoded by *npdC*) and the NDFR, generating the dihydride Meisenheimer complex of TNP ( $2H^-$ -TNP) (Fig. 1).

$2H^-$ -TNP was thought to be a dead-end metabolite of TNP degradation (15), although later, this concept was challenged, and it was suggested that nitrite is eliminated from  $2H^-$ -TNP to produce the Meisenheimer complex of 2,4-dinitrophenol ( $H^-$ -DNP) (6). Recently, another gene product of the *npd*-cluster of *Rhodococcus (opacus) erythropolis* HL PM-1 (NpdH) was purified and an activity with  $2H^-$ -TNP was found, generating product X (10).

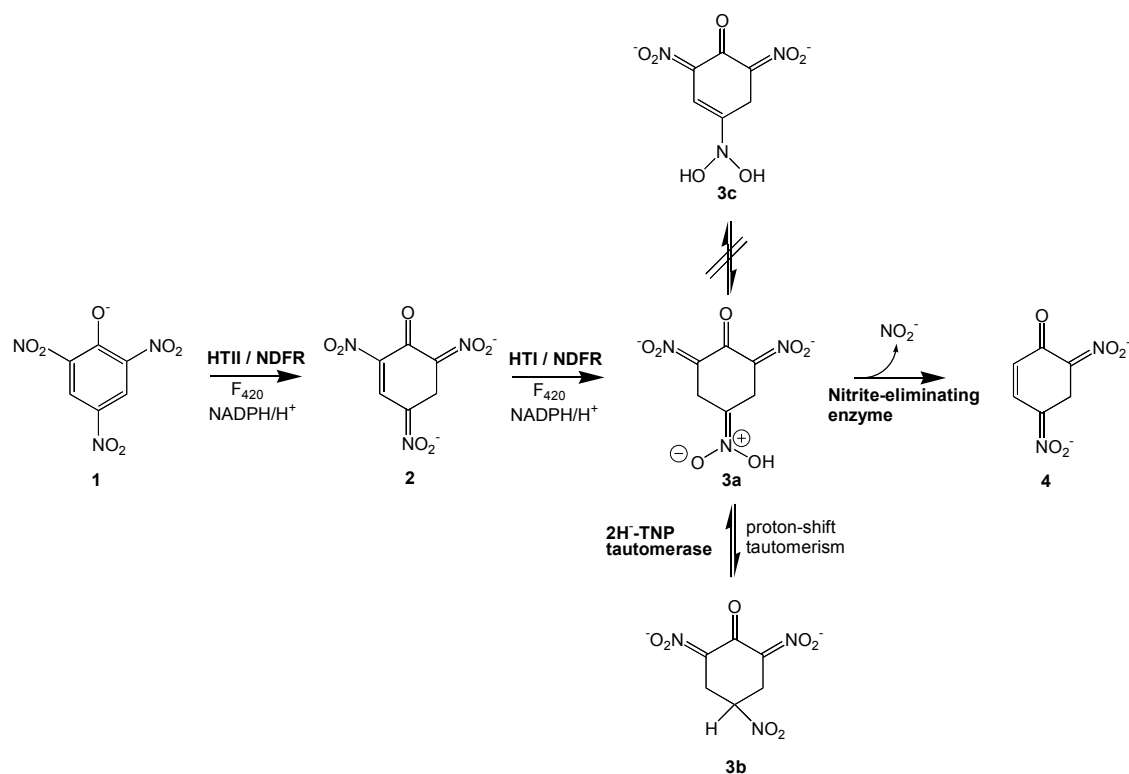


**Fig.1.** Upper degradation pathway of TNP. (1) TNP; (2) H<sup>-</sup>-TNP; (3a) aci-nitro form of 2H<sup>-</sup>-TNP; (3b) nitro form of 2H<sup>-</sup>-TNP; (3c) enamine form of 2H<sup>-</sup>-TNP; (4) H<sup>-</sup>-DNP. HTII: hydride transferase II; NDFR: NADPH-dependent F<sub>420</sub> reductase; HTI: hydride transferase I.

In the present study we describe the role of NpdH as a 2H<sup>-</sup>-TNP tautomerase, responsible for providing the substrate for the nitrite-eliminating enzyme. Furthermore, we purified and characterized a nitrite-eliminating enzyme, which specifically releases nitrite from the *aci*-nitro form of 2H<sup>-</sup>-TNP, and we established that H<sup>-</sup>-DNP is a true metabolite of TNP degradation.

## Materials and Methods

**Bacterial strains and growth conditions.** *Nocardiooides simplex* FJ2-1A (21) was grown in conical flasks at 30 °C in 50 mM phosphate buffer (pH = 7.5) containing 0.7 mM picrate, 20 mM sodium acetate, 0.5 g of yeast extract liter<sup>-1</sup>, 0.5 g of proteose peptone liter<sup>-1</sup>, 0.5 g of Casamino Acids liter<sup>-1</sup>, and mineral salts. Mineral salts without nitrogen contained 20 mg of Fe(III)-citrate liter<sup>-1</sup>, 1 g of MgSO<sub>4</sub>·7 H<sub>2</sub>O liter<sup>-1</sup>, 50 mg of CaCl<sub>2</sub>·2 H<sub>2</sub>O liter<sup>-1</sup>, and 1 ml of trace element solution SL 6 (20). After consumption of 0.7 mM picrate, 0.35 mM picrate was added to maintain induction of the cells. The culture was harvested by centrifugation immediately after decolorization of the medium. Cells were frozen in liquid nitrogen and stored at -30 °C.

*Escherichia coli* strains BL21 (DE3) (pNTG6) and *E. coli* BL21 (DE3) (pSLK2) were grown at 37 °C in Luria-Bertani (LB) medium containing 100 µg ml<sup>-1</sup> ampicillin. Overnight cultures were inoculated into LB and grown at 37 °C to an OD<sub>600</sub> of 0.4. The culture was induced for 4 h at 30 °C with 1 mM IPTG.

**Molecular techniques.** Standard protocols were used for manipulation of DNA (2, 23). Plasmid DNA was isolated using FlexiPrep Kit (Amersham Biosciences, Freiburg, Germany). *E. coli* was transformed according to Inoue et al. (12).

**Cloning of *npdH* from *N. simplex* FJ2-1A.** *npdH* was amplified by PCR. The PCR reaction mixture contained 1 ng template DNA, 2.5 U *Pwo*-DNA-polymerase (Peqlab, Erlangen, Germany), 3 mM MgSO<sub>4</sub>, 0.25 mM each dNTP and 50 pmol each primer. Thirty-five amplification cycles were performed as follows: 96 °C for 30 s, 63°C for 30 s, 68°C for 1 min, and 68°C for 5 min. The primers were designed to contain *NdeI* and *HindIII* sites (underlined) (5'-TTTTCATATGATCCACGAGCTGCGTGAGTACG-3' and 5'-TTTTAAAGCTTGAGAGCCGCAGGTTCCGAG-3'). Primers were purchased from Eurogentec (Köln, Germany). The PCR fragment was eluted from agarose using the Easypure DNA purification kit (Biozym Diagnostics, Hessisch Oldendorf, Germany), restricted with the appropriate restriction enzymes and ligated into pET22b (Novagen, Darmstadt, Germany). The resulting plasmid, pSLK2 was transformed into *E. coli* BL21 (DE3) to create *E. coli* BL21 (DE3) (pSLK2).



**Preparation of cell extracts.** About 20 g wet cells of *N. simplex* FJ2-1A and 2 g wet cells of *E. coli* BL21 were suspended in 50 mM Tris-HCl (pH = 7.5) and lysed with a French press as described before (10). The protein concentration was determined by the method of Bradford using a dye reagent concentrate (BioRad protein assay, BioRad, München, Germany) (5).

**Enzyme purification.** *npdH* was expressed in *E. coli* BL21 and purified as a His-tag fusion protein by Ni-NTA affinity chromatography as described before (10). Imidazole was removed from the enzyme-containing fractions by pD10 Desalting Columns (Amersham Pharmacia, Freiburg, Germany).

The nitrite-eliminating enzyme was purified at 4 °C by use of a fast-performance liquid chromatography system consisting of a LCC 500 controller, 500 pump, UV-1 monitor, REC-482 recorder, and FRAC autosampler (Pharmacia, Uppsala, Sweden). The cell extract of *N. simplex* FJ2-1A (340 mg of protein) was passed through a Q Sepharose column (HP HR 16/10, Pharmacia) preequilibrated with basic buffer (50 mM Tris-HCl [pH = 7.5]) at a flow rate of 1 ml min<sup>-1</sup>. The activity was eluted from the column with a linear gradient (200 ml) of 0 to 1 M NaCl in basic buffer at a NaCl concentration of approximately 0.25 M. Fractions (3 ml each) were collected, and enzyme activity was determined spectrophotometrically. The active fractions were pooled, and ammonium sulfate was added to a final concentration of 1 M. The solution was applied to a Phenyl Superose column (HR10/10, Pharmacia) preequilibrated with 1 M ammonium sulfate in basic buffer. The enzyme was eluted with a linear gradient (65 ml) of 1 to 0 M ammonium sulfate in basic buffer at a concentration of 0.41 M (NH<sub>4</sub>)<sub>2</sub>SO<sub>4</sub> and a flow rate of 0.5 ml min<sup>-1</sup>. The active fractions (2 ml each) were pooled and concentrated by ultrafiltration (Vivaspin 2, Vivascience AG, Hannover, Germany) to a total volume of 1 ml, loaded onto a gel filtration column (Superdex 200 Prep-Grade, Pharmacia), and eluted with basic buffer.

The molecular mass of native proteins was determined using a gel filtration calibration kit (Amersham Pharmacia, Freiburg, Germany). Purity and molecular mass of protein subunits was determined by MALDI-TOF with a G1025A Hewlett Packard LD-TOF system (GSG Mess- und Analysegeräte Vertriebsgesellschaft mbH,

Karlsruhe, Germany) and by SDS-PAGE with a 10 % polyacrylamide gel by the method of Laemmli (14) on a Mini-PROTEAN 3 electrophoresis cell (BioRad).

**Enzyme assays.** Enzyme assays were performed with a Cary 50 Biospectrophotometer controlled by Cary WinUV Biopackage software (Varian, Mulgrave, Australia). Reactions with the 2H<sup>-</sup>-TNP tautomerase were performed as previously described for NpdH (10).

The activity of the nitrite-eliminating enzyme was assayed by measuring the increase in absorbance of H<sup>-</sup>-DNP at 450 nm or repeated recording of UV-visible spectra between 280 and 600 nm in 1 min cycles. The test was conducted in 50 mM Tris-HCl (pH = 8.0) containing 0.1 mM 2H<sup>-</sup>-TNP and 6 µg of nitrite-eliminating enzyme. Reaction rates were calculated by using the experimentally determined extinction coefficient of 944 M<sup>-1</sup> cm<sup>-1</sup> (H<sup>-</sup>-DNP at 450 nm [20 °C, pH = 8.0]). One unit of enzyme activity was defined as the amount of enzyme that converts 1 µmol of substrate per min.

**Analytical Methods.** Metabolites were detected and quantified at 210, 340, 390, or 420 nm by HPLC analysis (Chromeleon Chromatography Data Systems 4.38, equipped with a Dionex UV/Vis detector, UVD 170S/340S, a Dionex pump, P 580, and a Dionex autosampler, Gina 50, Dionex, Idstein, Germany) with a Lichrospher 100 RP-18 column (250 x 4 mm, particle size 5 µm, Merck, Darmstadt, Germany). The mobile phase consisted of 20 % (v/v) methanol and 80 % (v/v) 50 mM phosphate buffer (pH = 8.0).

Liquid chromatography (LC) mass spectra were obtained by negative-mode electrospray ionization (ESI) on a HP1100 HPLC system (Hewlett Packard, Waldbronn, Germany) coupled to a VG Plattform II Quadrupol mass spectrometer (Manchester, GB). Samples were resolved on a C8 Reversed Phase column (Gromsil 100, particle size 5 µm, 125 x 4.6 mm, Grom, Herrenberg, Germany). The mobile phase consisted of 5 mM ammonium formate buffer (pH = 8.0).

Nuclear magnetic resonance (NMR) spectra were recorded with an ARX 500 spectrometer (Bruker, Rheinstetten, Germany) at a nominal frequency of 500.14 MHz (<sup>1</sup>H) and 125.76 MHz (<sup>13</sup>C), respectively. Samples were dissolved in D<sub>2</sub>O. Chemical

shifts ( $\delta$ ) are given in parts per million relative to tetramethylsilane as the internal standard.

Nitrite concentration was determined spectrophotometrically by the method of Griess-Ilosvay as modified by Shinn (16).

**Amino acid sequencing and sequence analysis.** The purified nitrite-eliminating enzyme was subjected to automatic sequencing with the Protein Sequencing System 476 (Applied Biosystems, Foster City, USA). Database searches were performed with BLAST (1) and FASTA (19).

**Chemicals.** 2H<sup>-</sup>-TNP and H<sup>-</sup>-DNP were prepared according to Severin & Schmitz (24, 25) and stored at -20 °C. All chemicals used were of the highest available purity and were purchased from Fluka (Taufkirchen, Germany), Merck (Darmstadt, Germany), Roth (Karlsruhe, Germany), and Sigma-Aldrich (Taufkirchen, Germany).

## Results

**Proton-shift tautomerization by a 2H<sup>-</sup>-TNP tautomerase.** Under alkaline conditions (pH 8) 2H<sup>-</sup>-TNP exists as a double charged anion (**3a** in Fig. 1), the so-called *aci*-nitro form. This structure was converted to the tautomeric nitro form (**3b**) by pH-dependent proton-shift tautomerization. HPLC analysis showed that the tautomeric structures had different retention volumes. The *aci*-nitro form was detected with a retention volume of 1.86 ml, whereas the nitro form was eluted from the column at 2.28 ml. Another theoretically possible tautomer, the enamine form (**3c**), was not detectable by HPLC or NMR. The tautomers were in equilibrium with an estimated concentration ratio of 20:80 (*aci*-nitro:nitro form), shown by HPLC measurements at 390 nm. Since the equilibration rate was pH-dependent, determination was carried out at pH 7.0, 7.5, and 8.0. When initiating the experiments, 2H<sup>-</sup>-TNP was present as its *aci*-nitro form, formed instantaneously by protonation of the trianion of the chemically synthesized dihydride complex (24, 25). The time taken to reach the final concentration ratio of 20:80 (*aci*-nitro:nitro form), was measured at 390 nm (Table 1). The result indicates that the equilibration rate accelerated at lower pH values. Further, Table 1 shows that NpdH from *R. (opacus) erythropolis* HL PM-1 catalyzed this proton-shift tautomerization of protonated 2H<sup>-</sup>-TNP, accelerating the equilibration rate 300- to 600-fold.

**Table 1. pH dependence of the spontaneous and the tautomerase-catalyzed proton-shift tautomerization of protonated 2H<sup>-</sup>-TNP.**

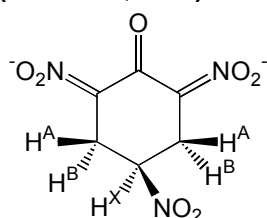
pH	spontaneous tautomerization	enzymatic tautomerization
8.0	300 min	1 min
7.5	180 min	0.5 min
7.0	60 min	0.1 min

min: time taken for equilibration. Each experiment was initiated with the *aci*-nitro form only at time zero. The final concentration ratio was 20:80 (*aci*-nitro:nitro form), determined by HPLC.

A 2H<sup>-</sup>-TNP tautomerase was purified from *N. simplex* FJ2-1A as a His-tag fusion protein. Comparison to NpdH from *R. (opacus) erythropolis* HL PM-1 showed a DNA sequence identity of 63 % and a protein sequence identity of 59 %. The enzyme function was confirmed to be the same as NpdH of *R. (opacus) erythropolis* HL PM-1.

The structures of the *aci*-nitro and the nitro form of 2H<sup>-</sup>-TNP were identified by <sup>1</sup>H NMR and <sup>13</sup>C NMR spectroscopy. The NMR data taken in D<sub>2</sub>O at pH 8.0 of the *aci*-nitro form corresponded with the data of authentic 2H<sup>-</sup>-TNP, also described by Ebert et al (6). The <sup>1</sup>H NMR spectrum (500 MHz, D<sub>2</sub>O) displayed one singlet at  $\delta = 3.8$  ppm, according to the four chemically equivalent protons in position 3 and 5 of the ring system. The <sup>13</sup>C NMR spectrum (126 MHz, D<sub>2</sub>O) showed one intense signal at  $\delta = 30$  ppm for the sp<sup>3</sup> carbon atoms C-3 and C-5. The sp<sup>2</sup> carbon atoms bearing the nitro substituents, C-2, C-4, and C-6 gave two signals at  $\delta = 119.76$  ppm and 120.55 ppm with a relative intensity of 2:1. The chemical shift at  $\delta = 175.19$  ppm was assigned to the carbonyl carbon atom C-1.

**Table 2. <sup>1</sup>H NMR (500 MHz, D<sub>2</sub>O) data of the nitro form of 2H<sup>-</sup>-TNP**



Position	$\delta$ [ppm]	Intensity	J [Hz]
H <sup>A</sup>	3.61	2	H <sup>A</sup> , H <sup>B</sup> (-) 11.73
H <sup>B</sup>	3.52	2	H <sup>A</sup> , H <sup>X</sup> 4.38
H <sup>X</sup>	3.74	1	H <sup>B</sup> , H <sup>X</sup> 6.53

The <sup>1</sup>H NMR spectrum (500 MHz, D<sub>2</sub>O) of the nitro form showed a heptuplet at  $\delta 3.74$  ppm and two doublets of doublets at  $\delta 3.61$  ppm and 3.52 ppm (Table 2). This resonance pattern was similar to the nitro form of protonated 2H<sup>-</sup>-TNT (26) and can be analyzed as an (AB)<sub>2</sub>X five-spin system. The signals at  $\delta 3.61$  ppm and 3.52 ppm correspond to the double set of diastereotopic methylene protons H<sup>A</sup> and H<sup>B</sup> at C-3

and C-5. The geminal coupling constant  $^2J$  ( $H^A$ ,  $H^B$ ) of 11.73 Hz demonstrated a doublet of doublets due to the symmetric equivalence of the diastereotopic methylene protons. The vicinal coupling constants (4.38 and 6.53 Hz) are assigned to the methylene spectrum between  $H^A$  and  $H^B$  on one side and the  $H^X$  proton on the other side. The  $H^X$  resonance displayed a heptuplet at  $\delta = 3.74$  ppm.

**Purification and molecular characterization of the nitrite-eliminating enzyme.** A nitrite-eliminating activity was found both in the crude extracts of *R. (opacus) erythropolis* HL PM-1 and *N. simplex* FJ2-1A, releasing stoichiometric amounts of nitrite from 2H-TNP. The enzyme was purified from *N. simplex* FJ2-1A according to the procedure shown in Table 3. The enzyme was purified 45-fold to a specific activity of 57 units  $mg^{-1}$  of protein. The overall yield was 3.3 % of the activity present in the cell extract. SDS-PAGE indicated a purity of > 95 % and an estimated molecular weight of 35.3 kDa. MALDI-TOF measurements gave a signal at  $m/z$  30.50 kDa. The molecular weight of the purified nitrite-eliminating enzyme as determined by gel filtration was estimated to be 42 kDa. N-terminal amino acid sequencing of the purified enzyme revealed the sequence M K N L E L A Y V G L (G) V H E X L V Y Y A A (Q/T) (H) L D (L) Y R (uncertain amino acids are in brackets). Database comparisons identified no similarity to any known protein sequences.

**Table 3. Purification of the nitrite-eliminating enzyme from *N. simplex* FJ2-1A.**

Purification step	Vol (ml)	Total protein (mg)	Sp act (U/mg)	Total activity (U)	Recovery (%)	Purification (fold)
Crude extract	35.0	340.20	1.27	432.68	100	1.0
Q Sepharose	9.0	37.10	4.10	151.0	35	3.2
Phenyl Superose	1.0	1.61	40.40	65.02	15	31.8
Gel filtration	0.4	0.25	57.0	14.3	3.3	44.9

**Conversion of the *aci*-nitro form of 2H<sup>-</sup>-TNP to H<sup>-</sup>-DNP by the nitrite-eliminating enzyme.** The enzymatic turnover of 2H<sup>-</sup>-TNP by the nitrite-eliminating enzyme was followed by repeated recording of UV-visible spectra (Fig. 2). The observation of isosbestic points at 338 and 413 nm indicated that the reaction mixture consisted of only the *aci*-nitro form of 2H<sup>-</sup>-TNP (pH = 8.0), assigned to the initial spectrum, and the reaction product H<sup>-</sup>-DNP, corresponding to the final spectrum.

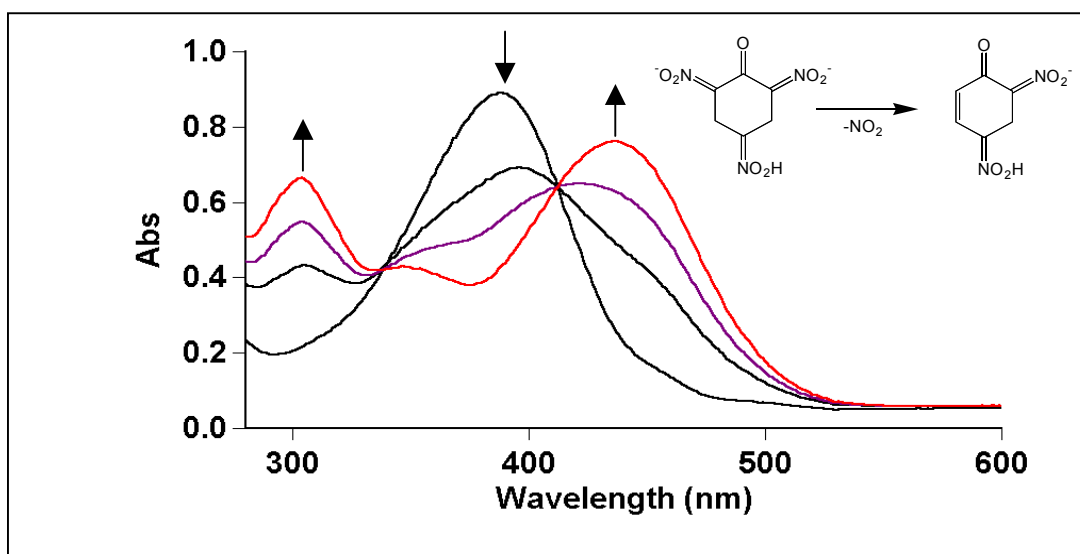


**Fig. 2:** Repeated recording of UV-visible spectra during an enzyme assay containing 0.1 mM 2H<sup>-</sup>-TNP and 6  $\mu$ g nitrite-eliminating enzyme (pH = 8.0). The spectra were recorded at intervals of 1 min.

During the turnover, stoichiometric amounts of nitrite were released. In order to identify H<sup>-</sup>-DNP, an authentic standard was prepared and identified by <sup>1</sup>H NMR (500 MHz, D<sub>2</sub>O) [ $\delta$  (H3, H3') = 3.83 ppm (s); d (H5) = 7.49 ppm (d); d (H6) = 5.89 ppm; J (H5, H6) = 10.2 Hz]. The results corresponded to the data presented by Behrend & Heesche-Wagner (3).

HPLC analysis of H<sup>-</sup>-DNP indicated a retention volume of 1.9 ml and the same UV-visible spectrum for both the standard and the product of the enzymatic conversion. Further evidence was given by HPLC-MS analysis, revealing a single peak at an ion mass of  $m/z$  185, which corresponded to the molecular ion [M]<sup>-</sup> of H<sup>-</sup>-DNP.

Since the results of the present study show that 2H<sup>-</sup>-TNP exists as two tautomeric structures, it was investigated whether the nitrite-eliminating enzyme possessed selectivity towards the *aci*-nitro or the nitro form. HPLC measurements gave evidence

that the nitrite-eliminating enzyme uses the *aci*-nitro form as the only substrate. The first columns in the diagram of Fig. 3 show that under physiological conditions (pH = 7.5) a concentration ratio of 20 % of the *aci*-nitro form and 80 % of the nitro form are present after equilibration (a). After addition of the nitrite-eliminating enzyme, only the *aci*-nitro form is transformed to H<sup>-</sup>-DNP (b). The proton-shift tautomerization by NpdH delivers the *aci*-nitro form (c). This is used as the sole substrate for the nitrite-eliminating enzyme (d).

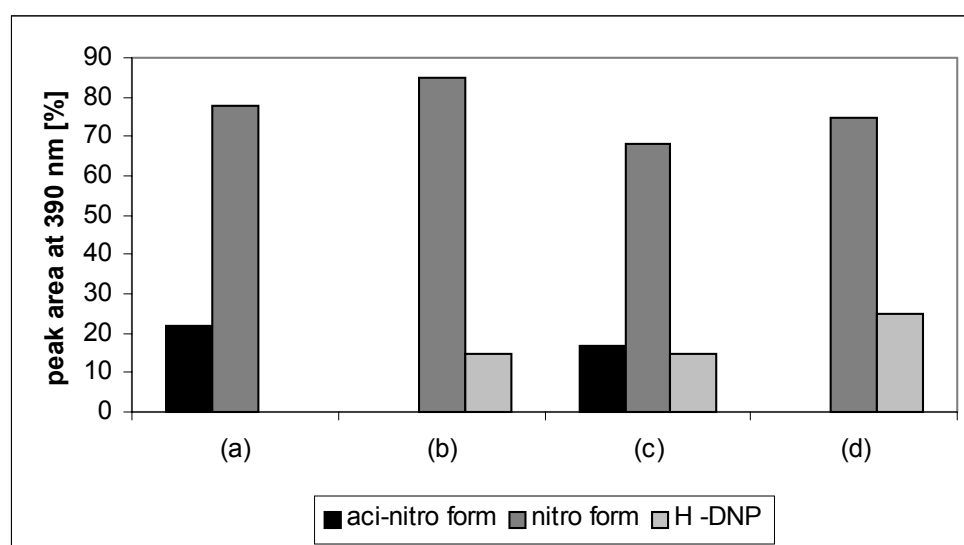


**Fig. 3:** Transformation of 2H<sup>-</sup>-TNP to H<sup>-</sup>-DNP by the 2H<sup>-</sup>-TNP tautomerase and the nitrite-eliminating enzyme: For each turnover the enzyme of the previous reaction was removed prior to HPLC analysis. (a) 2H<sup>-</sup>-TNP at pH = 7.5 after equilibration; (b) after addition of the nitrite-eliminating enzyme; (c) after addition of the 2H<sup>-</sup>-TNP tautomerase; (d) after addition of the nitrite-eliminating enzyme.



## Discussion

NpdH was formerly purified as a His-tag fusion protein from *R. (opacus) erythropolis* HL PM-1. Its activity was referred to as the transformation of 2H<sup>-</sup>-TNP to product X (10). However, no explicit function could be assigned to NpdH. The present results demonstrate that NpdH is a tautomerase, which catalyzes equilibration between the nitro form (previously referred to as product X) and the *aci*-nitro form of 2H<sup>-</sup>-TNP. Since the spontaneous proton-shift tautomerization occurred only from the protonated *aci*-nitro form of 2H<sup>-</sup>-TNP, it must be strictly pH dependent, i.e., the lower the pH value the more rapid is equilibration. This work provided evidence that under physiological conditions (pH = 7.4) 2H<sup>-</sup>-TNP exists as a mix of its *aci*-nitro and nitro form (Table 1). Nitrite elimination by the nitrite-eliminating enzyme was observed only from the *aci*-nitro form. Hence, the 2H<sup>-</sup>-TNP tautomerase appears to be responsible for avoiding accumulation of the metabolically inert nitro form.

A similar pH-dependent tautomeric equilibrium has been observed in the course of TNT degradation in *R. (opacus) erythropolis* HL PM-1, where the protonated dihydride-Meisenheimer complex of TNT (2H<sup>-</sup>-TNT) undergoes a pH-dependent tautomeric equilibration (26). Since *R. (opacus) erythropolis* HL PM-1 accumulates 2H<sup>-</sup>-TNT (26), the 2H<sup>-</sup>-TNP tautomerase seems to function only in 2,4,6-TNP catabolism. 2H<sup>-</sup>-TNT formed during TNT degradation is assumed to be a catabolic inert product (26). Pak et al. also described the formation of 2H<sup>-</sup>-TNT and suggested a misrouting by non-enzymatic dimerization, forming amino-dimethyl-tetranitrobiphenyl after partial denitration (18).

Oxygenolytic elimination of nitrite is frequently observed during the degradation of other nitroaromatic compounds. Nitrite is eliminated from mononitrophenols by monooxygenases yielding *ortho*- or *para*-dihydroxybenzenes (13, 27). Some bacteria eliminate a nitro group after initial vicinal dioxygenation to a dihydroxy intermediate, which was observed for 2-nitrotoluene (9) or 2,6-dinitrophenol (8, 17).

As far as we know, the nitrite-eliminating enzyme is the first enzyme in nitroaromatics degradation which can release nitrite by a non-oxygenolytic mechanism.

Although H<sup>-</sup>-DNP was formerly proven to be a metabolite of TNP degradation (3, 6), we have shown here that the conversion of the *aci*-nitro form of 2H<sup>-</sup>-TNP to H<sup>-</sup>-DNP is catalyzed by the nitrite-eliminating enzyme.

## Acknowledgements

Many sincere thanks to Silvia Lakner for biomolecular works, Peter Fischer and Jochen Rebell for NMR measurements, and Günther Tovar and Jürgen Schmucker for MALDI-TOF measurements. We thank DuPont de Nemours Company for supplying us with *Nocardioides simplex* FJ2-1A and Lacy Daniels for providing us F<sub>420</sub>. The work was supported by the German Research Foundation (DFG).

## References

1. **Altschul, S. F., T. L. Madden, A. A. Schaffer, J. Zhang, Z. Zhang, W. Miller, and D. J. Lipman.** 1997. Gapped BLAST and PSI-BLAST: a new generation of protein database search programs. *Nucleic Acids Res.* **25**:3389-3402.
2. **Ausubel, F. M., R. Brent, R. E. Kingston, D. D. Moore, J. G. Seidmann, J. A. Smith, and K. Struhl.** 2001. *Current protocols in molecular biology.* Wiley and Sons, Inc., New York.
3. **Behrend, C. and K. Heesche-Wagner.** 1999. Formation of hydride-Meisenheimer complexes of picric acid (2,4, 6- trinitrophenol) and 2,4-dinitrophenol during mineralization of picric acid by *Nocardioides* sp. strain CB 22-2. *Appl. Environ. Microbiol.* **65**:1372-1377.
4. **Blasco, R., E. Moore, V. Wray, D. Pieper, K. Timmis, and F. Castillo.** 1999. 3-nitroadipate, a metabolic intermediate for mineralization of 2, 4- dinitrophenol by a new strain of a *Rhodococcus* species. *J. Bacteriol.* **181**:149-152.
5. **Bradford, M. M.** 1976. A rapid and sensitive method for the quantitation of microgram quantities of protein utilizing the principle of protein-dye binding. *Anal. Biochem.* **72**:248-254.
6. **Ebert, S., Fischer P., and H. J. Knackmuss.** 2002. Converging catabolism of 2,4,6-trinitrophenol (picric acid) and 2,4-dinitrophenol by *Nocardioides simplex* FJ2-1A. *Biodegradation* **12**:367-376.
7. **Ebert, S., P. G. Rieger, and H. J. Knackmuss.** 1999. Function of coenzyme F<sub>420</sub> in aerobic catabolism of 2,4,6-trinitrophenol and 2,4-dinitrophenol by *Nocardioides simplex* FJ2-1A. *J. Bacteriol.* **181**:2669-2674.
8. **Ecker, S., T. Widmann, H. Lenke, Dickel O., Fischer P., C. Bruhn, and H. J. Knackmuss.** 1992. Catabolism of 2,6-dinitrophenol by *Alcaligenes eutrophus* JMP 134 and JMP 222. *Arch. Microbiol.* **158**:149-154.

9. **Haigler, B. E., W. H. Wallace, and J. C. Spain.** 1994. Biodegradation of 2-nitrotoluene by *Pseudomonas* sp. strain JS42. *Appl. Environ. Microbiol.* **60**:3466-3469.
10. **Heiss, G., K. W. Hofmann, N. Trachtmann, D. M. Walters, P. Rouviere, and H. J. Knackmuss.** 2002. *npd* gene functions of *Rhodococcus (opacus) erythropolis* HL PM-1 in the initial steps of 2,4,6-trinitrophenol degradation. *Microbiology* **148**:799-806.
11. **Hess, T. F., S. K. Schmidt, J. Silverstein, and B. Howe.** 1990. Supplemental substrate enhancement of 2,4-dinitrophenol mineralization by a bacterial consortium. *Appl. Environ. Microbiol.* **56**:1551-1558.
12. **Inoue, H., H. Nojima, and H. Okayama.** 1990. High efficiency transformation of *Escherichia coli* with plasmids. *Gene* **96**:23-28.
13. **Kadiyala, V. and J. C. Spain.** 1998. A two-component monooxygenase catalyzes both the hydroxylation of p- nitrophenol and the oxidative release of nitrite from 4-nitrocatechol in *Bacillus sphaericus* JS905. *Appl. Environ. Microbiol.* **64**:2479-2484.
14. **Laemmli, U. K.** 1970. Cleavage of structural proteins during the assembly of the head of bacteriophage T4. *Nature* **227**:680-685.
15. **Lenke, H. and H. J. Knackmuss.** 1992. Initial hydrogenation during catabolism of picric acid by *Rhodococcus erythropolis* HL 24-2. *Appl. Environ. Microbiol.* **58**:2933-2937.
16. **Montgomery, H. A. C.** 1961. The determination of nitrite in water. *Analyst* **86**:414-416.
17. **Nishino, S. F., G. C. Paoli, and J. C. Spain.** 2000. Aerobic degradation of dinitrotoluenes and pathway for bacterial degradation of 2,6-dinitrotoluene. *Appl. Environ. Microbiol.* **66**:2139-2147.

18. **Pak, J. W., K. L. Knoke, D. R. Noguera, B. G. Fox, and G. H. Chambliss.** 2000. Transformation of 2,4,6-trinitrotoluene by purified xenobiotic reductase B from *Pseudomonas fluorescens* I-C. *Appl. Environ. Microbiol.* **66**:4742-4750.
19. **Pearson, W. R. and D. J. Lipman.** 1988. Improved tools for biological sequence comparison. *Proc. Natl. Acad. Sci. U.S.A* **85**:2444-2448.
20. **Pfennig, N. and K. D. Lippert.** 1966. Über das Vitamin B12-Bedürfnis phototropher Schwefelbakterien. *Arch. Microbiol.* **55**:245-256.
21. **Rajan, J., K. Valli, R. E. Perkins, F. S. Sariaslani, S. M. Barns, A. L. Reysenbach, S. Rehm, M. Ehringer, and N. R. Pace.** 1996. Mineralization of 2,4,6-trinitrophenol (picric acid): characterization and phylogenetic identification of microbial strains. *J. Ind. Microbiol.* **16**:319-324.
22. **Russ, R., D. M. Walters, H. J. Knackmuss, and P. E. Rouviere.** 2000. Identification of genes involved in picric acid and 2,4-dinitrophenol degradation by mRNA differential display, p. 127-143. *In* J. C. Spain, J. B. Hughes, and H. J. Knackmuss (eds.), *Biodegradation of nitroaromatic compounds and explosives*. Boca Raton, Fla.
23. **Sambrook, J., E. F. Fritsch, and T. Maniatis.** 1989. *Molecular cloning: a laboratory manual*. Cold Spring Harbor Laboratory, Cold Spring Harbor, N.Y.
24. **Severin, T. and M. Adam.** 1963. Umsetzung von Nitroaromaten mit Borhydrid II. *Chem. Ber.* **96** :448-452.
25. **Severin, T. and R. Schmitz.** 1962. Umsetzung von Nitroaromaten mit Natriumborhydrid. *Chem. Ber.* **95**:1417-1419.
26. **Vorbeck, C., H. Lenke, P. Fischer, J. C. Spain, and H. J. Knackmuss.** 1998. Initial reductive reactions in aerobic microbial metabolism of 2,4,6-trinitrotoluene. *Appl. Environ. Microbiol.* **64**:246-252.
27. **Zeyer, J. and H. P. Kocher.** 1988. Purification and characterization of a bacterial nitrophenol oxygenase which converts ortho-nitrophenol to catechol and nitrite. *J. Bacteriol.* **170**:1789-1794.

## **Appendix 3**

# **Hydrolytic Ring Cleavage in the Biodegradation of 2,4,6-Trinitrophenol (Picric Acid) and 2,4- Dinitrophenol**

(Submitted at Appl. Environ. Microbiol.)

**Klaus W. Hofmann, Hans-Joachim Knackmuss\*, and Gesche Heiss**

Institute of Microbiology, University of Stuttgart, Allmandring 31, 70569 Stuttgart,  
Germany

Running title: 2,4-DNCH hydrolase in TNP and DNP biodegradation

\*Corresponding author: Phone: +49-(0)7152-52930. e-mail: imbhjk@po.uni-stuttgart.de

## Abstract

The hydride Meisenheimer complex of 2,4-dinitrophenol ( $H^-$ -DNP), a metabolite of 2,4,6-trinitrophenol and 2,4-dinitrophenol degradation in *Rhodococcus (opacus) erythropolis* HL PM-1 and *Nocardioides simplex* FJ2-1A, was hydrogenated to the dihydride complex of 2,4-DNP ( $2H^-$ -DNP), as shown by HPLC-MS. The enzyme for this hydride transfer is the hydride transferase I, which requires a NADPH-dependent  $F_{420}$  reductase and the coenzymes  $F_{420}$  and NADPH. Under physiological conditions  $2H^-$ -DNP is protonated, producing 2,4-dinitrocyclohexanone (2,4-DNCH). A 2,4-DNCH hydrolase from *N. simplex* FJ2-1A was purified and shown to be responsible for ring fission of 2,4-DNCH, generating 4,6-dinitrohexanoate (4,6-DNH). 4,6-DNH was identified by HPLC-MS and proven to be a true catabolite by turnover of 2,4-DNCH with crude extracts of *R. (opacus) erythropolis* HL PM-1 and *N. simplex* FJ2-1A.

## Abbreviations

2,4-DNCH, 2,4-dinitrocyclohexanone; DNP, 2,4-dinitrophenol;  $H^-$ -DNP, hydride  $\sigma$ -complex of 2,4-dinitrophenol;  $H^-$ -TNP, hydride  $\sigma$ -complex of 2,4,6-trinitrophenol;  $2H^-$ -TNP, dihydride  $\sigma$ -complex of 2,4,6-trinitrophenol; HTI, hydride transferase I; HTII, hydride transferase II; NDFR, NADPH-dependent  $F_{420}$  reductase; 2-NCH, 2-nitrocyclohexanone; TNP, 2,4,6-trinitrophenol.

## Introduction

Bacterial degradation of nitroaromatic compounds has been investigated with several bacterial strains, and different pathways were described. Mononitrophenols are hydroxylated by monooxygenases yielding *ortho*- or *para*-dihydroxybenzene (13, 23, 23), whereas initial dioxygenation to a dihydroxy intermediate was observed for 2-nitrotoluene (9) or 2,6-dinitrophenol (8, 18, 18). As with other aromatic compounds the general principle of aerobic degradation is initial hydroxylation generating 1,2- or 1,4-dihydroxy nitrocyclohexadienes. These diols are sufficiently reactive for oxygenolytic ring cleavage. In contrast, the initial reactions in the degradation pathway of 2,4,6-trinitrophenol (TNP) are two consecutive hydrogenation steps at the electron deficient carbon ring, catalyzed by a NADPH-dependent  $F_{420}$  reductase (NDFR) and two hydrid transferases (HTII and HTI) (Fig. 1). The product of the first hydrogenation step is the hydride complex of TNP ( $H^-$ -TNP), and the second hydrogenation yields the dihydride complex of TNP ( $2H^-$ -TNP) (7, 10, 14). Both reactions require the coenzymes NADPH and  $F_{420}$ . Recently it was shown that  $2H^-$ -TNP exists as two tautomeric structures, the *aci*-nitro and the nitro form. Furthermore a  $2H^-$ -TNP tautomerase was described, preventing the accumulation of the nitro form as a dead-end product (11). In the subsequent step a nitrite-eliminating enzyme catalyzes the release of nitrite from the *aci*-nitro form of  $2H^-$ -TNP, forming the hydride complex of 2,4-dinitrophenol ( $H^-$ -DNP) (11). Previous investigations also described  $H^-$ -DNP as a metabolite of the degradation pathway of TNP and DNP (4, 7).

In this communication we describe the hydrogenation of  $H^-$ -DNP by the HTI and the mechanism of the carbon ring fission by a 2,4-dinitrocyclohexanone (2,4-DNCH) hydrolase.



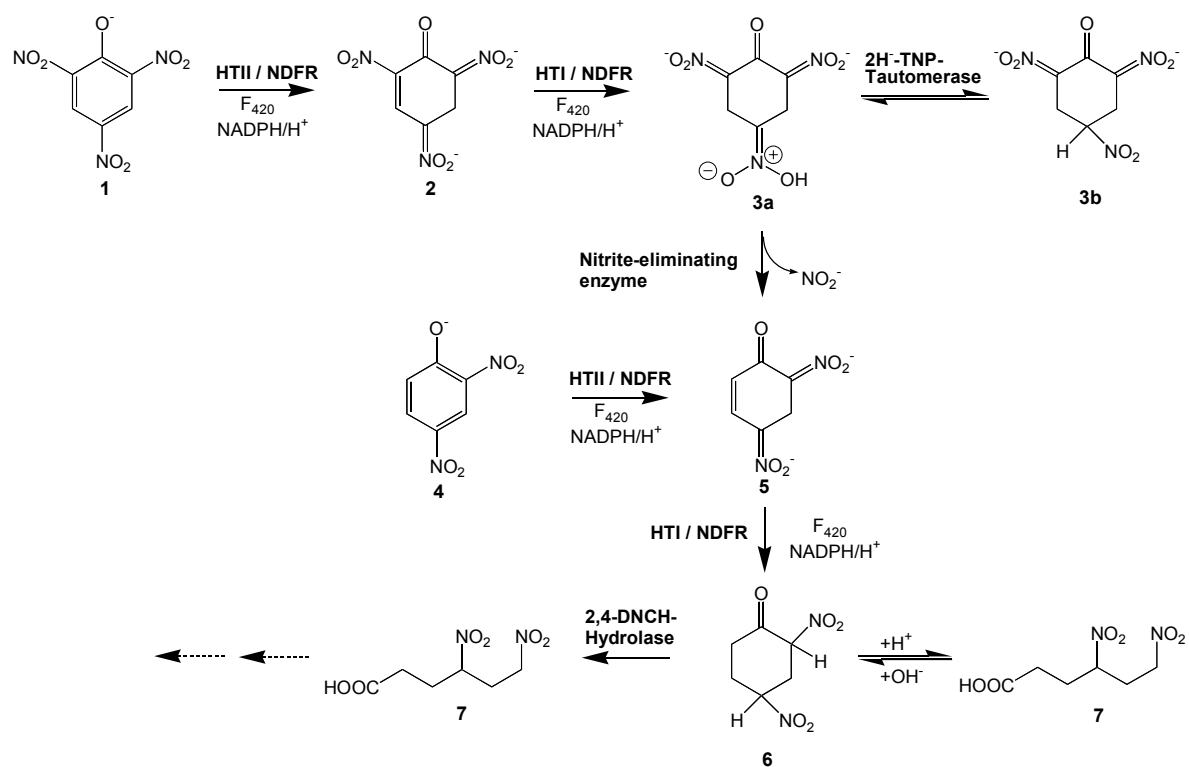


**Fig. 1:** Degradation pathway of TNP and DNP. (1) TNP, (2) H-TNP, (3a) *aci*-nitro form of 2H-TNP, (3b) nitro form of 2H-TNP, (4) DNP, (5) H-DNP, (6) 2,4-DNCH, (7) 4,6-DNH. HTI, hydride transferase I; HTII, hydride transferase II; NDFR, NADPH-dependent  $F_{420}$  reductase.

## Materials and Methods

**Organisms and culture conditions.** *Nocardiooides simplex* FJ2-1A was cultured and stored as described before (11). *N. simplex* FJ2-1A and *R. (opacus) erythropolis* HL PM-1 were also grown with 0.7 mM 2-nitrocyclohexanone (2-NCH) as the sole nitrogen source.

The recombinant strains *Escherichia coli* TOP10 (pDMW10), *E. coli* JM109 (pNTG6), and *E. coli* BL21 (DE3), and *E. coli* BL21 (DE3) (pSLK1) were cultured as described previously (10).

**Molecular techniques.** Standard protocols were used for manipulation of DNA (2, 2, 20, 20, 20). Plasmid DNA was isolated using FlexiPrep Kit (Amersham Biosciences, Freiburg, Germany). *E. coli* was transformed according to Inoue et al (12).

**Cloning of HTI from *N. simplex* FJ2-1A.** The PCR reaction mixture contained 1 ng template DNA, 2.5 U *Pwo*-DNA-polymerase (Peqlab, Erlangen, Germany), 2 mM MgSO<sub>4</sub>, 0.25 mM each dNTP and 25 pmol each primer. Thirty-five amplification cycles were performed as follows: 65 °C for 30 s, 68 °C for 1 min, and 96 °C for 30 s. The primers were designed to contain a *Nde*I restriction site (underlined) and blunt end, respectively (5'-CGTCATATGAAAGGTTGGAATCAGGATCCC-3' and 5'-TCACGGGAGCCGGTGCGCGGCG-3'). Primers were purchased from Eurogentec (Köln, Germany). The PCR fragment was eluted from agarose using the Easypure DNA purification kit (Biozym Diagnostics, Hessisch Oldendorf, Germany), restricted with the appropriate restriction enzymes and ligated into pET11a\* (10).

**Preparation of cell extracts.** Cells were lysed and the protein concentration determined as described before (11).

**Purification of the HTI and NDFR.** HTI and NDFR were expressed from *E. coli* JM109 (pNTG6), *E. coli* BL21 (pHTI-FJ), and *E. coli* TOP10 (pDMW10), respectively, and purified as His-tag fusion proteins as described before (10).

**Purification of the 2,4-DNCH hydrolase.** The cell extract of *N. simplex* FJ2-1A (340 mg of protein) was passed through a Q Sepharose column (1.6 X 10 cm) preequilibrated with basic buffer (50 mM Tris-HCl [pH = 7.5]). The protein was eluted from the column with a linear gradient (200 ml) of 0 to 1 M NaCl in basic buffer at a NaCl concentration of approximately 0.33 M. Ammonium sulfate was added to a final concentration of 1 M. The solution was applied to a Phenyl Superose HR column (1 X 10 cm) preequilibrated with 1 M ammonium sulfate in basic buffer. The enzyme was eluted with a linear gradient (65 ml) of 1 to 0 M ammonium sulfate in basic buffer at a concentration of approximately 0.54 M  $(\text{NH}_4)_2\text{SO}_4$ . The pooled protein fractions were concentrated with a Vivaspin 2 ml concentrator (Sartorius) to a total volume of 1 ml, loaded onto a Superdex 200 Prep-Grade gel filtration column (1 X 30 cm), and eluted with basic buffer.

The molecular mass of the native 2,4-DNCH hydrolase was determined, using a gel filtration calibration kit (Amersham Pharmacia, Freiburg, Germany). The purity and the molecular mass of the protein subunits was determined by MALDI-TOF with a G1025A Hewlett Packard LD-TOF system (GSG Mess- und Analysengeräte Vertriebsgesellschaft mbH, Karlsruhe, Germany) and by SDS-PAGE with a 15 % polyacrylamide gel by the method of Laemmli (1970) (7) on a Mini-PROTEAN 3 electrophoresis cell (Bio-Rad, München, Germany).

**Enzyme assays.** Enzyme assays were performed with a Cary 50 Biospectrophotometer controlled by Cary WinUV Biopackage software (Varian, Mulgrave, Australia). Enzyme activity of the HTI was measured by spectrophotometric determination of the decrease in absorbance of  $\text{H}^-$ -DNP at 450 nm. The test was conducted in 50 mM phosphate buffer (pH = 8.0) containing 100  $\mu\text{M}$   $\text{H}^-$ -DNP, 125  $\mu\text{M}$  NADPH, 11  $\mu\text{M}$   $\text{F}_{420}$ . 5  $\mu\text{g}$  NDFR was added and the assay was started after 1 min with 30  $\mu\text{g}$  HTI. Reaction rates were calculated by using the experimentally determined extinction coefficient of 944  $\text{M}^{-1} \text{cm}^{-1}$  ( $\text{H}^-$ -2,4-DNP at 450 nm, 20 °C, pH = 8.0). One unit of enzyme activity was defined as the amount of enzyme that converts 1  $\mu\text{mol}$  of substrate per min. The turnover was further observed by repeated recording of UV-visible spectra between 280 and 600 nm in 1 min cycles.

Enzyme activity of the 2,4-DNCH hydrolase was detected by repeated recording of UV-visible spectra between 280 and 600 nm. Spectra were recorded every minute. The reaction was performed in 50 mM Tris-HCl (pH = 8.0) or 50 mM phosphate buffer (pH = 8.0), containing 4  $\mu$ g 2,4-DNCH hydrolase and 100  $\mu$ M 2-NCH (commercially available substrate) or 2,4-DCNH (catabolic substrate, obtained by the turnover of H<sup>-</sup>-DNP by HTI and NDFR).

**Analytical Methods.** Metabolites were detected and quantified at 210, 340, 390, and 420 nm by an HPLC system (Chromeleon Chromatography Data Systems 4.38, equipped with a Dionex UV/Vis detector, UVD 170S/340S, a Dionex pump, P 580, and a Dionex autosampler, Gina 50, Dionex, Idstein, Germany) with a Lichrosphere 100 RP-18 column (250 X 4 mm, particle size 5  $\mu$ m, Merck, Darmstadt, Germany). The mobile phase consisted of 20 % (v/v) MeOH and 80 % (v/v) 50 mM phosphate buffer (pH = 8.0).

Liquid chromatography (LC) mass spectra were obtained by negative-mode electrospray ionization (ESI) on a HP1100 HPLC system (Hewlett Packard, Waldbronn, Germany) coupled to a VG Plattform II Quadrupol mass spectrometer (Manchester, GB). Samples were resolved on a Lichrosorb 100 RP-18 column (250 X 4 mm, particle size 5  $\mu$ m, Merck). The mobile phase consisted of 20 % MeOH and 5 mM ammonium formate buffer (pH = 8.0).

**Amino acid sequencing and sequence analysis.** The purified 2,4-DNCH hydrolase was subjected to automatic sequencing by a Protein Sequencing System 476 (Applied Biosystems, Foster City, USA). Database searches were performed with BLAST (1) and FASTA (19).

**Chemicals.** H<sup>-</sup>-DNP was prepared according to Severin & Schmitz (21) and stored at -20 °C. All chemicals used were of the highest available purity and were purchased from Fluka (Taufkirchen, Germany), Gerbu (Gaiberg, Germany), Merck (Darmstadt, Germany), Roth (Karlsruhe, Germany), and Sigma-Aldrich (Taufkirchen, Germany).

## Results

**HTI converts H<sup>-</sup>-DNP to 2,4-DNCH.** Repetitive spectroscopic scans during the turnover of H<sup>-</sup>-DNP by the HTIs of *R. (opacus) erythropolis* HL PM-1 and *N. simplex* FJ2-1A showed a decrease in absorbance at 441 and 306 nm, the absorption maxima of H<sup>-</sup>-DNP. A concomitant increase in absorbance at 340 nm demonstrated the generation of a new product (Fig. 2), and HPLC analysis revealed a metabolite with a retention volume of 3.2 ml. The corresponding UV-visible spectrum displayed absorbance maxima at 232 and 340 nm. For further identification the new product was subjected to coupled HPLC-ESI<sup>-</sup>-MS and the intense signal at *m/z* 187 was assigned to the molecular anion [M]<sup>-</sup> of 2H<sup>-</sup>-DNP. Under physiological conditions (pH = 7.5) 2H<sup>-</sup>-DNP is protonated to 2,4-DNCH.

In comparison with the HTIs, the HTIIs of *R. (opacus) erythropolis* HL PM-1 and *N. simplex* FJ2-1A did not possess activity for H<sup>-</sup>-DNP.

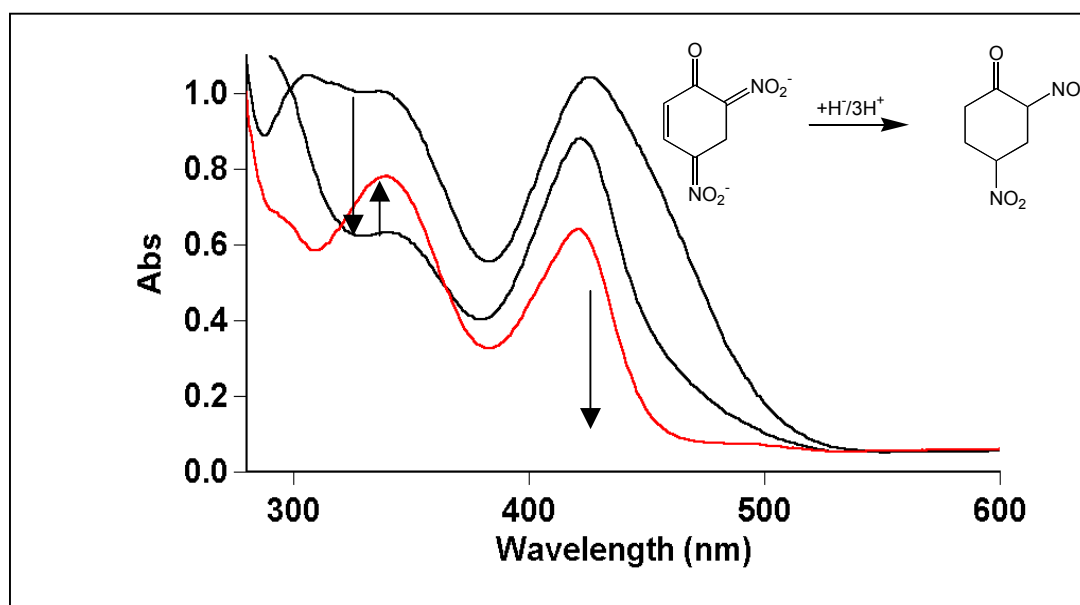


**Fig. 2:** Conversion of H<sup>-</sup>-DNP to 2,4-DNCH by the hydride transferase I in the presence of the NADPH-dependent F<sub>420</sub> reductase plus the coenzymes F<sub>420</sub> and NADPH. Scans were recorded at 1 min intervals. Residual absorbance at 420 nm is due to F<sub>420</sub>.

### **Purification and characterization of the 2,4-DNCH hydrolase.**

2,4-DNCH was unavailable by chemical synthesis. Since the analogous compound 2-NCH was commercially obtainable, it was used for further experiments. Both *N. simplex* FJ2-1A and *Rhodococcus (opacus) erythropolis* HL PM-1 were able to grow on 2-NCH as the sole source of nitrogen. Crude extracts of both strains grown with DNP and 2-NCH showed activity for 2-NCH and biologically generated 2,4-DNCH. To identify the enzyme, cell extract of *N. simplex* FJ2-1A was subjected to FPLC purification, using 2-NCH as a test substrate. After three purification steps SDS-PAGE showed one polypeptide band at 15.3 kDa with a purity of > 98 %. The molecular mass was determined by MALDI-TOF measurements, giving a signal at  $m/z$  16.989 kDa. Since the molecular weight of the purified enzyme estimated from gel filtration was 63 kDa, it can be assumed that the enzyme consists of four identical subunits. N-terminal amino acid sequencing of the purified protein by automated Edman degradation revealed the sequence M R K F W (H) V G I N V T D M D K S I E F Y R K V G F D V (S) Q (S) K (uncertain amino acids are in brackets). FASTA (19) search assigned a sequence identity of 78 % to the product of *orfF*, which encodes a putative lyase in *R. (opacus) erythropolis* HL PM-1 (accession number AAK38100) (22). Comparison with *orf3* of *N. simplex* FJ2-1A (6) showed 100 % sequence identity.

The 2,4-DNCH hydrolase was specific for 2,4-DNCH and 2-NCH and showed no activity for other metabolites of the catabolic pathway (such as TNP, H<sup>-</sup>-TNP, 2H<sup>-</sup>-TNP, or H<sup>-</sup>-DNP). Repeated UV-visible spectroscopic scans displayed a decrease in absorbance at 340 nm, indicating the disappearance of 2,4-DNCH. HPLC analysis revealed a new product with a retention volume of 3.4 ml. The corresponding UV-visible spectrum displayed a maximum in absorbance at 203 nm and a band of low intensity at 255 nm. The data were in agreement with the properties of 4,6-dinitrohexanoate (4,6-DNH) described by Lenke et al. (16). Further confirmation of the structure was obtained by coupled HPLC-ESI<sup>-</sup>-MS analysis. A signal at  $m/z$  205 corresponded to the molecular anion [M<sup>-</sup>] of 4,6-DNH.

### **Chemical and enzymatic hydrolysis of 2,4-DNCH.**

Hydrolysis of 2,4-DNCH, generating 4,6-DNH, was shown to be a pH dependent equilibrium by comparing UV-visible spectra under basic and acidic conditions. In

alkalic solution ( $\text{pH} > 8$ ) the equilibrium contained only 2,4-DNCH, whereas 4,6-DNH predominated under acidic conditions ( $\text{pH} < 5$ ).

Fig. 3 shows the gradual formation of 4,6-DNH from 2,4-DNCH under physiological conditions at  $\text{pH} = 7.5$ . The spontaneous reaction rate was very low. In the presence of  $2 \mu\text{g}$  2,4-DNCH hydrolase, ring cleavage accelerated dramatically: after 10 min, a 15-fold increase in the amount of 4,6-DNH was measured. Chemical decomposition of 4,6-DNH at  $\text{pH} 7.5$  became apparent after 30 min. This was due to the instability of 4,6-DNH, as described formerly (16).

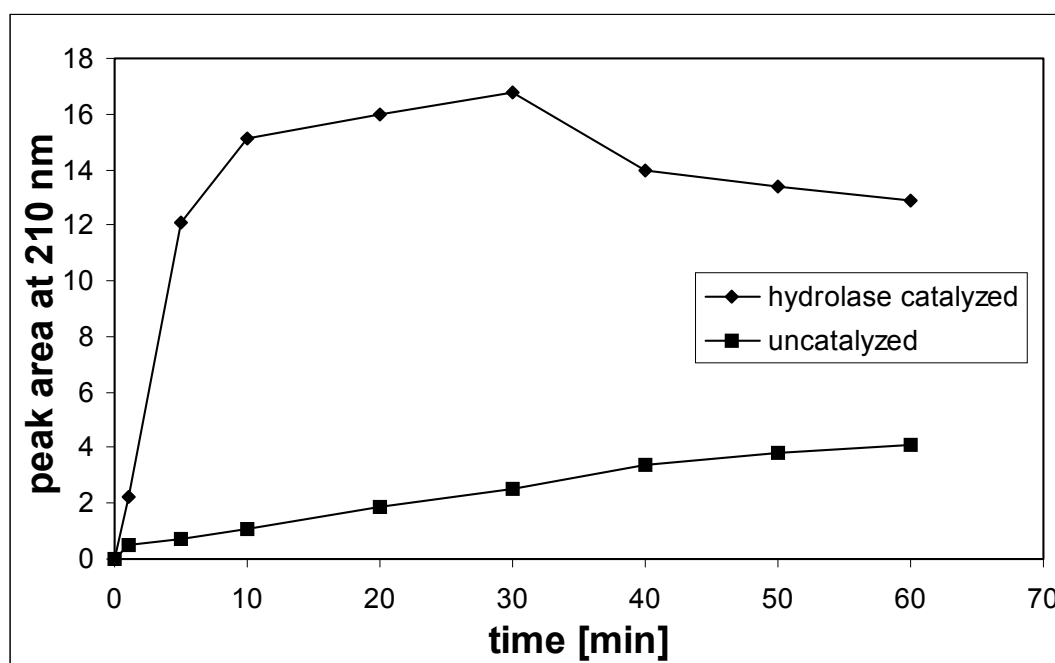


**Fig. 3:** Increase of 4,6-DNH during chemical or enzymatic ring fission of 2,4-DNCH at  $\text{pH} = 7.5$ , measured by HPLC.

**Conversion of 4,6-DNH by crude extracts.** Experiments were conducted to examine whether 4,6-DNH was further metabolized. Turnover of 4,6-DNH by crude extracts of *R. (opacus) erythropolis* HL PM-1 and *N. simplex* FJ2-1A was followed by HPLC analysis. The peak with a retention volume of 3.4 ml immediately disappeared after incubation with crude extracts, whereas a new product could not be detected by HPLC. Reactions in the absence of crude extract or performed with crude extracts of *E. coli* BL21 (DE3) only showed the disappearance of 4,6-DNH after 3-4 h, due to the chemical decomposition.

## Discussion

H<sup>-</sup>-DNP is the first denitration product of TNP, generated by a nitrite-eliminating enzyme with 2H<sup>-</sup>-TNP as substrate (11). The HTIIs of *R. (opacus) erythropolis* HL PM-1 and *N. simplex* FJ2-1A, hydrogenate not only picric acid but also DNP, forming H<sup>-</sup>-DNP as product (7, 10). Thus, H<sup>-</sup>-DNP is a common metabolite of the convergent pathway of picric acid and DNP. Until recently the fate of H<sup>-</sup>-DNP was unclear. Behrend & Heesche Wagner found that NADPH is required for further degradation by *Nocardioides* sp. CB 22-2 (4) and suggested that a monooxygenolytic hydroxylation at the *para* position may take place, forming 2-nitrohydroquinone with release of nitrite. An alternative hypothetical pathway for H<sup>-</sup>-DNP transformation was assumed by Lenke et al. (14). The authors proposed that H<sup>-</sup>-DNP could be converted to 2H<sup>-</sup>-DNP by another hydride transfer, which finally could give rise to 4,6-DNH.

The results of the present work confirm the latter hypothesis. The HTIs of *R. (opacus) erythropolis* HL PM-1 and *N. simplex* FJ2-1A were shown to hydrogenate H<sup>-</sup>-DNP, forming 2H<sup>-</sup>-DNP, which gives rise to 2,4-DNCH after protonation. The mechanism is analogous to the reduction of H<sup>-</sup>-TNP (Fig. 1). In the presence of NDFR, the coenzyme F<sub>420</sub>, and NADPH, hydride is transferred to the C5 carbon atom of H<sup>-</sup>-DNP. Since the HTIIs of *R. (opacus) erythropolis* HL PM-1 and *N. simplex* FJ2-1A showed no activity with H<sup>-</sup>-DNP, the additional hydride transferase, HTI, is necessary to catalyze the hydrogenation of H<sup>-</sup>-DNP.

A 2,4-DNCH hydrolase was identified and purified from *N. simplex* FJ2-1A, catalyzing the hydrolytic ring fission of 2,4-DNCH. Since the sequence showed high similarity to the N-terminal end of the gene product of *orfF* of *R. (opacus) erythropolis* HL PM-1, we suggest that the gene product of *orfF* is a hydrolase and we thus name the gene *npdF*.

Chemical hydrolysis of 2-NCH under basic conditions has been described by several groups as a reverse Claisen condensation (3, 17). We also confirmed that the hydrolytic ring opening is part of a pH-dependent equilibrium between 2,4-DNCH and 4,6-DNH. However, under physiological conditions (pH = 7.5) the reaction is very slow and a 2,4-DNCH hydrolase is necessary to increase the reaction rate



dramatically and to produce high amounts of 4,6-DNH within a short time period (Fig. 3).

Crude extracts of *R. (opacus) erythropolis* HL PM-1 or *N. simplex* FJ2-1A further converted 4,6-DNH. This suggests that 4,6-DNH is a true metabolite in the biodegradation of TNP and DNP. This differs from previous findings, in which 4,6-DNH was suggested to be chemically formed as a minor dead-end product by spontaneous hydrolysis (15).

Blasco et al. (5) proposed an alternative pathway of DNP degradation based on the detection of 3-nitroadipate in the supernatant of resting cell experiments with *Rhodococcus* sp. strain RB1. The authors hypothesized that Meisenheimer intermediates, H<sup>-</sup>-DNP and 2H<sup>-</sup>-DNP, are generated by two successive hydride transfers. Subsequent *ortho* ring fission of 2H<sup>-</sup>-DNP with a concomitant release of nitrite, catalyzed by an oxygenase, was proposed to form 3-nitroadipate.

Behrend & Heesche-Wagner (4) published another hypothetical mechanism for NADPH-dependent conversion of H<sup>-</sup>-DNP in *N. simplex* CB22-2, proposing 2-nitrohydroquinone as an intermediate and subsequent oxygenolytic ring opening. Neither Blasco et al. nor Behrend & Heesche-Wagner gave evidence for their mechanisms, whereas the present communication confirms the generation of 2,4-DNCH by hydrogenation and the subsequent oxygen-independent ring fission.

In contrast to what has been known about aerobic catabolism of aromatic compounds, the high electron deficiency in polynitroaromatics favors initial hydrogenation steps rather than oxygenation reactions. As a consequence, hydrolytic ring fission of 2,4-DNCH, instead of oxygenolytic cleavage, is promoted.

## Acknowledgements

Many sincere thanks to Silvia Lakner for biomolecular works and Günther Tovar and Jürgen Schmucker for MALDI-TOF measurements. We thank DuPont de Nemours Company for supplying us with *Nocardioides simplex* FJ2-1A and Lacy Daniels for providing us F<sub>420</sub>. The work was supported by the German Research Foundation (DFG).

## References

1. **Altschul, S. F., T. L. Madden, A. A. Schaffer, J. Zhang, Z. Zhang, W. Miller, and D. J. Lipman.** 1997. Gapped BLAST and PSI-BLAST: a new generation of protein database search programs. *Nucleic Acids Res.* **25**:3389-3402.
2. **Ausubel, F. M., R. Brent, R. E. Kingston, D. D. Moore, J. G. Seidmann, J. A. Smith, and K. Struhl.** 2001. *Current protocols in molecular biology.* Wiley and Sons, Inc., New York.
3. **Ballini, R. and M. Petrini.** 1986. Ring cleavage of cyclic 2-nitroketones by KF catalyst: a general synthesis of  $\omega$ -nitroacids and  $\omega$ -nitroesters. *Synth. Commun.* **16**:1781-1788.
4. **Behrend, C. and K. Heesche-Wagner.** 1999. Formation of hydride-Meisenheimer complexes of picric acid (2,4, 6- trinitrophenol) and 2,4-dinitrophenol during mineralization of picric acid by *Nocardioides* sp. strain CB 22-2. *Appl. Environ. Microbiol.* **65**:1372-1377.
5. **Blasco, R., E. Moore, V. Wray, D. Pieper, K. Timmis, and F. Castillo.** 1999. 3-nitroadipate, a metabolic intermediate for mineralization of 2, 4- dinitrophenol by a new strain of a *Rhodococcus* species. *J. Bacteriol.* **181**:149-152.
6. **Ebert, S.** 2001. Enzyme, Gene und Mechanismen des oberen Abbauweges von Pikrinsäure und 2,4-Dinitrophenol durch *Nocardioides simplex* FJ2-1A. Ph.D. thesis. University of Stuttgart, Stuttgart, Germany.
7. **Ebert, S., Fischer P., and H. J. Knackmuss.** 2002. Converging catabolism of 2,4,6-trinitrophenol (picric acid) and 2,4-dinitrophenol by *Nocardioides simplex* FJ2-1A. *Biodegradation* **12**:367-376.
8. **Ecker, S., T. Widmann, H. Lenke, Dickel O., Fischer P., C. Bruhn, and H. J. Knackmuss.** 1992. Catabolism of 2,6-dinitrophenol by *Alcaligenes eutrophus* JMP 134 and JMP 222. *Arch. Microbiol.* **158**:149-154.

9. **Haigler, B. E., W. H. Wallace, and J. C. Spain.** 1994. Biodegradation of 2-nitrotoluene by *Pseudomonas* sp. strain JS42. *Appl. Environ. Microbiol.* **60**:3466-3469.
10. **Heiss, G., K. W. Hofmann, N. Trachtmann, D. M. Walters, P. Rouviere, and H. J. Knackmuss.** 2002. *npd* gene functions of *Rhodococcus (opacus) erythropolis* HL PM-1 in the initial steps of 2,4,6-trinitrophenol degradation. *Microbiology* **148**:799-806.
11. **Hofmann, K. W., Knackmuss, H. J., and Heiss, G.** The role of a tautomerase and a nitrite-eliminating enzyme in 2,4,6-trinitrophenol (picric acid) degradation. 2003, submitted to *Appl. Environ. Microbiol.*
12. **Inoue, H., H. Nojima, and H. Okayama.** 1990. High efficiency transformation of *Escherichia coli* with plasmids. *Gene* **96**:23-28.
13. **Kadiyala, V. and J. C. Spain.** 1998. A two-component monooxygenase catalyzes both the hydroxylation of p- nitrophenol and the oxidative release of nitrite from 4-nitrocatechol in *Bacillus sphaericus* JS905. *Appl. Environ. Microbiol.* **64**:2479-2484.
14. **Lenke, H., C. Achtnich, and H. J. Knackmuss.** 2000. Perspectives of bioelimination of polynitroaromatic compounds, p. 91-126. *In* J. C. Spain, J. B. Hughes, and H. J. Knackmuss (eds.), *Biodegradation of nitroaromatic compounds and explosives*. Lewis Publishers, Boca Raton.
15. **Lenke, H. and H. J. Knackmuss.** 1996. Initial hydrogenation and extensive reduction of substituted 2,4-dinitrophenols. *Appl. Environ. Microbiol.* **62**:784-790.
16. **Lenke, H., D. H. Pieper, C. Bruhn, and H. J. Knackmuss.** 1992. Degradation of 2,4-dinitrophenol by two *Rhodococcus erythropolis* strains, HL 24-1 and HL 24-2. *Appl. Environ. Microbiol.* **58**:2928-2932.
17. **Matlack, A. S. and D. S. Breslow.** 1967. Cleavage of 2-nitrocyclohexanone by base. *J. Org. Chem.* **32**:1995-1996.

18. **Nishino, S. F., G. C. Paoli, and J. C. Spain.** 2000. Aerobic degradation of dinitrotoluenes and pathway for bacterial degradation of 2,6-dinitrotoluene. *Appl. Environ. Microbiol.* **66**:2139-2147.
19. **Pearson, W. R. and D. J. Lipman.** 1988. Improved tools for biological sequence comparison. *Proc. Natl. Acad. Sci. U.S.A* **85**:2444-2448.
20. **Sambrook, J., E. F. Fritsch, and T. Maniatis.** 1989. *Molecular cloning: a laboratory manual.* Cold Spring Harbor Laboratory, Cold Spring Harbor, N.Y.
21. **Severin, T. and R. Schmitz.** 1962. Umsetzung von Nitroaromaten mit Natriumborhydrid. *Chem. Ber.* **95**:1417-1419.
22. **Walters, D. M., R. Russ, H. J. Knackmuss, and P. E. Rouviere.** 2001. High-density sampling of a bacterial operon using mRNA differential display. *Gene* **273**:305-315.
23. **Zeyer, J. and H. P. Kocher.** 1988. Purification and characterization of a bacterial nitrophenol oxygenase which converts *ortho*-nitrophenol to catechol and nitrite. *J. Bacteriol.* **170**:1789-1794.

## Acknowledgements

Herrn Prof. Dr. H.-J. Knackmuss danke ich für sein ständiges persönliches Interesse am Fortgang dieser Arbeit, sowie für viele nützliche Anregungen aus zahlreichen Diskussionen.

Insbesondere bedanke ich mich bei Frau Dr. Gesche Heiss für ihr reges Engagement und ihre fortwährende Diskussionsbereitschaft.

Herrn PD Dr. Andreas Stolz danke ich für die Übernahme des Korreferates.

Ein herzliches Dankeschön an meine Laborkolleginnen Natalie Trachtmann und Dang Phuong Nga für ihre Hilfsbereitschaft und die gute Laboratmosphäre.

Ich bedanke mich ganz herzlich bei allen Mitarbeitern des Instituts für Mikrobiologie für ihre Offenheit, die gute Zusammenarbeit und nicht zuletzt den vielen Spaß innerhalb und außerhalb des Labors.

Für viele interdisziplinäre Diskussionen im "Maulwurf" und spannende Bowling-Abende ein großes Dankeschön an Mathias Lehmann, Jürgen Schmucker, Marc Herold und Dr. Christian Hoffmann.

Reinhard Braaz, Regine Zocher und meinem Patenkind Nicholas Braaz danke ich für die Unterstützung und die Freundschaft, die mir stets Kraft gegeben hat.

Nicht zuletzt bedanke ich mich bei Silvia Lakner für die Unterstützung bei vielen molekularbiologischen Arbeiten und vor allem für die schöne Zeit zusammen in Stuttgart.

## Curriculum Vitae

Klaus Walter Hofmann

Geboren am 07. Februar 1970 in Coburg

1980 - 1989 Meranier-Gymnasium Lichtenfels

05/1989 Abitur

06/1989 - 08/1990 Wehrdienst in Amberg

09/1990 - 08/1992 Studium der Biologie (Diplom) an der  
Friedrich-Alexander Universität Erlangen-Nürnberg

09/1992 - 11/1999 Studium der Chemie (Diplom) an der  
Friedrich-Alexander Universität Erlangen-Nürnberg

11/1999 Diplom Chemie

03/1999-11/1999 Diplomarbeit bei Prof. Dr. E. Schweizer am Lehrstuhl für  
Biochemie der Friedrich-Alexander Universität Erlangen-  
Nürnberg,

Thema: "Herstellung und enzymchemische Charakterisierung  
eines hybriden Fettsäuresynthase-Komplexes aus der  $\alpha$ -  
Untereinheit von *Saccharomyces cerevisiae* (FAS2-kodiert) und  
der  $\beta$ -Untereinheit von *Yarrowia lipolytica* (FAS1-kodiert)"

03/2000 Beginn der experimentellen Untersuchungen zur vorliegenden Arbeit  
bei Prof. Dr. H.-J. Knackmuss am Institut für Mikrobiologie der  
Universität Stuttgart

